METHODS TO CREATE AND CHARACTERISTICS OF POROUS POLY(VINYL) ALCOHOL FOR THE PURPOSE OF FACIAL IMPLANTS

A Thesis
Presented to
The Academic Faculty

by

Kathleen Carmen Bernhard

In Partial Fulfillment
of the Requirements for the Degree
Master of Science in the
School of Mechanical Engineering

Georgia Institute of Technology
December 2014

METHODS TO CREATE AND CHARACTERISTICS OF POROUS POLY(VINYL) ALCOHOL FOR THE PURPOSE OF FACIAL IMPLANTS

Approved by:

Dr. David N. Ku, Advisor
School of Mechanical Engineering
Georgia Institute of Technology

Dr. Jonathan S. Colton
School of Mechanical Engineering
Georgia Institute of Technology

Dr. Felmont F. Eaves, III
Department of Surgery
Emory University

Date Approved: December 5th, 2014

DEDICATION

I dedicate this to my grandfather, Anthony Calandro.

A man I never met, but who's lasting legacy helped make this thesis possible. I hope you're proud to know your granddaughter is a Ramblin Wreck from Georgia Tech.

ACKNOWLEDGMENTS

First and foremost, I would like to thank my adviser Dr. David Ku. His willingness to take me into his lab and give me this research opportunity has meant the world to me. I will always appreciate his constant efforts to strengthen my creativity, critical thinking, and ability to problem solve. His wisdom and mentorship have been invaluable and I will never forget the kindness he has shown towards me.

I would like to thank my lab mates, both past and present, who have imparted their knowledge and shown me support: Marmar Mehrabadi, Lauren Casa, Daniel Tanner, Sumit Khetarpal, Max Nguemeni, Susan Hastings, and Joav Birjiniuk. The presence of you all was the most enjoyable aspect throughout this experience. I wish you all nothing but the best in life.

I would like to thank my parents, Rudolph and Judith Bernhard, for constantly pushing me to do my best in all aspects of life. They emphasized the importance of education from an early age and instilled in me the work ethic that was required to make it through six years at Georgia Tech and achieve my two degrees. From addition flash cards on my bedroom floor, to weekly vocabulary words on my bed, to physics on the kitchen table, they spent countless hours tutoring and studying with me. When they saw an early interest in math and science, they fostered it with science books, a telescope, and trips to space camp. They taught me to never be ashamed of who I am and to have the belief in myself that I can accomplish my dreams. Everything I am today is because of their unyielding love and support.

I would like to thank my younger sister, Kristina Bernhard, whose companionship from childhood through today has been my most treasured gift. I have tried to live by

your example of fearlessness and self confidence. No matter what happens, I know you will always be there to help me celebrate my victories in life.

Finally, I would like to thank my best friend and partner Harrison Jones. His decision of a graduate degree is what prompted me to pursue one as well. He has been by my side through every victory and defeat as well as always there to hold me during a breakdown. Although so much as changed since we met in that freshman dorm, his comforting presence and constant support has been unwavering. His encouraging smile and confidence in my abilities pushed me to achieve all that I have during these six years at Georgia Tech. His love has made a positive everlasting impact on my life and for that I will always be grateful.

TABLE OF CONTENTS

LIST OF TABLES

LIST OF FIGURES

SUMMARY

Facial implants are becoming more common in America and across the world. In the United States last year, over 260,000 augmentation and reconstruction surgeries were performed on facial cartilage areas, while over two million soft tissue fillers were administered. The current implants on the market, though, are deficient in three major areas: they are too rigid, susceptible to migration, and require a large incision. Alternatively, dermal fillers lack shape and biodegrade too quickly. Poly(vinyl) alcohol (PVA) cryogel is a promising hydrogel alternative due to its softness, durable nature and ease of cast molding. While biocompatible, it does not elicit a fibrous response with firm adhesion and could migrate. The goal of this study is to develop a biodurable implant material that has soft-tissue elasticity, pores for adhesion, and swelling for small incisions.

In this research, multiple porosity inducing methods are applied to PVA cryogel. These include a casting PVA cryogel over a porogen then leaching it in a solvent, a gaseous exothermic reaction, creating composites with biodegradable components, as well as using molds to alter the surface texture. Once created, the samples then underwent a series of tests to determine their mechanical properties which include elasticity, tensile strength, elongation, tear strength, pore size, and porosity. Swelling ratio of nonporous PVA cryogel was also considered.

Porous PVA cryogel made with a high PVA weight percentage (30%) showed equivalent mechanical properties to that of cartilage. Porous PVA cryogel manufactured with a lower weight percent (10% and 20%) were shown to have similar elastic properties

to that of adipose tissue. The surface texture methods, gas method, casting and leaching method, and composites made with CaPO4 and chitosan were all shown to create pores large enough for ingrowth. Samples created with a porosity large enough to encourage ingrowth include the gas method, casting and leaching method, and the CaPO4 composites. The swelling ratio was shown to increase as the weight percentage of PVA in the samples decreased. These quantified characteristics can be used to select the appropriate porous PVA cryogel required for a range of applications including facial implants.

CHAPTER 1

BACKGROUND

Introduction

The purpose of prosthetics is to replace portions of damaged or missing body parts in order to improve physiological function and/or appearance. With this purpose in mind, volume filling implants were examined to determine whether there was a need for improvement in any category. After reviewing current products on the market, facial implants arose as a promising field. In 2013, over 260,000 augmentation and reconstruction surgeries were performed on facial cartilage areas. Many biomaterials are currently on the market for this purpose, however each has issues including rigidity and a tendency to migrate. In addition, over two million soft tissue fillers were administered last year. Most of these fillers, however, are only temporary. The one brand that is permanent is made up of microspheres that, if they become infected, can lead to scaring and disfigurement.

Poly(vinyl) alcohol (PVA) cryogel has emerged as a new biomaterial for prosthetic implants. Its characteristics include biocompatibility, high water solubility, resistance to degradation within the body, and the ability to mimic a wide range of characteristics similar to soft tissues.[1, 2] Its softer nature in comparison to current biomaterials will allow it to feel more natural underneath the skin. It is currently used in an array of medical products from vein valves to soft contact lenses.[1] Its application towards volume filling implants could be limited however because of its nonporous

structure within the body. This may lead to lack of adhesion to the body and subsequent migration of the implant.

In this study, one pathway to promote implant adhesion was examined – the manufacture of pores at the surface and throughout the implant. Porosity inducing techniques were applied to PVA cryogels in order to create open and closed cell pores. The purpose is to determine which methods are feasible as well as characterize key mechanical properties of the manufactured porous PVA cryogel. These properties include elasticity, tensile strength, tear strength, elongation percentage, pore size, porosity percentage, and swelling ratio. These values were quantified to provide a reference database when designing volume filling implants with porous PVA cryogels.

Choosing Volume Filling Facial Implants

The goal is to research volume filling implants to determine one that could be improved or enhanced with PVA cryogel. Through the FDA's list of implantable devices[3], 18 types of space occupying implants were identified. These are listed in Table 1 with a description, prevalence, and usage of each type of implant. The prevalence data were obtained from the American Society of Plastic Surgery[4] and are for the Unites States only.

The categories on Table 1 were narrowed down to determine which implants would be the most feasible for PVA cryogel. Since PVA cryogel's mechanical characteristics cannot be made to mimic that of bone, categories intended for bone replacement such as JAZ (mandibular implant facial prosthesis composed of materials such as stainless steel and titanium) were excluded. MIC (pectoral muscle implant) was removed because of such a small implantation rate in comparison to other implants. Since PVA cryogel is a hydrogel, it must always be hydrated. Implants that have contact with the air such as ESZ (endolymphatic shunt) and HPZ (eye sphere implant) were excluded because the PVA cryogel would dehydrate and shrink. While MRD (breast implant) is one of the most common augmentation implants with 290,000 operations in 2013, thus about 680,000 breast implants[4], the Class III regulation pathway required by the FDA is lengthy, complicated, and expensive.[5]

With function, material, prevalence, implantation area, and regulatory pathway taken into account, facial implants arose to be a favorable and promising choice for PVA cryogel implants. These include categories FWP (internal chin prosthesis), FZE (internal nose prosthesis), MIB (facial silicone block), and LMH (wrinkle filler). These implants

were extensively researched to determine the tissue's physiological characteristics; a series of experiments were conducted to see whether PVA cryogel can meet these conditions and become a more suitable material for these implants than those currently sold on the market. It is hypothesized that PVA cryogel can be substituted for the current implant materials to create a line of more natural feeling and long lasting facial implants.

Table 1: List of FDA's Volume Filling Implant Categories

References [3, 4, 6]

Code	Description	Specialty	Uses	Examples	Material	Prevelance
ESF KDA ODU	Space-occupying implant material	General & Plastic Surgery, ENT	For plastic and reconstructive surgery of soft tissue deformaties of chin, jaw, nose, or bones or tissue near the eye or ear. Shaped and formed by surgeon	Ceravital ceramic ear canal wall prosthetic, Hearing aid	Polytetraflouroethylene with carbon fibers composite	Hard to determine because it encompases many types of surgeries
ESH JOF MIB	Synthetic polymer material (Polymer, Synthetic-Pife, Silicon Elastomer, Polyethylene, Polyurethane)	Ear Nose & Throat	Space occupying substance	Nose, ear, chin, calf, gluteal, and pectorial implants. Closing defects in esophagus. Silicone blocks that can be shaped	Synthetic polymer material (Polymer, Synthetic-Pife, Silicon Elastomer, Polyethylene, Polyurethane)	Hard to determine because it encompases many types of surgeries
ESY FZD	Otoplasty (Ear) prosthesis	General & Plastic Surgery	For reconstruction of the external ear	Ear Lobe	Silicone rubber solid	24,000 in 2013
ESZ	Endolymphatic shunt	Ear Nose & Throat	Used to relieve Ménière's disease	Tube that is inserted in endolymphatic sac	Polytetrafluoroethylene or silicone elastomer	100,000 cases a year
ETC	Middle ear mold	Ear Nose & Throat	Repair of the tympanic membrane	Preformed device that is implanted to reconstruct the middle ear cavity	Polyamide, polytetrafluoroethylene, silicone elastomer, or polyethylene, but does not contain porous polyethylene	150,000 cases a year
FAE	Penile rigidity implant	Gastroenterology/Urology	Erectile disfunction	Semi-rigid rods implanted in the corpora cavernosa		20,000 a year
FWP MNF	Internal and temporal chin prosthesis	General & Plastic Surgery	Augment or reconstruct the chin (Mentoplasty)	Chin Prosthesis	Silicone rubber solid	20,000 in 2013
FZE	Internal nose prosthesis	General & Plastic Surgery	Augment or reconstruct the nasal dorsum (Rhinoplasty)	Nosal Prosthesis	Silicone rubber solid	250,000 a year
GXO	Preformed craniosynostosis strip	Neurology	Prevents the bone from regrowing in patients whose skull sutures are abnormally fused together	Strip used to cover bone edges of craniectomy sites (sites where the skull has been cut)	Plastic	
HPZ	Eye sphere implant	Ophthalmic	Implanted in the eyeball to occupy space following the removal of the contents of the eyeball			
JAZ	Mandibular implant facial prosthesis	Ear Nose & Throat	Functional reconstruction of mandibular (lower jaw bone) defects		Stainless steel, tantalum, titanium, cobalt-chromium based alloy, polytetrafluoroethylene, silicone elastomer, polyethylene, polyurethane, or polytetrafluoroethylene with carbon fibers composite	
KHK	Polymer, Ent Natural-Collagen Material	Ear Nose & Throat			Collagen	
KIG	Wrist joint polymer constrained prosthesis	Orthopedic	For replacement of a wrist joint	Consists of a single flexible across-the-joint component that prevents dislocation in more than one anatomic plane	Polyester-reinforced silicone elastomer	

Code	Description	Specialty	Uses	Examples	Material	Prevelance
LBL	Porous polyethylene tympanostomy tube	Ear Nose & Throat	For ventilation or drainage of the middle ear by permit a free exchange of air between the outer ear and middle ear	Malleous clip tube	Polytetrafluoroethylene, polyethylene, silicon elastomer, or porous polyethylene	668,245 in 2006
MIC	Implant, Muscle, Pectoralis	General & Plastic Surgery	Implanted under chest muscle	Pectorial Implant	Silicone rubber solid	342 in 2013
FWM FTR	Sizer, Mammary, Breast Implant Volume	General & Plastic Surgery	Implanted under the breast tissue or under the chest muscle to increase breast size (augmentation) or to rebuild breast tissue after mastectomy or other damage to the breast (reconstruction).	Breast Implant	Saline-filled and silicone gel-filled. Both types have a silicone outer shell	290,000 in 2013
NRO	Surgical Lip Implant	General & Plastic Surgery		All injectable are temporary	Polytetrafluoroethylene	25,000 in 2013
MQV MBP OIS	Calcium Salt Bone Void Filler	Orthopedic	To fill defects not intrinsic to the stability of the bony structure	Fills bony voids of the extremities, spine, and pelvis	Calcium Salt	
LMH	Wrinkle filler	General & Plastic Surgery	To fill in facial wrinkles or fat loss in order to create a smoother appearance.	Many absorbable materials, but only one non-absorbable	Polymethylmethacrylate beads in gel like solution	2,242,000 in 2013

Nose and Chin Replacements

Facial implants are used for augmentation, correction of developmental or traumatic deformities, and to help improve the feature's functionality.

Market Size

In 2013, 19,000 chin implants were implanted within the United States. While 14% of the patients were in their twenties, the highest percent of patients were in the age bracket of 55 and older. In addition, gender distribution was split. 51% of chin implants were administered to males while 49% were for females.[4]

221,000 rhinoplasty procedures were performed in the United States in 2013, however it is not specified what percentage of these were for augmentation. The most common age group for this procedure was the 20-29 year old range. 26% percent of rhinoplasties were performed on males while 74% was on females. [4]

Regulatory Pathway

The most basic volume filling implant category is MIB. This category is defined as a synthetic polymer material meant for implantation for augmentation or reconstruction of the head and neck.[6] It is a Class 2 device and requires a 510K pathway for clearance. Its predicate devices range from basic silicone carving blocks to gluteal and calf implants.

More specific facial implant categories are FWP (internal chin prosthesis) and FZE (internal nose prosthesis). These are described as chin/nose prosthesis made of a silicone rubber solid device for augmentation or reconstruction. Within their previously

cleared device summaries, there is a trend that they reference their own carving block made of equivalent material in MIB as a predicate device. Once the basic material is approved, companies produce specific shapes and usages for it can be more easily passed through the FDA. Also listed is a standard recommended by the FDA for submission: *ASTM F881-94 (Standard Specification for Silicone Elastomer Facial Implants).* Completing the standards set out for silicone should be considered when submitting porous PVA cryogel to the FDA. These include determining tensile strength, elongation percentage, elastic modulus, and tear strength.

Current Materials

The three main types of implants are autographs (grafts derived from the patient's own tissue), homografts (where the tissue for the graft is from a donor), and alloplasts (in which the implants are completely or partially synthetic).[7, 8] A summary of the main advantages and disadvantages between autografts, homografts, and allografts provided by Lin, et. al. and is shown in Table 2.[8] A list of pros and cons specific to each material on the market is presented in Table 3.

Table 2: Advantages/Disadvantages of Autografts, Homografts, and Allografts

Reference: [8]

Table 3 Advantages/disadvantages of autografts, homografts, and allografts

	Autografts	Homografts	Allografts
Advantages	Biocompatibility Strength (bone) Ability to contour (cartilage) Ability to camouflage (fascia)	Biocompatibility Strength (bone) Ability to contour (cartilage) Ability to camouflage (fascia, alloderm) No donor site morbidity Unlimited supply Decreased surgical time	Strength Elasticity Durability No donor site morbidity Unlimited supply Decreased surgical time
Disadvantages	Donor site morbidity Memory (cartilage) Resorption Limited material Warping Displacement Increased surgical time	Increased resorption Warping (cartilage) Extrusion Higher infection rate Higher cost Patient confidence with implant safety	Higher extrusion rate Higher infection rate Higher cost

Table 3: Pros and Cons for Current Cartilage Replacing Materials

References [8-13]

Type	Material	Description	Pro	Con	Failure Rate (%)
Biologic	Bone graft	Bone harvisted from patient	Encourages bone growth	Always reabsorbed Ridgid appearance to nose Requires bone contact Pain and scaring at donor signt	
	Cartilige graft	Cartilage harvisted from patient	Gold standard of grafts Minimal resorption rate Good vitality even with low blood supply Long-term survival rate	Sometimes not enough material for large defects, especially for trama or infection cases Chance of warping Difficult to carve	
	Septal Cartilage	Cartilage harvisted from patient	More ridgid Easy to shape	Frequently defective, insufficient, or missing	
	Homograft Rib	Harvested from human cadaveric donors	Readily available Easy to carve	High resorption rate	
	Dermis and Fat grafts	Fat harvisted from patient	Redily available Good for small deformities	10-20% reabsorption for dermis, 33-50% for fat Requires an extra surgery	
	Zyderm	Collagen	Fibrous encapulation occurs and breaks it broken down to replace with host's collagen Injection (non surgical)	Defect always returns to some degree 3% of patients sensitive to bovine collagen	
	Avitene	Microfibrillar Collagen Hemostat	Smoothing effect Low rejection/reactivity rate	Resorption is highly variable	
Synthetic	Teflon	Polytetrafluoroethylene	Injectable Quite stable and practically inert in tissues Fibrous encapsulation anchors in place	Initial mild foreign body reaction Requires very large needle	
	Silastic	organosilicone polymer	Inert, no reactivity Fibrous incapsulation	Mild tissue reaction High rate of extrusion, migration, infection	
	Supramid	organopolymer similar to dacron	Safe, reliable implant Texture and firmness simulates soft tissue Fibrous incapsulation	Few reports of extrusion Moderate foreign body response Some resorption after ~15 years, loss of use	
	Mersilene	Polyethylene terephthalate [PETP]	Easily shaped	No structural support Extnesive fibroblast ingrowth makes almost impossible to remove	7
	Proplast (I and II)	Prepared from Teflon polymer and carbon fibers	Highly porous (79%) but firm Allows for host fibrous-tissue ingrowth Resistance of extrusion because filled with host tissue Easy to shape	Tendency to fragment and collapse under pressure and shear forces Initial inflamatory response Black substance, which may show through skin No longer available in US Less resistant to infection	7.0-9.0
	Medpore	High-density porous polyethylene	Porous (46% of vol) Rapid tissue/bone growth within a month Very biocompatible Easily sculptable Minimal inflamation Long term structural stability Resistant to infection High suscess in 2nd and 3rd revision surgeries White in color	Stiffness can create an unnatural appearance Rough surface makes insertion cumbersome	3 - 6%
	Silicone	Polydimethylsilaxane	Enert Easy to shape Thick fibrous incapsulation Easy to remove Maintains its shape within body	High rate of migration, extrusion, inflamation, calcification, patient disatisfaction Feels like foreign body underneith skin Slipery surface Abnormal skin color, even after implant removal	4-36%
	Gore-Tex	Microporous Polytetraflouroethylene	Low tissue reactivity Low cost High biocompatibility Microporous tissue ingrowth gives stability Easily shaped Can be removed without disrupting surroung tissue Proved long term patency No resorption	Develop prominent edges over time Slippery, not easily carved Recently discontinued in plastic surgery applications Small pores increases liklyhood of infection	1.5%-3.2

Autografts

Autografts are regarded as the most preferred option for facial augmentation. Grafts are materials that are combined with a patient's own cartilage, bone, dermis, or fat. Its most important attribute is that it has extremely high biocompatibility. They also provide strength and can be easily shaped. Disadvantages include the potential for donor site morbidity, warping, and increased surgical time to obtain the extra material. In addition, since it is made with the patient's own body, there is a chance of partial or full absorption of the biomaterials. There is also a risk of not enough supply of the biological components. This is especially in the case of facial reconstruction where there is usually a shortage of donor sites from the body to achieve desired results.[7, 8]

Bone

The biomaterials from the bone grafts come from the rib, calvarium, iliac chest, and nasal septum. Because this graft is made from a bone, it is much stiffer than surrounding facial tissue and is more likely to fracture than other grafts. Noses reconstructed with these grafts tend to be more rigid and unnatural looking in appearance. They have lost favor over the years because of a high resorption rate and donor site morbidity which can include pain and paresthesia.[8] In order to help prevent resorption, these grafts must have contact with bone. If they are placed in contact with only soft tissue, the bone will be absorbed and replaced by fibrous tissue within a few years of implantation.[11, 13]

Cartilage

Cartilage is currently the most commonly used material for autografts of facial implants. It has a low infection and extrusion rate, as well as excellent elasticity and resistance. It is easy for the surgeon to shape, survives in areas with low blood supply, and has a minimal resorption rate (as low as 2%). The three sources for the graft come from septal, rib, and auricular cartilage with septal being the most preferred. Unfortunately, in the case of reconstruction and other forms of rhinoplasty, there is usually too little septal cartilage available. [13, 14] Like all autographs, an insufficient amount of cartilage will prevent it from being an option to surgeons. Cartilage from the rib is almost always in large supply and offers great structural support, however there is a risk of potential donor site morbidities that include scar visibility and chest wall deformity. Rib grafts also have a high rate of warping and must be added deeper under the skin than other cartilage grafts.[8] Unlike bone grafts, cartilage grafts do not require contact with bone or other cartilage to survive. This allows them to be used in many more corrective surgeries because they do not need to be buried deep within the face.[11, 15]

Fat

Fat is appealing because of the wide availability, however its absorption rate ranges anywhere between 20 and 90%.[16] Because of this, it is typically used as a filler for small imperfections. It is commonly paired with liposuction surgeries where some fat is removed with a large bore needle then injected into the face.[11]

Homografts

Homografts have long term unpredictability making them not an preferred substitute for autogenous grating material. Because they are not made with the patient's own cells, homografts typically have a higher absorption rate (33%) and revision surgery rate (44.4%) than autografts.[8] There is also the fear of transmitting diseases from the donor to the patient as well as a chance of extrusion. To help prevent the transmission of diseases, donor bodies must comply with rigorous standards as well as the donated tissue is exposed up to 60,000 Gy gamma waves.[13] This leads them to be offered at a higher cost to the patient. They do, however, still have the same advantages of autografts like high biocompatibility, ability to be easily shaped, and easily camouflaged within the face. In addition, there is no donor site morbidity to the patient, reduced surgical time, and supply is no longer a limiting factor. The most common biomaterial for homografts is irradiated costal cartilage (ICC). This, unfortunately, has a high likelihood of warping as well as an absorption rate of 75% over 10 years.[8, 17]

Alloplasts

Alloplasts are synthetic implants that provide strength, elasticity, and durability for the face. They are readily available, and because they are not from the patient's own body there is no donor site morbidity, reduced trauma to the patient, and a decreased surgical time. Unfortunately, since they are synthetic, they have higher extrusion and infection rate and typically cost more. The biggest issue with alloplasts is the risk of incompatibility with the patient. An immuno-responce can happen soon after surgery or even years later. [8, 14]

Silicone

Silicone appeared in the 1950s and was the first alloplast to have gained widespread use. It is a polymer of silicone-oxygen chains that are crosslinked by methyl side groups. The crosslinking determines its physical state in which increasing crosslink leads to decreased elasticity. This allows it to be provided in a range of mechanical properties. It is nonporous, inert, and does not decompose nor change its shape over time.[8, 11] Because it is manufactured using a mold, it can be produced in any shape to allow customization for an individual's needs.[15] Its physical properties allow it to give excellent structural support for a facial implant. Its firmness makes it easy to sculpt but can make it feel foreign underneath the skin and can even cause bone erosion.[13]

After implantation, silicone becomes surrounded by a thick capsule of fibrous tissue which give it poor anchoring within the body and does little to stop migration.[8] This barrier also prevents penetration of antibiotics in the case of infection. In addition, it has been observed to discolor the skin near the implant which usually persists even after the implant has been removed. Within the nose it experiences constant movement and frequent midface trauma. This, combined with only a thin soft tissue cover, leads to a high chance of movement and extrusion.[11] An example of silicone extrusion is shown in Figure 1.

Ham et.al. reviewed 1500 cases of silicone implants and found 357 complications (20.8%). Of those complications, 6.6% were due to infections, 18% were inserted incorrectly, 8.5% migrated, 7.5% extruded, and 62.4% discolored the patient's skin.[18] Because of the high rate of complication, silicone has become widely abandoned by western cultures.[13] Although it has lost popularity in America, it is still widely used in Asian countries because of its low cost in comparison to other alternatives. In this

population, the patient's skin also tends to be thicker which reduces the extrusion rate of the implant. The complication rate is still estimated around 10-16% within this ethnicity.[8, 10]

Figure 1: Extruding Silicone Implant

Medpor

Medpor is a porous high density polyethylene produced by Stryker and is described in literature as safe and effective[10, 19, 20]. It is considered one of the stiffer options for implants and is commonly used in surgeries that add more support for facial features.[21] It has been noted that its stiffness gives an unnatural appearance for more prominent features like the nose and its rough surface makes displacement infrequent but insertion into the face a cumbersome task.[13] When heated between 90-100°C, this material can be easily shaped, cut, pierced, and sutured. Its shape becomes permanent when cooled.[14] Its pore size ranges in between 100 and 250 µm, which is an optimal range for rapid fibrovascular ingrowth.[8] This size is also large enough for the immune system to be effective which reduces its rate for infection and extrusion in comparison to

other porous implants. It has been shown to have ingrowth of soft tissue within the implant after one week and bone after three.[10, 15] Romo et. Al.[22] found a complication rate of 2.6% after implantation of Medpore into 187 patients. While extrusion was the main complication, it was noted that those who experienced extrusion had thinner skin because of their smoking habits.

Gore-Tex

Polytetraflorethylene (Gore-Tex) is a microporous plastic material with a soft, textile feel that is more commonly used for volumetric compensation of smaller defects than support. It is very pliable and is manufactured in sheets of variable thickness in which the surgeon can easily cut and carve for the desired shape.[14] It contains micropores with sizes ranging from 10 to 30 μm. The pores are large enough to give limited collagen ingrowth and graft stabilization to prevent movement and encourage minimal capsule formation to allow easy removal that will not disrupt the surround tissues. The small pores do, however, limit the immune system's effectiveness.[8]

While Gore-Tex has been shown to have high biocompatibility and a minimal foreign body response, there is a chance of it slightly deforming and developing prominent edges over time as well as infection.[13] Godin et al. [23] reviewed Gore-Tex 4 years after implantation and found that 3.2% of the implants were infected and required removal. Jin et al. [24] found a 2.5% complication rate of Gore-Tex due to infection in a group of 853 patients after 1.5 years. Conrad et al. [25] examined 521 rhinoplasty patients who received a Gore-Tex implant over a span of 17 years. They observed a complication rate of 3.4% and an implant removal rate of 1.9% with infection being the

main reason. It is also important to note that it will always extrude if placed in contact with the dermis.[10] While Gore-Tex sheets for general surgery are still being produced, its manufactures chose to discontinue its plastic surgery usage in 2006.[13]

Supramid Mesh

Supramid (polyamide mesh) was common in the 1970s and was considered the standard of its time. It has a texture and firmness that is similar to soft tissue. There were very little reports of adverse reactions and extrusion, and most of these were because of infection. It caused some tissue reaction of macrophages and foreign-body giant cells, but that ceased within the year of implantation and became filled and surrounded by fibrous tissue that minimized the chance of migration. It was more difficult to carve than other options.[11, 13] By the mid 80s, however, it had almost completely been abandon by surgeons. While it did show great initial results, it was discovered to fragment and degrade over time in the body.[8] This hydrolytic degradation was caused by the reversal of the polymerization reaction that forms the polymer. This causes a gradual 20% loss of tensile strength per year of the material. Within a decade, it is completely absorbed by the body.[8, 11]

Mersilene Mesh

Mersilene (polyethylene terephthalate) is the successor of Supramid. It is a woven polyester fiber mesh produced by Ethicon, and is superior to Supramid mesh because it maintains its tensile strength, has minimal tissue reaction, and has little to no degradation within the body.[11] Its average pore size is 125 μ.[26] It is primarily used for volumetric correction because of its lack of structural support and has been shown to

not degrade nor absorb in the body over time. Being made out of fiber, there is a large biological response in which it becomes filled with fibroblasts and ingrown with connective tissue.[14] This makes it much more difficult to remove in the need of revision surgery which is required about 7% of the time with this product in nasal surgeries.[8] The main reason for removal of this implant is the risk of infection which is about 4%.[13] It has found success when used as a chin implant. Gross et al. [27] used it for chin augmentations on 264 patients over a 14 year span. It was found to have a 0.8% infection rate and 1.5% displacement rate.

Proplast

Proplast (polytetrafluorethylene) by Vitek is a firm and porous implant made from PTFE polymer and carbon fibers. With pore sizes ranging from 100-500µm, the implant is surrounded and filled with fibrous tissue within a few months on implementation. Originally, the carbon fibers were black making it visible as an implant, especially for the nose, but Proplast II soon appeared which was made out of white aluminum oxide instead of carbon. Its main advantages are that it is firm enough to provide support as well it is flexible and one of the easiest materials to shape. It does, however, have a higher chance of extrusion when compared to other options like Mersilene.[11] With it being highly porous (73%) and flexible, its primary limitation is its tendency to fragment and collapse under pressure and shear forces.[13] It is most commonly used in malar augmentation with an implant removal rate of 7.6%.[10] While it is still used abroad, the United States Food and Drug Administration (FDA) withdrew its approval for the material in 1990.[14]

The fragmentation of the material was found to lead to progressive bone degeneration for the patient in as little as 1-2 years.[28]

Dermal Fillers

As people age, facial wrinkles and folds of the skin appear and become more prominent. Dermal fillers are natural or synthetic injections into the mid to deep dermis of the face for correction of these wrinkles. Recently they have started to be used to augment and contour small facial imperfections as well as fill in divots left by acne scars.[29]

Market Size

After Botox, a procedure which prevents the development of wrinkles by paralyzing facial muscles, soft tissue fillers are the second most common minimally invasive cosmetic procedure. In 2013, the procedure was performed over 2.2 million times in the United States. In addition, the use of soft tissue fillers is on the rise. Its usage has increased 243% since 2000.[4] Housman et al. found that it encompassed 18.4% of all office based cosmetic visits.[30]

Figure 2 was obtained from the FDA's Executive Summary of Dermal Fillers. After reviewing 533 reports, the FDA found patient's age's ranged from 17 to 86 years old with the largest age bracket being 50-60 years.[29]

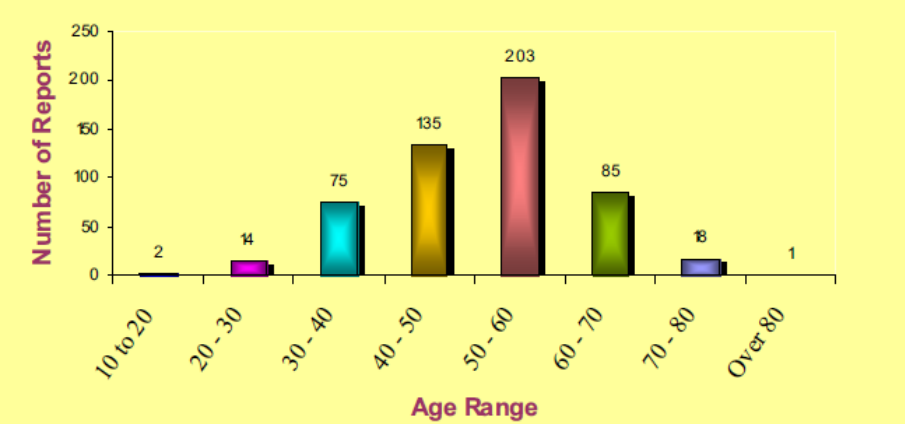

Figure 2: Patient Age Range for Dermal Fillers

Reference: [29]

While dermal fillers have traditionally been used for the face, lately the market has expanded to include improving the look of crow's feet, horizontal neck and chin folds, aging in hands, and nipple definition. Although the FDA has not specifically approved fillers for these usage, doctors are allowed to use their own discretion for the benefit of the patient.[31]

Regulatory Pathway

The FDA approved the first wrinkle filler with the Zyderm Collagen Implant in 1981. Since then, another 20 have been approved with the most recent being in 2013[32]. Their FDA product code is LMH and they are considered a Type 3 device. Currently, they must be submitted through the premarket approval (PMA) pathway.[6]

In 2008 the *Executive Summary for Dermal Filler Devices* was published by the FDA[29] to give a pathway for pre-market approval. It includes the requirement of a randomized, controlled, multi-center clinical trial with a sample size around 150 patients. The assessment of patient's wrinkle severity should be scored based on the Lemperle

Rating Scale (LRS) 3 and 6 months after injections through pictures by an independent reviewer. In addition, the patients should receive follow up meetings at 3 and 14 days after injection as well as after 1, 3, 6, 9, and 12 months to determine if any adverse reaction had appeared.

Another possible route to consider is through MIB (Elastomer, Silicone Block). The FDA defines this implant as an "ear, nose, and throat synthetic polymer material intended to be implanted for use as a space-occupying substance in the reconstructive surgery of the head and neck."[6] While not specifically used to minimize wrinkles and folds in the face, attempting to have the implant pass as just a facial space filler would reduce the time and money required for approval. An argument could be made that since the implant would be a solid rod shape instead of microspheres within a gel, it does not belong within LMH. MIB encompasses any space-occupying polymer within the face while LMH is specifically for dermal implants. Products under MIB are considered to be Class II devices and require a 510K instead of a PMA. Predicate devices under this code include silicone carving blocks for facial implants and gluteal, calf, and pectoral implants.

Current Materials

Materials for dermal fillers range from biologic to synthetic and absorbable to nonabsorbable. They are considered short lasting if their affects are not evident after 6 months, semi-permanent if they last to 3 years, and permanent if they last longer than 3 years.[33]

Hyaluronic Acid

Hyaluronic acid ($(C_{14}H_{21}NO_{11})_n$) is a naturally occurring glycosaminoglycan in the extracellular matrix. Because the acid's half life in the body is 1-2 days, all injectables have been chemically crosslinked with various chemicals to increase the lifetime of the product.[29] These dermal fillers have become the material of choice. In 2013, 75% of all dermal fillers administered were from the four approved brand names: Hylaform, Restylane, Juvederm, and Elevess.[4] Duration of the injection ranges from label to label. Restylane's and Perlane's effects last up to 6 months while Juvéderm lasts from 9-12 months. Site of injection also determines its duration within the body. It lasts longer in areas of less muscle movement such as under the eyes as opposed to high usage muscle areas like the lips.[34]

These injections have been proven safe for patients many times over.[34, 35] Nicholas et al. [36] injected these fillers into over 700 patients from 1996-2000. Only 3 patients (0.42%) had complications which was skin reactions 8 weeks after injection due to allergies and took 6 to 24 weeks to resolve.

Collagen

Collagen was the first type of dermal filler approved with Zyderm in 1981. While it is composed of bovine collagen, Evolence is composed of porcine collagen, and Cosmoderm is made up of human collagen.[29] Until the early 2000s, collagen based dermal fillers were the only option available. Since 2000, however, their usage has decreased 90% while the overall usage of dermal fillers has increased 243%.[4]

Hypersensitivity reactions occur in 1-3% of patients using collagen. In addition, since they are derived from a different species, there is a greater chance of eliciting an immune response.[37]

Hydroxylapatite

Hydroxyapatite is a biocompatible substance that has been used in implants for over 20 years. Radiesse is synthetic biodegradable hydroxylapatite (particle diameter 25-45 μm) suspended in carboxymethylcellulose. It is approved for both the correction of facial folds and the signs of lipoatrophy in HIV patients. It was injected into 285,000 patients in 2013.[29] The gel is absorbed and replaced with soft tissue within a few weeks. HA exhibits little, if any, foreign body response and is highly biocompatible.[33]

The longevity of Raduesse depends on many factors including age and metabolism. Silvers et al found that 91% of patients still showed improvement at the end of an 18 month trial and there was a 97% satisfaction rate.[38] With a population of 102 patients, Bass et al claimed 40% still showed slight improvement at 2.5 years, however it was not nearly as prominent as it was at 6 months.[39] Jansen et al found that 12.4% of patients developed nodules, but they were easily treated with steroids. Patient satisfaction rate in that study was 89%.[40]

Poly(methyl methacrylate)

Poly(methyl methacrylate) (PMMA) microspheres, known on the market as ArteFill, was approved by the FDA in 2006.[29] It consists of non-resorbable PMMA microspheres (30-50 μm in diameter) suspended in a bovine collagen and saline mixture. This is the only long lasting injection on the market currently. Patients have the same

wrinkle improvement at six months as they did after one year as well as results have been shown to last up to 15 years.[31] In 2013, it was used in 17,000 instances which was a decrease of 6% from the year before.[4]

Its smooth surface and uniform size leads to minimum foreign body reaction. Its potential complications include redness, itching, intradermal nodules, and hypertrophic scaring. These usually arise from improper injection technique and are typically treated with steroids or extraction if the issues persists. For three days after injection the spheres sit in a viscous paste before encapsulation, and muscle movement can push the microspheres deeper or closer to the surface of the skin. Figure 3 shows intradermal nodules that were removed from a patient.[41] In addition, wrinkles may appear 5-10 years after injection from muscle movement shifting the spheres.[31]

Figure 3: Intradermal Nodes Formed from Injected PMMA Microspheres

Characteristics for Facial Implants

After reviewing facial implants, multiple issues became apparent with the current material options available for patients. Characteristics of a facial implant need to be determined and quantified in order to help identify and create potential alternative materials. The values of these characteristics are derived from those of the surrounding tissues (cartilage for nasal and chin implants and adipose tissue for dermal fillers) as well as thresholds given by the FDA through the standard ASTM F881.[42]

Elasticity

The main issue that arose with the most prominent market materials (silicone, Medpor, and Gore-Tex) is the unnatural feeling of the implants. This is due to their rigidity being greater than the surrounding tissues. An implant should have a similar firmness to the tissue it was trying to mimic or replace. This characteristic is quantified as the elastic modulus or Young's modulus and its value ranges depending on the tissue type.

Due to the change in elasticity between tissue types, values were found for both cartilage and adipose tissue. The Young's modulus of cartilage is depth dependent. Most of facial cartilage falls within the range of [0.3,1.3]MPa, however the deepest 20% could increase as high as 2.3MPa.[43] Due to the nature of adipose tissue, determining it mechanical characteristics has been a difficult task. The only mechanical characteristic of fat found in literature was its Young's modulus. Krouskop et al.[44] found the modulus to range between 0.018 and 0.024MPa and Sarvazyan et al.[45] found a greater range at 0.005-0.050MPa.

Tensile Strength

Tensile strength is the maximum stress a material can withstand while being stretched before breaking. ASTM F881 states that the material for facial implants must have a minimum tensile strength of 1.38MPa. The yield tensile strength for nasal cartilage was found by Richmon, et al. to be 1.95MPa ±0.24, or a range of [1.71,2.19]MPa.[46] Thus, even if the material meets the FDA requirement, it still may not be strong enough to handle the everyday forces experienced by the face. A minimum tensile strength of 1.71MPa, the lower end of its standard deviation, was chosen as the value's standard in this research in order to better mimic the characteristics of surrounding tissue.

Elongation

When choosing a material for an implantable device, an important characteristic is that the implant can stretch as much as its surrounding biological tissues. ASTM F881 states that implantable silicone should have a length increase of at least 200%. Even if the material does not achieve 200% elongation, an argument should be made that it does not have to reach this benchmark, just that it can stretch as much as its surrounding tissue. Human cartilage has a linear stress/strain behavior up to 15% strain.[47] After that, cartilage deformation ensues to at least 30% elongation.[48] Thus, a minimum threshold of 30% would be a suitable elongation percentage of a facial implant due to the fact that it satisfies the characteristic of both elastic and even potential inelastic deformation of its surrounding tissues.

Tear Strength

Tear strength is the measure of a material's resistance to tearing. A desired value for tear strength is not mentioned for silicone facial implants in ASTM F881.[42] It only states that it must be determined and recorded. Tear strength for cartilage is 2.2kN/m.[48] An implant should at minimum have the same tear strength as cartilage if not higher to prevent it from becoming damaged when experiencing everyday stresses within the face. For this reason, a minimum tear strength of 2.2kN/m should be required for facial implants.

Pore Characteristics

The lack of porosity in some current materials like silicone gives rise to a higher migration and ejection rate than its porous competitors. In order to help integrate an implant into the surrounding tissue and prevent unwanted movement, pore characteristics such as pore size and porosity should be considered.

The required pore size for implants is dependent on the kind of desired biological ingrowth. Fibrous ingrowth can be seen in pores with diameters between 5 and 15µm while bone regeneration typically requires pore diameters ranging from 100 to 400µm but can be as high as 700µm.[49-51] While a microporous structure (under 50µm) does show some cellular attachment from the fibrous ingrowth, the strength of the bond is much less than one attached by bone ingrowth and the implant can more easily be dislodged. This means that the implant can be more easily removed in the case of reconstruction; however it more likely to be shifted when placed under stress. In

addition, the pore size is too low for macrophages to enter and can increase the risk of infection.

The higher the porosity percentage of a material, the more structural linkage of the ingrowth material appears within the implant to ensure attachment and prevent slippage. There is a wide range of porosity values within current biomedical materials, but Bruchman, et al. states that an implant should strive to have a minimum porosity of 30% to help this bonding.[52]

Swelling

Hydrogels have the ability to absorb water and swell in size. While finding a swelling percentage is not required by the FDA, it is a useful property to know when using hydrogels for implants and can be used as an advantage in the design. When administering an implant, the incision should be as small as possible to reduce noticeably and pain. A smaller implant that grows within the body would reduce the incision. One particular example is with dermal fillers. If the PVA cryogel is smaller in size during injection and slowly swells within the body, this would allow doctors to use smaller diameter needles and cause less pain to the patient.[53] In this case, the larger the volume increase of the PVA cryogel when placed in an aqueous environment, the more preferred it would be. A minimum volume increase of at least 50% was considered large enough to be useful in this application.

Summary of Acceptance Criteria for Facial Implants

A summary of the range of acceptable values for facial implant characteristics is shown in Table 4.

Table 4: Acceptable Values for Facial Implant Characteristics

Basis	Characteristic	Acceptance Criteria	Reference
Adipose Tissue	Young's Modulus (MPa)	[0.005,0.05]	[44, 45]
Cartilage	Young's Modulus (MPa)	[0.3,2.3]	[43]
	Tensile Strength (Mpa)	≥1.71	[46]
	Elongation (%)	≥30	[47, 48]
	Tear Strength (kN/m)	≥2.0	[48]
Fibrous	Pore Size (μm)	[10,30]	[49-51]
Bone	Pore Size (μm)	[100,700]	[49-51]
Cellular Ingrowth	Porosity (%)	[30,90]	[49-51]
Volume Growth	Swelling (%)	≥50	

Poly(Vinyl) Alcohol Cryogel

Hydrogels are swollen networks of a hydrophilic polymer and water via physical or chemical crosslinking. They exhibit the ability to swell in water and retain a significant fraction of water in its interior structure without dissolving. The appropriateness of poly(vinyl alcohol) (PVA) cryogel hydrogels for various biomedical applications has been recognized because of their excellent biocompatibility, high water content, and chemical stability. It has been examined for use as intervertebral disk nuclei [54], artificial articular cartilage[55], and as a contact lens material [1]. PVA hydrogels have been investigated extensively for articular cartilage applications due to their ability to mimic human tissue [1, 2, 54, 55]. PVA cryogel can be made with a wide range of physical properties to create soft materials made up of 10% wt PVA. Very stiff hydrogels can be made with PVA weight percentage ranges up to 60%.[56]

PVA is soluble in water but it must be crosslinked to form a hydrogel. Crosslinking can be performed through either chemical or physical methods. Chemical techniques include chemical crosslinkers like glutaraldegyde and radiation. A physical crosslinking method of PVA cryogel is to cook with water in an autoclave to create an aqueous solution then thermally crosslink it using the freeze/thaw cycling method.[56, 57] This involves freezing the PVA cryogel in a chilled environment of at least -20°C then bringing it back to room temperature. Both the number of freeze/thaw cycles and the duration of the freezing time influence the mechanical properties of the PVA cryogel.[54] PVA cryogels formed through freeze–thaw cycling offer the additional advantage of being biocompatible as no toxic cross-linkers are required for physical cross-linking to occur.[57]

While PVA cryogel is desirable due to its range of properties that include biocompatibility, elastic softness that can mimic both fat and cartilage, elastic strength, durability within the body, manufacture-able at low cost, and FDA cleared for some medical areas, a main drawback is its lack of adhesion within the body. Due to the lack of pores within PVA cryogel, there may be no attachment of the implant to the surrounding tissues. Using porosity inducing methods, PVA cryogel should be manufactured with pores that will lead to implant integration with the surrounding tissues.

Current Methods for Manufacturing Porosity in Polymers

Cellular ingrowth is imperative in facial implants to help prevent movement and detachment. This is achieved through either creating a porous material or texturing the surface. The field of tissue engineering has been attempting to create porous materials for cellular scaffolds for decades. Scaffolds for cells should have highly interconnected open pore networks for cellular ingrowth and nutrition diffusion, highly biocompatible, mechanical properties similar to the surrounding implantation area, and large and suitable surfaces for cellular attachment and growth.[58, 59] Hydrogels (crosslinked macromolecular networks formed from hydrophilic polymers immersed with water) are typically used when creating scaffolds because of their biocompatibility, similarities with human tissue, and good cellular interaction capabilities.[49, 57]

Solvent Casting/Particulate Leaching

One method of creating pores is through particulate leaching. During this process, the hydrogel is cast over a porogen and solidifies. The material is then placed in a solvent of the porogen in order for the porogen to slowly diffuse out of the hydrogel.[49, 59] After the porogen is dissolved, an open void is left as a porous matrix within the hydrogel. The porogen most often used is sodium chloride because of its low cost, ease of use, and high availability. Other common materials used are paraffin wax, sugar, and gelatin.[60] With this method, porosity can be controlled by the amount of the particle added, while the size of particle dictates the size of the pores. Even the shape dictates the structure with circular porogens creating a more interconnected matrix than cubic ones.[49] Another method to increase interconnectivity is to heat the porogens to where

they ‘sweat’ and start to combine together. This has been proven effective with salt and paraffin wax.[61-63] The areas of the porogens that combine together to create open pores after the particles are removed.

The salt leaching method has been tested extensively with many cell types and has shown no adverse effects on new tissue formation.[64-66] This method does however require the use of organic solvents and the leaching component increases manufacturing time at a rate dependent on the thickness of the molded shape.[59] In addition, some leaching methods include cytotoxic solvents, such as xylene for paraffin wax as well as there is the chance that not all of the porogen dissolves.[49, 67]

Gas Foaming

Conventional gas foaming techniques are commonly used to create porous materials. In this method, N2 or Co2 are generated via a chemical reaction typically involving sodium bicarbonate or ammonium bicarbonate. The inert gas is formed from a reaction and is dispersed throughout the polymer to create the pores.[49, 68, 69] A surfactant is typically used to stabilize the foam while the polymer hardens to preserve these pores. The microstructure created from this process is dependent on the foaming agent concentration, surfactant type and concentration, and the length of time of the solidification process of the polymer.

Keskar et al. [69] used the chemical reaction of citric acid and sodium bicarbonate to create foam within a 15% wt polyethylene glycol diacrylate (PEGDA) solution. Interconnected pores with diameters ranging from 100-600μm were formed from the resulting CO2 from the reaction. Cells then were seeded on the porous scaffold and

cellular ingrowth was seen in the pores after 2 weeks. In addition, this method does not require a solvent and a dissolving period.[49, 70]

Another gas foaming method is supercritical CO2–water emulsion templating. This involves forming a high internal phase emulsion made up of a polymer and CO2 at a high pressure (120-150 bar) in a reaction chamber. After the polymer has solidified from chemical crosslinking, the pressure is released and the CO2 evaporates to leave behind the highly porous material.[49] Surfactants are typically added to maintain the CO2 within the polymer during the solidification stage.[71] This method leaves no residues in the polymer matrix and the product does not require any other purification steps. [72] It leads to a well-defined closed cell porous structure[73] and the use of CO2 is beneficial due to its inexpensive and non-toxic nature.[71]

Porosity percentage is dependent on the value of the CO2 pressure as well as the viscosity of the polymer. The higher the concentration of the polymer, the smaller the pore size.[72] The expected pore size from the gas chamber method ranges from 2-100μm.[74] Cooper et al. [72, 73] performed this technique with low molecular weight 10% PVA hydrogel and the average pore size ranged from 8-15μm.

Composites

Another method used extensively in tissue engineering involves creating a composite hydrogel by combining PVA cryogel with another material. This other material could be either biodegradable or not, but it should encourage fibrinogen and bone growth to help for cellular attachment. Some examples include titanium fiber mesh[75] and poly(vinyl pyrrolidone)[76]. While composites made with nonabsorbable

materials are used to enhance the mechanical properties of PVA cryogel, mixing with biodegradable materials may provide a porous matrix for cellular ingrowth as the material is absorbed by the body.[77] Two notable examples are hydroxyapatite and chitosan.[70, 77-80]

Hydroxyapatite (HA) ($Ca_{10}(PO_4)_5(OH)_2$) is a major inorganic component (about 60% wt) of bone and teeth.[67] Because of its ability to encourage bone attachment, differentiation, and proliferation, it is used to coat implants such as hip replacements and dental implants as well as implanted on its own.[81] Its absorption rate in the body is slow and can take months or even years.[67] PVA cryogel/HA composites in *in vivo* studies have been proven to be biocompatible and they encourage osteoid tissue growth (the precursor to bone tissue) within two weeks of implantation.[70, 77] The HA particles within the composites ranged from 0.07-5μm.[81]

Chitosan (CS) ($(C_6H_{11}NO_4)_n$) is a polysaccharide derived from chitin. It is an extremely favorable material in the biomedical field because of its biocompatibility, biodegradability, and bioactivity, however its brittle nature has limited its usage.[78, 82] The biological effects of PVA cryogel/CS composites have been studied both *in vitro* and *in vivo*. Nontoxicity has been proven and cellular proliferation is seen within 2 weeks.[80, 82] In a 3 month *in vivo* rabbit implantation study, bone cells had grown and proliferated throughout the small implanted composite within the cartilage.

Creating a composite material of PVA cryogel with HA or CS could encourage cellular growth into the implant as well as slowly give a porous matrix for ingrowth as the material is absorbed by the body.[77]

Summary

Implants for facial augmentation provide a structural framework, minimize defects, and bring the area to an pleasing anesthetic look. A facial implant's material must be biocompatible, easily shapeable, prevent migration, and possess similar mechanical properties to the surrounding tissue. Current materials on the market, however, have many issues associated with them. Cartilage replacements have a range of problems that include displacement and ejection to an unnatural feel within the body. Most dermal fillers are only temporary while those that are permanent can lead to disfigurement if they become infected or rejected. Poly(vinyl) alcohol cyrogel is a permanent biocompatible hydrogel that can be made in a range of mechanical properties similar to tissues within the body. A potential drawback is its lack of fibrous attachment. Adhesion may be achieved with the incorporation of pores through pore forming techniques and changing the surface texture. Further, an implant that could be inserted through a small incision that swells in situ would have insertion advantages. In this thesis, porous PVA cryogel was created and its mechanical, pore, and swelling characteristics were measured to determine its feasibility for facial implants.

CHAPTER 2

MATERIALS AND METHODS

Experimental Design

Due to issues of current biomaterials, poly(vinyl) alcohol cryogel has arisen as a promising replacement for facial implants. Its many positive traits include its biocompatibility, ability to be manufactured with a range of mechanical properties similar to biological tissues, and resistance to degradation within the body. The implant may be subject to movement and migration. Pores may encourage adhesion. Porosity inducing techniques were applied to PVA cryogel to help combat this issue.

A range of experiments were designed to manufacture porous PVA cryogel and to determine its mechanical and porous characteristics. These properties include elasticity, tensile strength, elongation percentage, tear strength, pore size, and porosity percentage. The mechanical tests were performed on the samples in tension and are adapted from the standards ASTM D412[83] and ASTM D624[84]. The pore characteristics were determined from sectioned sample images and analyzed through programs such as Matlab and Image J. To determine PVA cryogel's ability of swelling, nonporous PVA cryogel was dried then placed in water to measuring the increase in size. Molds were created as well to help visualize the shape of the porous samples as facial implants.

General Method of Manufacturing Poly(Vinyl) Alcohol

Poly(vinyl alcohol) (PVA cryogel) is made by dissolving its granular form in water, pouring the solution into a mold, then putting it through multiple freezing and thawing cycles. The hydrogel forms to the exact shape of the mold.

Granular PVA was obtained from Sigma (Milwaukee, WI) (catalog number 363065) with an average molecular weight of 124,000-186,000 and 99+% hydrolyzed. It is mixed with deionized water, the container is capped, and it is cooked in the autoclave at 255°C for 30 minutes to dissolve the PVA in water. For a 10% weight solution of PVA cryogel, 11.111g of PVA is used for every 100mL of deionized water. To obtain 30% weight PVA cryogel, 42.853g of PVA is used for every 100mL of deionized water.

Once removed from the autoclave, the viscous PVA cryogel solution is poured into a mold of the desired shape of the PVA cryogel. This can be done by either pouring the PVA cryogel directly into the mold or when constricted with smaller insertion areas, poured into a 20mL syringe then injected into the mold. The injection method can be used for a solution up to 25% weight PVA cryogel. Greater weight percentages are too viscous to easily press through. Multiple shaped molds were used for prototyping and mechanical testing. These include molds to create chin and nose shapes, extruded cylinders, and shapes required for mechanical testing.

The hydrogel becomes solid by thermal crosslinking through a freeze/thaw cycle process. Once secured within the mold, PVA cryogel is placed within a freezer of at least -20°C to begin the freezing process. When the specimen is frozen (about 4 hours), it turns from clear to white in color. The mold is then removed from the freezer and placed at room temperature to begin the thawing process. When the specimen warms up to room

temperature (2 hours), a full freeze/thaw cycle has been completed and it is placed back into the freezer to begin the next cycle. All specimens underwent 6 freeze/thaw cycles during the course of this project.

Manufacturing the Molds

Chin and Nose

Shapes for the chin and nasal implant were designed using SolidWorks® V2013 CAD software (Dassault Systèmes Solidworks Corporation, Waltham, MA). To obtain accurate sizes, dimensions were pulled from current products on the market shown in Figure 4.

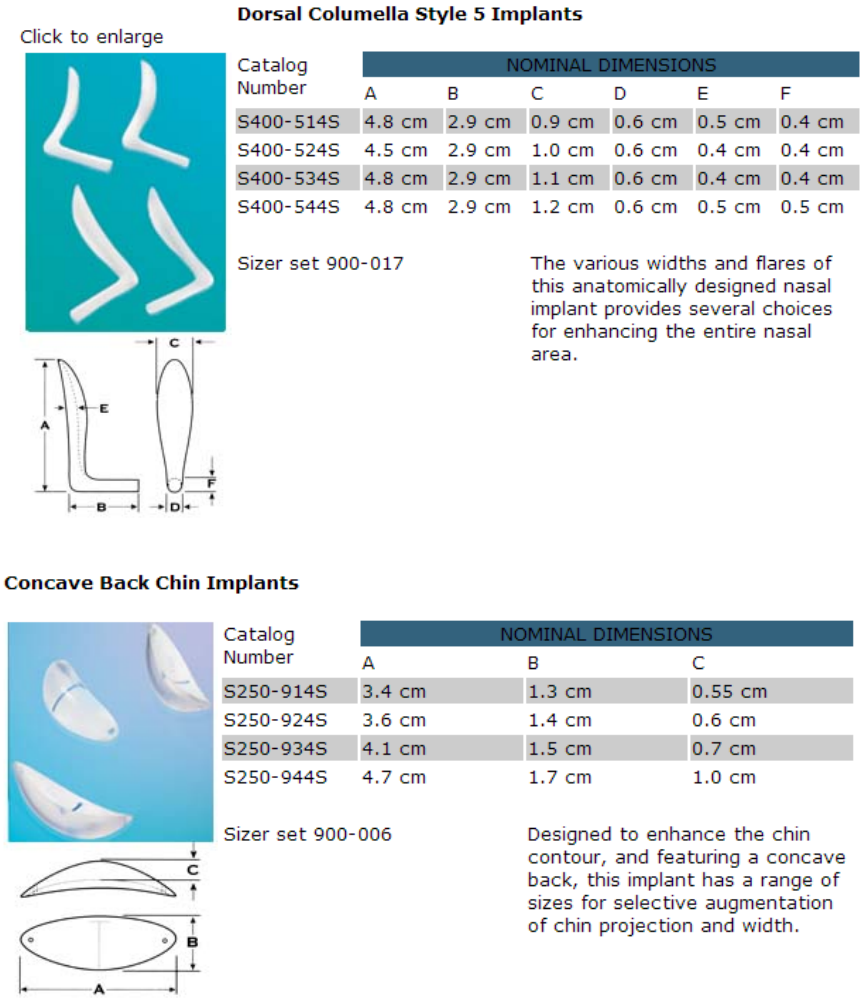

Dorsal Columella Style 5 Implants

Click to enlarge

Catalog Number	NOMINAL DIMENSIONS					
	A	B	C	D	E	F
S400-514S	4.8 cm	2.9 cm	0.9 cm	0.6 cm	0.5 cm	0.4 cm
S400-524S	4.5 cm	2.9 cm	1.0 cm	0.6 cm	0.4 cm	0.4 cm
S400-534S	4.8 cm	2.9 cm	1.1 cm	0.6 cm	0.4 cm	0.4 cm
S400-544S	4.8 cm	2.9 cm	1.2 cm	0.6 cm	0.5 cm	0.5 cm

Sizer set 900-017

The various widths and flares of this anatomically designed nasal implant provides several choices for enhancing the entire nasal area.

Concave Back Chin Implants

Catalog Number	NOMINAL DIMENSIONS		
	A	B	C
S250-914S	3.4 cm	1.3 cm	0.55 cm
S250-924S	3.6 cm	1.4 cm	0.6 cm
S250-934S	4.1 cm	1.5 cm	0.7 cm
S250-944S	4.7 cm	1.7 cm	1.0 cm

Sizer set 900-006

Designed to enhance the chin contour, and featuring a concave back, this implant has a range of sizes for selective augmentation of chin projection and width.

Figure 4: Images and Dimensions of Silicone Facial Implants

Reference: Spectrum Design Medical [85]

From these dimensions found online, nasal and chin implants were designed in Solidworks. The nose is in the shape of an 'L' with dimensions 1.1cm width x 3.3cm length x 4.80cm height and shown in Figure 5. The chin is in the shape of a half-moon with dimensions 1.40cm width x 3.98cm length x 0.65cm height. Details of the designed chin and nasal implant can be seen in Figure 6.

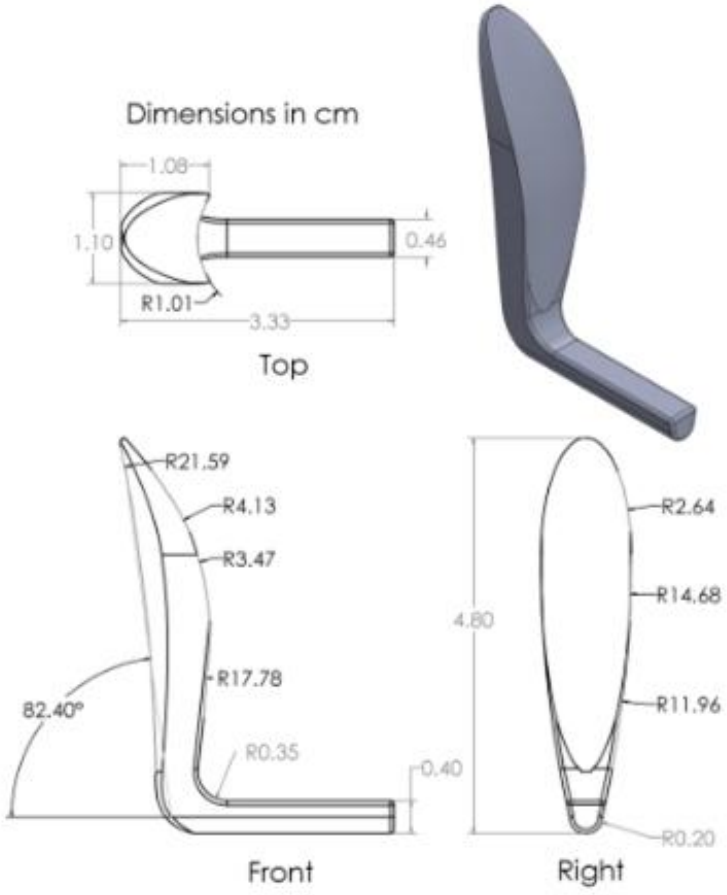

Figure 5: Design of the Nasal Implant

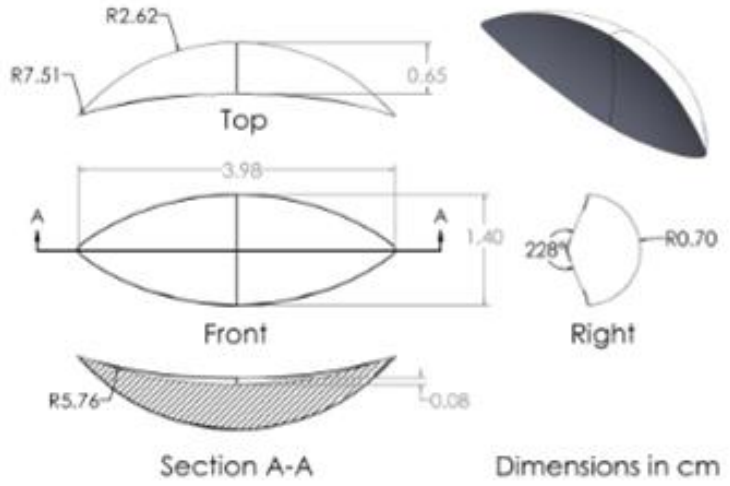

Figure 6: Design of the Chin Implant

Molds were created from the CAD of the implants. The two-part molds are held together with screws that run its length. The parting lines follow the main edge of the implants. This was done to minimize flash from the manufacturing process as well as make it easier to cut the implant away after it is removed from the mold. During early prototyping stages, molds for these implants were created through additive manufacturing using the 3D printer Dimension (Stratasys, Eden Prairie, Minnesota). While inexpensive and quick to produce, these molds gave a rough surface to the implants. The layers of the mold were evident on the implant and gave it a rough appearance. An example of these molds are shown in Figure 7. When a final design was chosen, aluminum molds for the chin and nose were manufactured by the Georgia Tech Machine Shop. The implants used in these molds have a much smoother surface, which are shown in Figure 8.

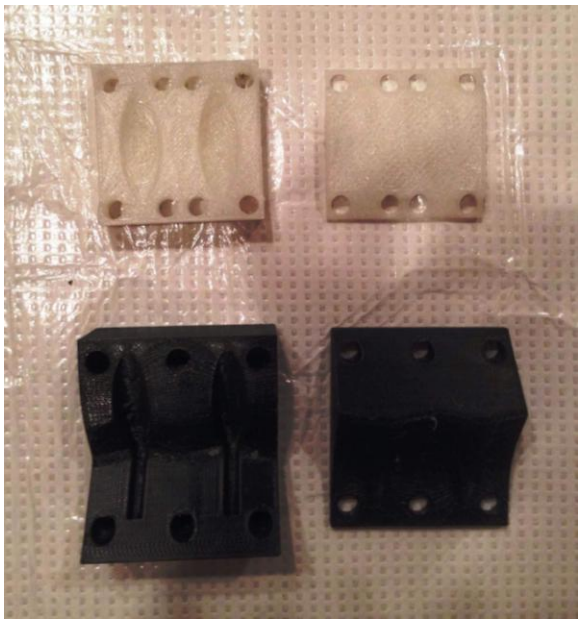

Figure 7: 3D Printed Molds for Chin and Nasal Implant

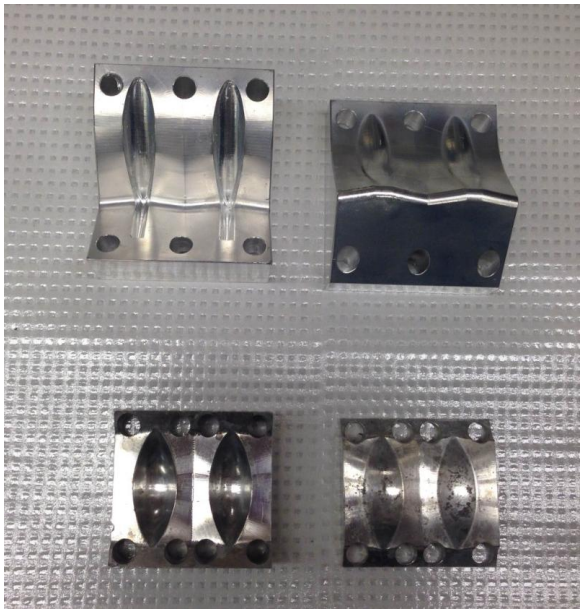

Figure 8: Aluminum Molds of for Chin and Nasal Implant

Extruded Cylinders

The extruded cylinder implants are created using Tygon® tubing (Saint-Gobain S.A, Paris) of a length of 25cm. The 3mm diameter tubing is injected and filled with PVA cryogel pushed from a 10cc syringe. To prevent the PVA cryogel from spilling out of the tubing, the tubes are orientated in a 'U' shape within a bowl with the edges of the tubing pointing upward. This is shown in Figure 9. After the completion of the first freeze/thaw cycle, the mold is removed from the bowl and straightened. At this point the PVA cryogel has solidified enough that it will not run out of the mold, and straightening the tubes will help prevent the PVA cryogel from curving. Once 6 freeze/thaw cycles are completed, the PVA cryogel is removed from the tubing by pressing down on one side of the tube and it slips out the other end. The PVA cryogel 'noodle' can then be segmented with scissors to create whichever length of cylinder is required. An image of the noodle implant is shown in Figure 10.

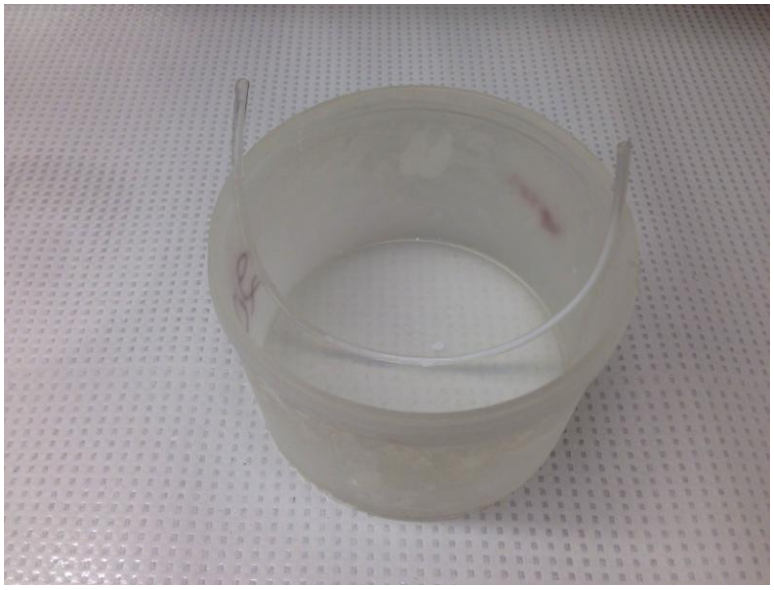

Figure 9: Mold Setup for Extruded Cylinders

Figure 10: Image of Extruded Cylinders

Molds for Mechanical Testing Samples

Two mold shapes were created for the purpose of mechanical testing. Their shape and dimensions are in accordance with ASTM D412[83] and ASTM D624[84]. ASTM D412 calls for "dog bone" shaped molds to determine tensile strength, elongation, and elasticity. ASTM D624 requires a "zig-zag" shape to complete tear strength tests.

Acrylic sheets purchased from McMaster Carr (Atlanta, GA) were used to manufacture these molds. Each mold was comprised of one 2mm thick sheet sandwiched between two 13mm thick sheets. The shape of the samples was designed in SolidWorks (shown in Figure 11) then cut into the thin middle sheet using the Trotec Speedy 300 laser cutter (Trotec, Wels, Austria). The thin newly cut piece was then super glued using Professional Liquid Super Glue (Loctite; Düsseldorf, Germany) to one of the thicker sheets. This gave a sunken mold that the PVA cryogel could easily be poured into. The molds are pictured in Figure 12. The other thick sheet of acrylic is used to cover the PVA cryogel after it has been poured into the mold. Because this mold is flatter and wider than the chin and nasal molds, clamps are used instead of screws to secure the mold. The parting line for this mold also runs along the edge of the shape which reduces flash and makes it easy to remove.

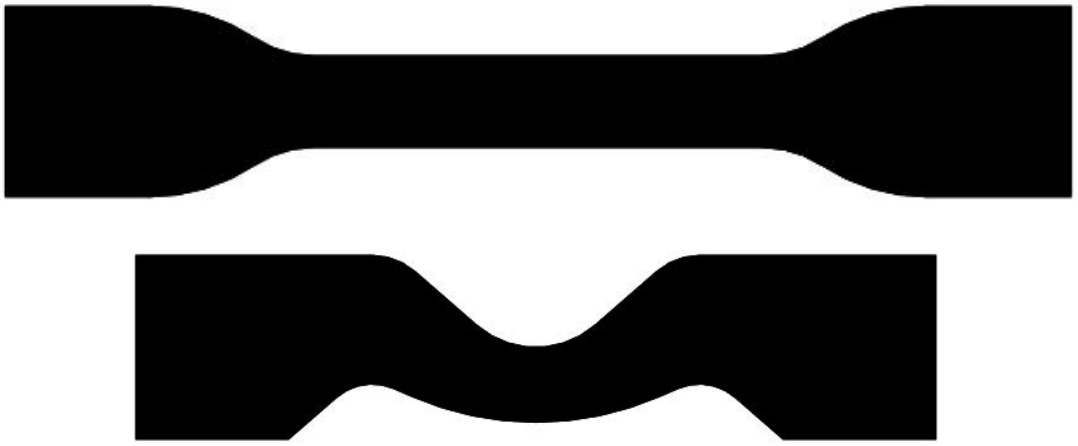

Figure 11: Mechanical Testing Shapes

Created in Solidworks A) dog bone shape from ASTM D412 B) zigzag shape from ASTM D624

Figure 12: Acrylic Molds Used to Create Samples for Tensile Tests

Overview of Tests

Tensile Strength, Elongation Percentage, and Elasticity

Samples of PVA cryogel were tested in accordance with ASTM D412 [83] to determine tensile strength, elongation percentage, and elasticity. This protocol published by the American Society for Testing and Materials is meant to evaluate the tensile properties of vulcanized thermoset rubbers and thermoplastic elastomers. This standard is listed in ASTM F881 (Standard Specification for Silicone Elastomer Facial Implants) as a recommended test for silicone intended for facial implants. ASTM F881 [42] is a standard noted by the FDA in the Guidance Documents for facial implants in product categories FWP, FZE, and MIB.[6]

The PVA cryogel test strips were manufactured by using the 'dog bone' acrylic mold described earlier. After the PVA cryogel was removed from the autoclave, it was poured into the slots of the mold and a 13mm thick sheet of acrylic was pressed down on top. The sheets were then compressed between two large clamps and the mold underwent 6 freeze/thaw cycles. After the PVA cryogel was removed from the mold, each 'dog bone' sample was examined and any with imperfections were discarded.

The machine used for testing was the DDL 650 (Distribution Dynamics Labs, Minnesota). It is equipped with software-driven computerized controls and automated data collection. Wedged jaw clamps were used to hold the specimen in place. The surface of the clamps was rough to prevent slippage of the PVA cryogel during the test. The 'dog bone' specimen was placed within the grips of the machine with care to make sure the specimen was aligned as straight as possible. The clamps were spread

approximately 70mm before the start of the test with zero load applied. The exact clamp distance as well as the specimen's thickness and width were noted, and the force and distance measurements were zeroed before the test began.

The test was conducted by the upper clamp moving away from the lower clamp of a rate of grip separation of 500mm/min (20in/min). Pictures of the process over time can be seen in Figure 13. Using a sensor built into the machine, data were collected for the force (in pounds) and change in position (in inches). Data collection began when the pulling force exceeded 0.1lb. The specimen was stretched until rupture and the data were saved.

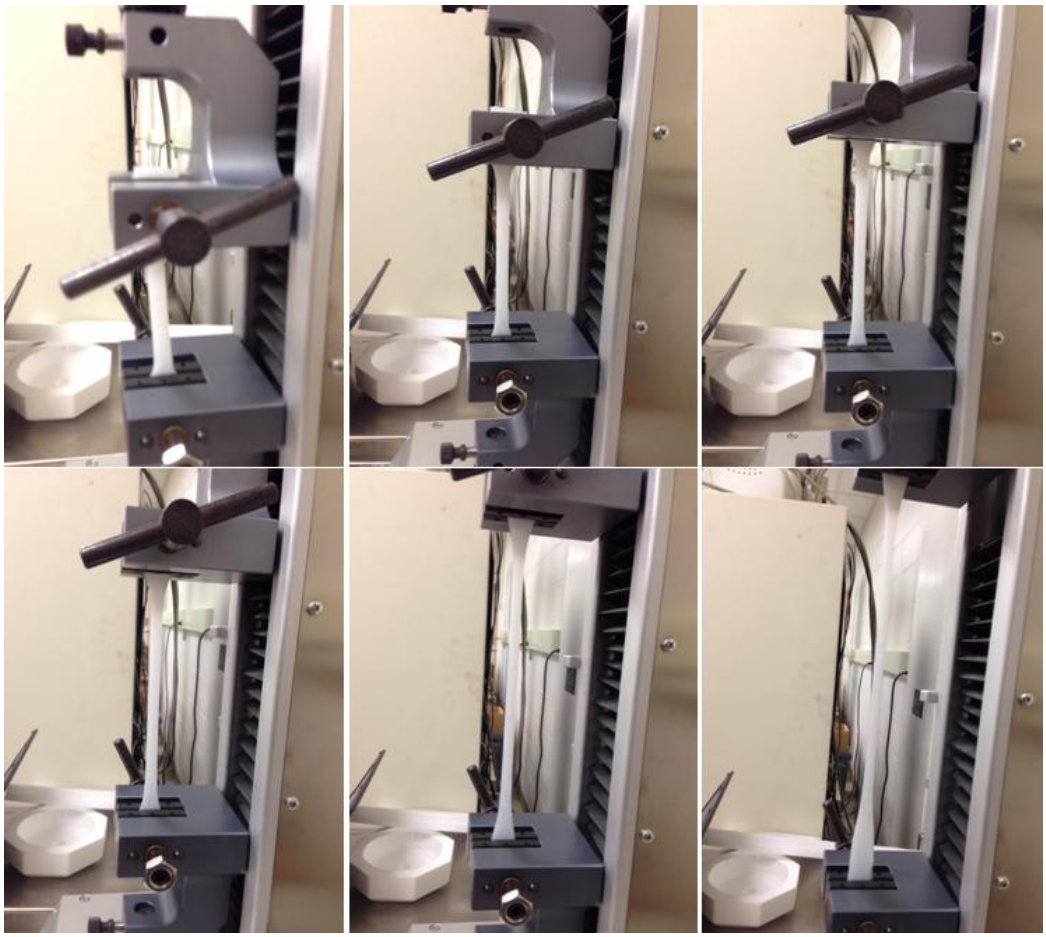

Figure 13: Tensile Test Over Time

Tear Strength

Samples of PVA cryogel were tested in accordance with ASTM D624 [83] to determine tear strength. This protocol published by the American Society for Testing and Materials is meant to evaluate the tear strength of conventional vulcanized thermoset rubbers and thermoplastic elastomers. As with ASTM D412, this standard is listed in ASTM F881 as a requirement for facial silicone implants.

The PVA cryogel test strips were manufactured by using the created 'zig-zag' shape acrylic mold. Similar to the 'dog bone' samples, the PVA cryogel was removed from the autoclave, poured into the opening slots of the mold, and a 13mm thick sheet of acrylic was pressed down on top. The sheets were then compressed between two large clamps and the mold underwent 6 freeze/thaw cycles. After the PVA cryogel was removed from the mold, each specimen was examined and any with imperfections were discarded. A scalpel was used to create a 1mm long nick in the middle of each specimen as described by the standard.

The machine used for testing and the testing procedure was the same one used for the tensile testing. The thickness of the specimen was noted, and the machine collected the force (in pounds) and change in position (in inches) when the pulling force exceeded 0.1lb. The test ended when the specimen split in half. All specimens were monitored to make sure the tear fell along the line of the administered nick. If not, then the sample was not recorded.

Pore Characteristics

The device used to section the specimens was the Leica CM3050 S Cryostat (Leica; Wetzlar, Germany). It was found that the PVA cryogel sectioned most easily when frozen. An attempt to section it was made on a microtome, however the PVA cryogel shriveled in the warm paraffin wax embedment and fell out of its wax casing during the sectioning process. The warm PVA cryogel also did not cut easily or cleanly.

After the PVA cryogel had undergone its 6 freeze/thaw cycles and was removed from the mold, it was cut into a 0.5 cm cube. This cube was placed inside a plastic 1.0 cm cube container and the remainder of the cube was filled with Tissue-Tek O.C.T. Compound (Sakura Finetek; Torrance, California). Embedding the PVA cryogel allowed it to be easily sectioned later. To remove any excess bubbles and to ensure the OTC compound fully penetrated the pores of the PVA cryogel, the plastic container was placed inside a vacuum chamber and the air was removed until the pressure reached -25 atm.. The specimen was left in the chamber until all bubbles had been removed from the OTC compound liquid. This process took about 20 minutes. Afterwards, the specimen was placed in a freezer at -20°C and remained there until both the OTC compound fluid and the PVA cryogel fully froze (about 30 minutes).

The temperature of the sectioning area of the cryostat was set to -25°C. Once the PVA cryogel and OTC compound had frozen and solidified, then were removed from the plastic container and attached to the sectioning pad. Once this pad was attached to the cryostat, the specimen was sectioned into samples 20μm thick and placed onto microscope slides.

The Nikon Eclipse E600 microscope (Nikon; Tokyo, Japan) was used to view and take pictures of the samples. The images were taken at 4X magnification.

Pore Size

Public domain image processing program Image J® (National Institutes of Health; Bethesda, Maryland) was used to determine pore sizes within the porous PVA cryogel samples. This was done through the Measuring Tool within the program. Pores were identified as the empty void areas within the PVA cryogel with dark perimeters. At least 20 pores were measured within each image to determine the pore size range. An example of this process is shown in Figure 14. Lines were drawn across the length of the pores and the diameter length was calculated as a ratio to the scale bar in the bottom right corner. The mean pore size was also calculated through this program. A example of the summary of the measurements is shown underneath the measurements in Figure 14.

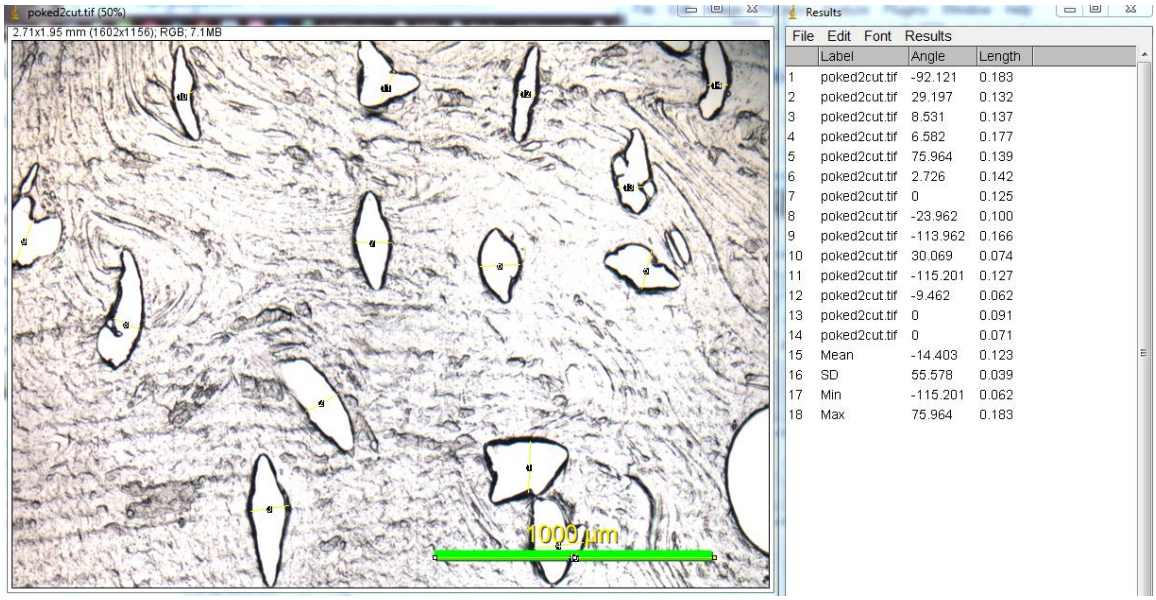

Figure 14: Example of Measuring Pore Size

Porosity Percentage

The porosity percentage of the manufactured porous PVA cryogel was also obtained using images of the sectioned samples. Samples were sectioned at multiple depths as well as images were taken in multiple areas of each picture. At least 5 samples were used for each type of porous PVA cryogel. These images then were analyzed through Matlab® (Natick, Massachusetts). A simplified version of the code is presented below. To summarize, images were opened and converted into 2-tone black and white images. The threshold was chosen to be high enough such that the grey PVA cryogel would be converted to black in the image while the white background (the open pore part of the sample) would remain white. Each white pixel then was assigned a value of 1 while each black pixel became 0. Summing the pixel values of the image gave the number of white pixels within the image. The size of the image was determined by multiplying its length and width together. The number of white pixels over the total number of pixels in the image gave the percent of the image that was white or the percent porosity.

```
I = imread('image.png'); % Opens the image
BW = im2bw(I,.9999); % Creates black/white two tone image
[x,y]=size(BW); % Calculates image pixel width and height
total_pixles = x*y; % Calculates number of pixels in image
white_pixles = sum(BW(:)); % Finds number of white pixels
                           % in image
porosity = (white_pixles ./ total_pixles); % Finds
                      %percentage of white space in image
```

This code was used for all images except those using CaPO4. Unlike the others, the black part of these images is the porosity. The Matlab code below shows that it was calculated by finding the difference of 1 and the white space.

```
porosity = 1 - (white_pixles ./ total_pixles); % Finds percentage
                                               %of black space in image
```

Swelling Ratio

The swelling ratio test was performed on nonporous 10, 20, and 30% wt PVA cryogel. Five samples were used for each group.

After the specimen has completed its 6 freeze/thaw cycles, it was removed from the mold and placed in an open air space. This was done to dry out the sample. The specimen dehydrated over the next week. To determine if all the water had be removed from the specimen, its weight was measured every two days. When the specimen's weight did not change between weighings, it was deemed to no longer have any water in its composition. The weight of the sample was noted.

The sample was then placed in deionized water for a week to allow it to swell. Again, its weight was monitored until there was no change. At this point the specimen was deemed to be fully swelled. The weight was noted again. From the weight and density, the volume of the specimen was calculated. The calculated volume increase, or the swelling percent increase, is the change in volume from the dehydrated to saturated PVA cryogel. It was calculated as

$$Volume\ Increase\ Percentage = \frac{(V_S - V_D)}{V_D} * 100$$

Where V_S is the volume of the saturated PVA cryogel and V_D is the volume of the dehydrated PVA cryogel.

Density was calculated for each sample in both hydrated and dehydrated states. A large sample of each specific weight PVA cryogel (plain 10, 20, and 30%) was dehydrated in open air. When all the water was removed, the specimen was weighed

then placed in a graduated cylinder filled with water. The increase of the water level was taken as the volume of the specimen. The weight of the specimen over the volume was determined to be the density. Weight and volume were measured again after the specimen was saturated with water to determine the density at that state as well. Knowing the density of each sample type allowed for only the measurement of weight of each individual sample. The volume of the sample was then calculated by dividing the weight by the density.

Manufacturing Porous Poly(Vinyl) Alcohol Cryogel

PVA cryogel was subjected to multiple porosity inducing techniques in the effort to make pores. Samples that did not undergo these methods and remained completely solid are considered 'plain' PVA cryogel.

Solvent Casting/Particulate Leaching

The salt was prepared for this method by first shifting it through sieves to have a set range of pore diameter of 100-600µm. The sieves were purchased from McMaster Carr (Atlanta, GA) and were certified by the manufacturer to meet all standards required by ASTM E11 (Standard Specification for Woven Wire Test Sieve Cloth and Test Sieves). The width openings of the sieves were 100 and 600µm.

Once selected according to size, the salt particles were poured in 100mL syringes and then subjected to 95% humidity at 50°C for 24 hours. This method was adapted from Murphy et al. [61] Salt crystals are cubic in shape and are not as effective as spherical shapes when trying to create an open pore structure.[49] An example of two salt crystals interacting together is shown in Part A of Figure 15. The incubation of the salt in humidity for 24 hours causes the salt to ‘sweat’ and partially fuse together, as shown in Part B of Figure 15. The salts bridge together to allow for an open cellular matrix as well as the edges of the crystals become more curved. When the salt is removed after 24 hours, it has become a connected skeletal-like structure to create a porous open cellular matrix.

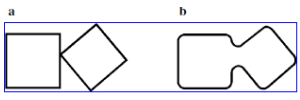

Figure 15: Salt Crystals

PVA cryogel from the autoclave is poured directly into the syringes that hold the cooked salt. The plunger part of the syringe is then pressed down and the pressure created forces the PVA cryogel into the salt matrix. Once the PVA cryogel had been forced as deep as possible (1cm for 10% wt PVA cryogel, 2mm for 20% wt PVA cryogel), the mixture was removed from the syringe and placed in the desired mold. It then underwent the necessary 6 freeze/thaw cycles.

The final step is to remove the porogens from the PVA cryogel to reveal the porous matrix. The salt particles were leached out over time by placing the specimen in deionized water. This solvent was refreshed every 4 hours until all the salt was removed. The time for this process is dependent on the size of the molded part and the depth of the porogen pressed within the PVA cryogel. The salt was leached out of the samples for these experiments within 4-5 days. The samples were felt by hand to determine if the salt had been removed. This involved squeezing the sample and feeling for any hard granular substance within the softer porous PVA cryogel. Once no more salt could be felt the sample was soaked for another 2 days.

This technique was attempted with a wide range of concentrations of PVA cryogel, however it was determined that concentrations above 20% are too solidified to enter the salt matrix when the salt's diameter is between 100 and 600μm. A larger porogen diameter would leave larger gaps between particles and allow higher concentrations of PVA cryogel to be utilized.

Paraffin wax was also attempted as a porogen. While it is dissolvable in xylene and can be heat treated (between 35 and 45°C) to bridge the particles together to help create an interconnected matrix, wax easily melts and deforms when exposed to

temperatures over 58°C. PVA cryogel would have to be cooled to below this temperature threshold after removal from the autoclave for use, and at temperatures this low PVA cryogel starts to harden and becomes almost impossible to press into the wax matrix. Ma et al. [62] utilized paraffin wax to create porous PVA cryogel, however the PVA cryogel concentration used was only 0.5%. While at this concentration the PVA cryogel solution can be cooled low enough to still be fluid, concentrations this low are not suitable for the implants currently under consideration which require a range of 10-30% weight PVA cryogel.

Gas Forming Method

Sodium bicarbonate ($NaHCO_3$) (Sigma, St. Louis) was chosen as the foaming agent because of its low cost, accessibility, and biocompatibility. It was combined with citric acid ($C_6H_8O_7$) (Sigma, St. Louis) according to the methods described by Kabiri et al.[68] The exothermic reaction of sodium bicarbonate and citric acid in the presence of water creates the products trisodium citrate ($Na_3C_6H_5O_7$), carbon dioxide, and water. This equation in shown in the equation below.

$$3NaHCCO_3 + C_6H_80_7 \rightarrow Na_3C_6H_5O_7(aq) + 3CO_2(g) + 3H_2O(l)$$

Trisodium citrate is used as an anticoagulate in the medical field and is a common food preservative.

This method begins right after PVA cryogel is removed from the autoclave. 20% wt PVA cryogel (25g PVA cryogel, 100mL of deionized water) was used in all data collecting experiments. 10, 20, and 30% wt PVA cryogel were originally tested with this method. It was observed that 10% wt PVA cryogel did not contain enough PVA cryogel

to maintain the porous structure through the first freezing process while 30% did not contain enough free water to fully activate the chemical reaction. The PVA cryogel is poured into a 1L beaker that holds a mixture of 6.0g sodium bicarbonate and 4.574g citric acid. The chemical reaction begins as soon as the PVA cryogel solution touches the chemical mixture. The solution was stirred vigorously for 1 minute with a stirring utensil. From this, a frothy white column of foam forms within the beaker. The volume of the foam fills up two thirds of the 1L beaker.

While some of the gas foaming procedures in the literature used surfactants to help stabilize and maintain the porous matrix, it was decided that surfactants would not be used in this experiment. Liquid Dove soap (Unilever; Rotterdam, Netherlands) was tested as a surfactant for this procedure because it is inexpensive, widely available, and is composed of surfactants sodium lauroyl isethionate, lauryl alcohol, tallow acid and palmitic acid. Dove soap, however, was determined to have no effect on maintaining the porous matrix and left the PVA cryogel sticky and soapy. Freezing time was determined as a factor in keeping the pores intact. The sooner the PVA cryogel was frozen, the less bubbles popped and CO_2 escaped from the foam. For the conventional gas method then, the PVA cryogel's first freeze was at -80°C instead of -20°C to quicken the freezing process. The molds were also prefrozen to help chill the PVA cryogel mixture as fast as possible.

Dry ice was used as the freezing agent to create an environment of -80°C. It was placed into a thermally insulated cooler along with the intended mold. Once the PVA cryogel was mixed and the column of foam appeared in the beaker, the foam was removed, spooned into the mold, and quickly placed with the dry ice. After an initial

freezing time of 1 hour, the mold was removed and thawed to room temperature. This marked the end of the first freeze/thaw cycle. The remaining 5 freeze/thaw cycles were performed as usual.

It should be noted that conventional gas formation was the only gas forming method attempted. C/W emulsion was considered, but the lab lacked the required laboratory equipment such as a high pressure reaction vessel. This made performing this type of test unfeasible. When looking at the literature, no studies were found that used this method that produced pores larger than 15μm.[71, 74] In addition, this method creates closed cell hydrogels which do not allow cellular ingrowth and adhesion.[86]

PVA Cryogel Composites

Methods to create composite materials of PVA cryogel and biodegradable polymers were also examined. Because of the plethora of literature available, chitosan (CS) and hydroxyapatite (HA) were chosen for experimentation. HA, however, is difficult to find and a very expensive compound. Manufacturing it proved to be a difficult and costly task. It was decided to replace HA with a similar compound for these experiments: calcium phosphate ($CaPO_4$).

Multiple methods to combine chitosan with PVA cryogel were given in the literature including chemical crosslinking[80] and cooking together at low temperatures.[82] Chemical crosslinking introduces extra, sometimes toxic chemicals into the implant as well as reduces the rate of absorption of the CS. While PVA cryogel at lower molecular weights can be cooked at temperatures 80°C and under, the PVA cryogel used in these experiments required a high temperature and pressure to dissolve in

the water. CS percentages of 2.0% and 4.0% were chosen to be added to the PVA cryogel mixture. This weight percent is similar to that used in the literature[78, 80, 87] as well as it felt to have a similar strength to plain 30% PVA cryogel in comparison to other CS weight percents. At 5% and greater the composite started to become brittle. 2.0g and 4.0g of CS were each combined with 42.583g PVA cryogel and 100mL of water in the autoclave at 255°C for 30 minutes. They were placed into molds and underwent 6 freeze/thaw cycles like normal.

Like CS, calcium phosphate also was mixed with PVA cryogel and cooked in the autoclave. Mixtures of 5.0g and 10.0g $CaPO_4$ were used with 100mL of saline and 30% weight PVA cryogel. Additions of 5% and 10% $CaPO_4$ were chosen because these values are equivalent to what is seen in the literature for HA[77].

While these materials would be implanted as composites, the CS and $CaPO_4$ molecules need to be leached out of the PVA cryogel to determine the pore size and porosity the material will have after the body absorbs the CS and $CaPO_4$ and leaves an open matrix.

Molded Surface

Another method to create porous PVA cryogel is to have the mold designed to create the pores. This method requires no extra chemicals or steps. The surface of the mold is textured in a way that will reflect in the surface of the mold; ideally to encourage cellular ingrowth. This can be done by having extrusions on the surface of the mold. The PVA cryogel will form around these extrusions which will lead to void space in the implant's area after the mold is removed. This idea is especially appealing when the

implant would only require a slight attachment on the surface to prevent slippage and migration.

A few types of surface textures were considered such as extruded cylinders and domes, but the one selected for testing is similar in shape to a light bulb. An image of the proposed structure is shown in Figure 16. This shape is appealing because it increases in area as it is farther from the surface of the mold which will lead the area of the holes in the implant it increase with its depth from the surface. The cells can expand in this area which can allow better anchorage of the implant to the surrounding tissue.

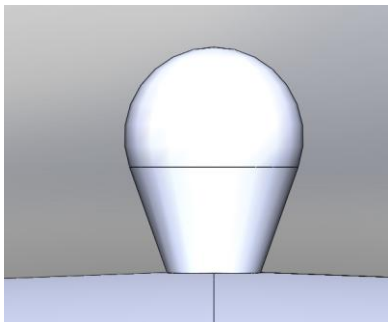

Figure 16: Image of Proposed Light Bulb Shape

A chin mold was designed and attempted to be 3D printed with this surface area, however the details were too fine. With extrusions of diameters 300-500μm and heights 1mm, the 3D printer's tolerance levels were too large. The extrusions formed together into one mass. It was then realized that this shape is equivalent to that found on Velcro. The idea was conceived by lab mate Max Nguemeni. 3M Dual Lock brand Velcro (3M, Minnesota) was used in all experiments. An image of the Velcro used is pictured in Figure 17. The Velcro was glued to some of the manufactured molds, such as the chin mold, to be used in experiments. The Velcro was used on only one side of the molds, including the samples used for the mechanical testing. During manufacturing, the PVA

cryogel was just pressed into the Velcro surfaced mold and underwent the 6 freeze/thaw cycles like normal.

Figure 17: Velcro Used to Mold Pores in PVA cryogel

Removing Material

The final method that was undertaken was to remove sections of the PVA cryogel after it had undergone its freeze/thaw cycles. Like the method using Velcro for the mold's surface, this requires no extra chemicals, porogens, and solvents. It does, however, require the extra step of removing the PVA cryogel after it has solidified.

The method used to remove the PVA cryogel is to press a stainless steel needle through the PVA cryogel. An example is shown in Figure 18. The needle used in all experiments was 10cm in length and had a diameter of 0.6mm. Once pressed through, the needle leaves an extruded hole within the implant that the cell can grow into. While this method was performed by hand in these experiments, it could be easily automated. The samples were skewered at least one hundred times each before testing.

Figure 18: Method to Create Poked Holes in PVA

CHAPTER 3

RESULTS

The test materials were measured for mechanical properties, porosity and swelling. Certain combinations provided appropriate mechanical, porosity, and swelling for use as facial implants.

Images of Porous PVA Cryogel Samples

The PVA cryogel samples were molded in the chin molds and are presented in the figures below.

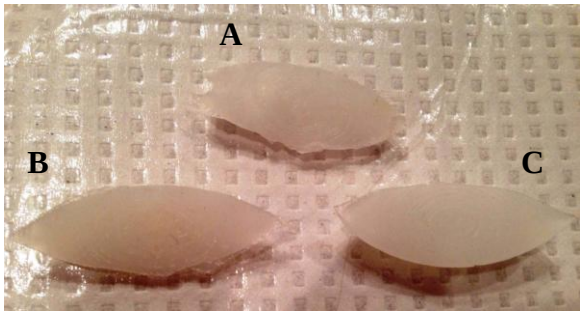

Figure 19: Plain PVA cryogel

A) 10% wt PVA cryogel B) 20% wt PVA cryogel C) 30% wt PVA cryogel

Figure 20: 30% wt PVA Poked with Needle

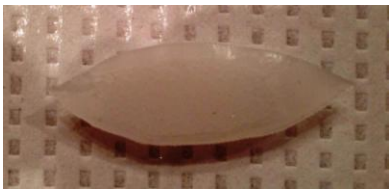

Figure 21: 30% wt PVA Molded over Velcro

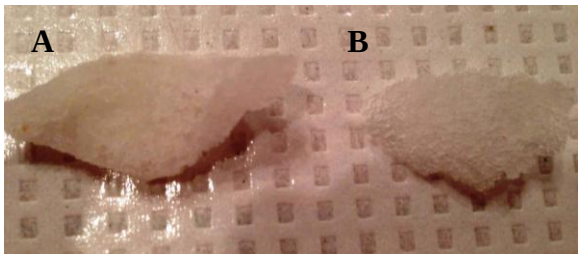

Figure 22: Porous PVA Cryogel Created through Solvent Casting/Particulate Leaching Method

A) 10% wt PVA cryogel B) 20% wt PVA cryogel

Figure 23: Porous PVA Cryogel Created through Gas Method with 20% wt PVA cryogel

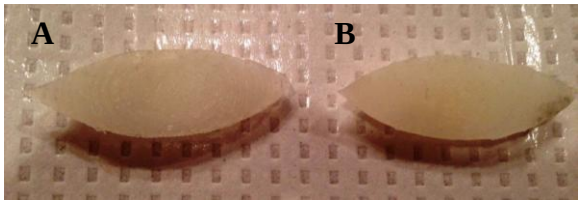

Figure 24: PVA/Chitosan Composite

Made with 30% wt PVA cryogel A) 2% wt Chitosan B) 4% wt Chitosan

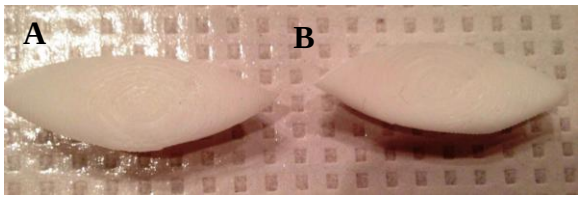

Figure 25: PVA/CaPO4 Composite

Made with 30% wt PVA cryogel A) 2% wt CaPO4 B) 4% wt CaPO4

Tensile Strength, Elongation, and Elasticity

Samples of 10%, 20%, and 30% wt PVA cryogel and all porous PVA cryogel samples were tested in tension (n>=3). A representative force elongation curve for a 30% PVA cryogel material is shown in Figure 26.

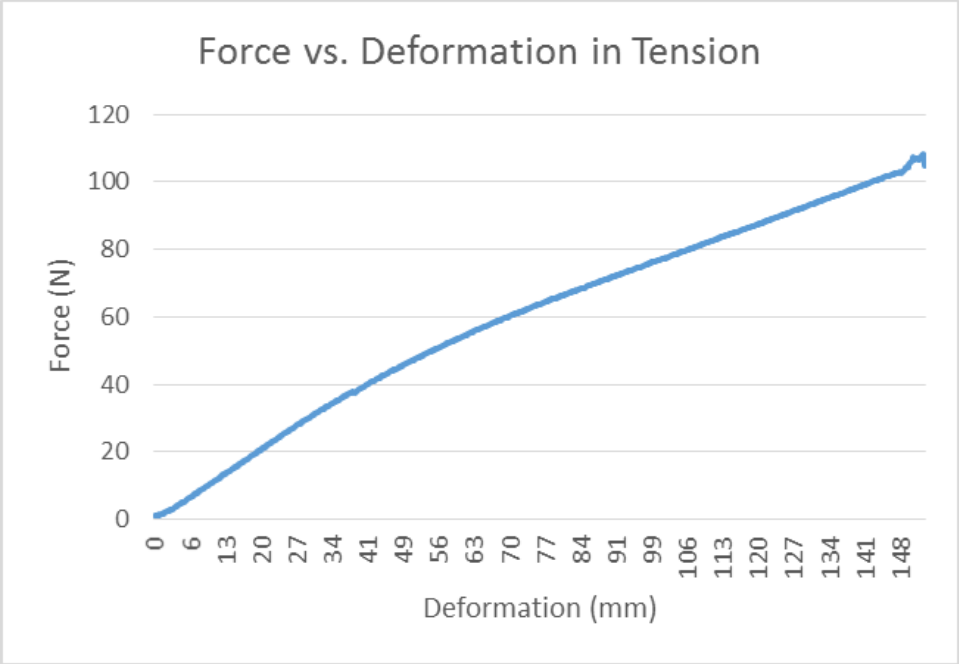

Figure 26: Force vs. Deformation in Tension Test

Data used are from Sample 4 of 30% wt PVA cryogel

Mechanical values were determined using the process given in ASTM D412. Tensile stress (MPa) at a specific increase (xxx) in elongation is defined as:

$$T_{(xxx)} = \frac{F_{(xxx)}}{A}$$

Where $F_{(xxx)}$ (N) is the force measured at a specific elongation and A is the cross-sectional area (mm^2) of the unstrained specimen. This means that engineering stress was determined, not true stress. The tensile strength (MPa) is then:

$$TS = \frac{F_{(\max)}}{A}$$

The maximum force recorded is the magnitude of the force at the specimen's yield point.

Elongation (percent increase of the original length) is calculated as:

$$E_{\%} = 100\,\frac{[L - L_{(0)}]}{L_{(0)}}$$

L (meters) is the observed distance between the machine's clamps on the extended specimen and $L_{(0)}$ (meters) is the original distance between the clamps. The ultimate elongation is the L at $F_{(max)}$ and specimen rupture.

A tensile strength vs elongation graph is presented in Figure 27. The specimen shows a linear elastic elongation for the first quarter of the test then around 50% elongation exhibits a change in slope. This signifies that the specimen has entered plastic deformation. From the slope of the first linear part of the data, the modulus of elasticity (E) can be determined.

$$E = \frac{\Delta TS}{\Delta E}$$

The modulus of elasticity is the change in stress over the change in strain, i.e., the slope of the early part of the graph in Figure 27. It was calculated in Microsoft Excel® using the SLOPE function over the beginning portions of the data before the slope change. Each sample was examined to determine where this slope change took place to help accurately determine the modulus.

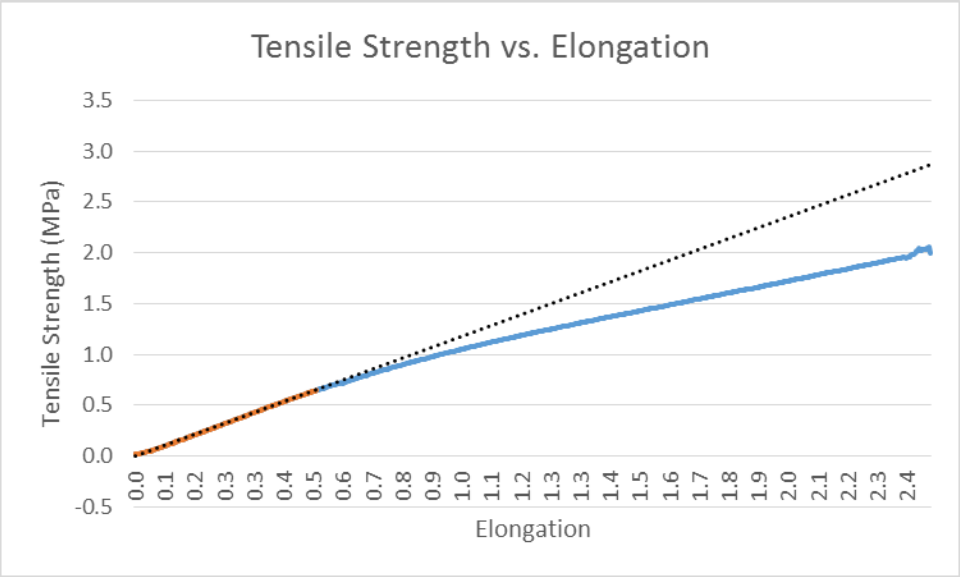

Figure 27: Tensile Strength vs. Elongation in Tension

Data used are from Sample 4 of 30% wt PVA cryogel. Portion used to determine elasticity highlighted in red. Treadline of slope shown as dotted black line.

The stress/strain graph presented in Figure 27 is that of a nonporous 30% wt PVA cryogel sample. The graphs created from porous PVA cryogel samples had much more fluctuating data, most likely due to the fact porous materials are not completely solid but filled with void space. The elasticity was still determined as the slope of the beginning portion of the data. Examples of this are presented in Figure 28. A stress/strain graph of a sample created through the gas method is shown below.

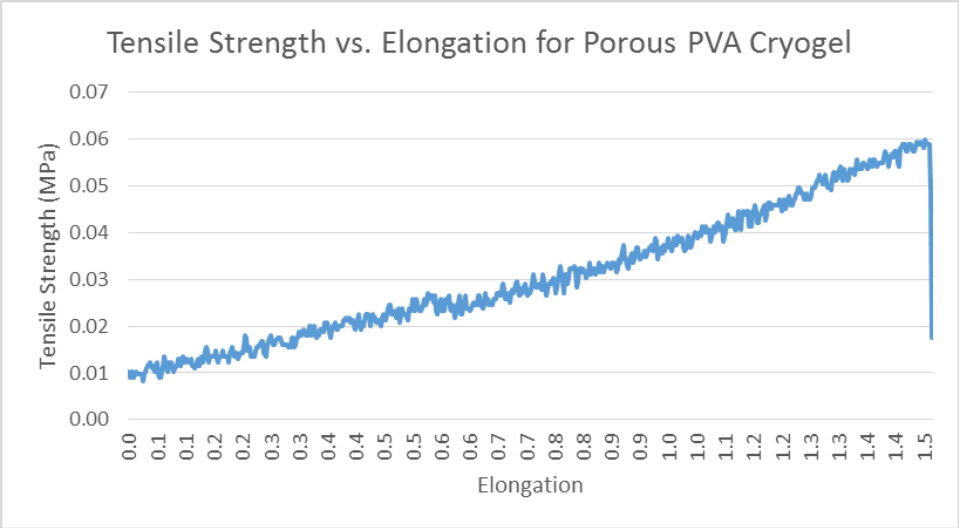

Figure 28: Tensile Strength vs. Elongation in Tension for Porous PVA cryogel

Data used are from Sample 1 of 20% wt porous PVA cryogel created with salt method

The data collected from all tests performed in tension with the calculated yield tensile strength, percent elongation at break, and modulus of elasticity are presented in Table 6. Visual comparisons in bar graph form for these mechanical properties are shown in Figure 29, Figure 30, and Figure 31 respectively.

Due to small sample sizes (<30 samples), a t-test (1 way, unequal variance) was performed in Microsoft Excel® on multiple pairings of the types of porous PVA cryogel to determine statistical difference between them. A p-value less than 0.05 was considered statistically significant. These pairing compared the mechanical values of porous PVA cryogel to its plain weight percent counterpart as well as the other porous sample created through the same method with a different PVA cryogel weight percent. The p-values are displayed in Table 7. The highlighted values display those that are statistically different.

Elastic Modulus

The Young's Modulus was calculated as the slope created from the beginning portion of the stress/strain curve found from the samples. Tensile strength (MPa) over elongation (unitless) gives the modulus a unit of MPa, or N/mm^2. The modulus for each type of PVA cryogel is listed in Table 8, a graph for comparison is shown in Figure 32, and a statistical comparison is listed in Table 9.

A distinct difference can be seen in the elastic modulus between the plain PVA cryogels tested. 10% wt PVA cryogel has a modulus of 0.08MPa, 20% wt PVA cryogel is three times greater at 0.20MPa, and 30% wt PVA cryogel is five times greater with an average of 1.20MPa.

Poked 30% wt PVA cryogel has an elastic modulus of 1.24MPa which is similar to that of plain PVA cryogel. With a P-value of 0.24, they are not statically different. The molded PVA cryogel did show a 27% reduction though with a modulus of .8MPa.

The gas method produces the smallest modulus of 0.04MPa. This is six times less than the plain 20%.

In regards to the PVA cryogel cast over salt, both showed the elastic modulus reduced 25%. 10% salt became 0.06MPa while 20% salt became 0.18MPa.

A trend can be seen in the composites in that the more of the non-PVA cryogel compound that was added the greater the elastic modulus. 2% CS's modulus was 1.20MPa and is considered statistically similar to plain 30%. Doubling the percentage weight of chitosan increased the modulus 32% to 1.58MPa. 4% CS is also the only sample tested that showed a increase in the modulus from the original. 5% CaPO4

showed a 34% reduction from plain 30% PVA cryogel. Doubling the CaPO4 showed a similar increase to the chitosan of 34%.

In Relation to Facial Implant Criteria

Most of cartilage falls within an elastic range of [0.3,1.3]MPa, however the deepest 20% could increase as high as 2.3MPa.[43] While none of the samples had a modulus as high as 2.3MPa, the elasticity of 30% wt plain PVA cryogel fell within the typical cartilage range as did all its porous counterparts.

The Young's modulus for adipose tissue has been found to range between 0.005-0.050MPa.[44, 45] At 0.04MPa, gaseous 20% wt PVA cryogel falls within this range. The modulus of plain 10% wt PVA cryogel was 0.08MPa and 10% cast over salt had a value of 0.06MPa. Although larger than the range of human fat, they are within the same magnitude.

In Relation to Shore A Hardness

The ASTM F881Standard Specification for Silicone Elastomer Facial Implants gives a requirement that the durometer shall have a maximum of shore A80.[42] A durometer, which is used to measure the hardness, was unavailable for use during the time of experimentation. To help determine the hardness of the PVA cryogels, an equation was found from Qi et al. that converts the Young's modulus to shore A hardness.[88] This equation is shown below, where S is the shore A hardness and E is the elastic modulus in units of MPa.

$$S = 100\,\mathrm{erf}(.0003186 * E^{\frac{1}{2}})$$

After substituting the experimental values of the elastic modulus for each PVA cryogel sample into the equation, the shore A hardness conversions are shown in Table 5. The largest hardness value found was A43 (4% chitosan and PVA cryogel composite), which is well below the A80 requirement for facial implants.

Table 5: Converting Young's Modulus to Shore A Hardness

PVA	Young's Modulus (Mpa)	Shore A Hardness
10%	0.08	10
20%	0.24	17
30%	1.2	38
Poked	1.28	39
Velcro	0.88	33
Gas	0.04	7
10% Salt	0.06	9
20% Salt	0.18	15
2% CS	1.2	38
4% CS	1.58	43
5% CaPO4	0.79	31
10% CaPO4	1.06	36

Maximum Tensile Strength

For the nonporous PVA cryogel, the maximum tensile strength doubled with each 10% increase in PVA cryogel within the samples. Strength increased from 0.39MPa at 10% wt PVA cryogel to 1.14MPa at 20% wt PVA cryogel to then 2.48MPa at 30% wt PVA cryogel. The standard deviation of all three of them is less than 8.0% of the total value.

The average maximum tensile strength for 30% wt PVA cryogel was slightly decreased when filled with a over one hundred holes created from having a needle

pressed into it. The strength was decreased 14% to a value of 2.13MPa. The 30% wt PVA cryogel molded over Velcro had a decrease of 40% from the original to have a strength of 1.5MPa. The imperfections in the solid PVA cryogel created through these methods weakened the strength of the 30% wt PVA cryogel.

20% wt PVA cryogel that underwent the gas method had an average ultimate tensile strength of 0.06MPa with a standard deviation of ±0.02. This is a 95% reduction from the plain 20% wt PVA cryogel. This method created closed pores with diameters up to 600μm. These samples have on average 75% porosity with thin walls separating the pores.

Porous PVA cryogel created through the salt casting and leaching method also showed a decrease in tensile strength in comparison to their plain PVA cryogel counterparts. 10% wt PVA cryogel with salt decreased 46% to have a strength of 0.21MPa and 20% salt decreased 78% to 0.25MPa. Once again, open space from the pores greatly impacted the strength of the material. In addition, both data ranges were within each other's standard deviation. 10% salt has a standard deviation range of [0.15,0.27]MPa and 20% has a range of [0.12,0.38]MPa. As presented in Table 7 the tensile strengths were compared between both salt weight percents. With a calculated P-value of 0.328, there is no statistical difference in strength between them.

The materials used in the composites were still embedded within the samples during the tensile tests. 2% CS had a tensile strength of 1.53 and a standard deviation of ±0.26. This is a 38% decrease in strength from the plain 30%. 4% CS had a strength of 2.54MPa ±0.25 and was the only tested porous PVA cryogel that had a strength statistically similar to its nonporous counterpart. Doubling the percent weight of

embedded CS increased the average tensile strength by 40%. Calcium phosphate was also still embedded within the 30% wt PVA cryogel for tensile testing. 5% CaPO4 had an average strength of 2.11MPa ±0.26, a 15% decrease from the plain PVA cryogel. 10% CaPO4 gave the highest value of tensile strength out of all methods at 2.66MPa ±0.12. While this is only a 7% increase in strength from the plain 30% wt PVA cryogel, a p-value of 0.018 deemed this increase significant.

In relation to cartilage, an implant should have a minimum strength of 1.71MPa. The average tensile strength of cartilage falls between the values found for 20% and 30% plain PVA cryogel. The porous implants that had an average that met this threshold were the poked PVA cryogel and the composites made up of 4% CS and 5% and 10% CaPO4. The PVA cryogel molded over Velcro and the composite of 2% CS showed averages below this threshold, however their standard deviation range did meet this standard.

Yield Elongation Percentage

A graph comparing the elongation percentage of all the samples is exhibited in Figure 30, and the statistical comparison is listed in Table 7. Plain 10%, 20%, and 30% wt PVA cryogel all have a similar yield elongation strain of 250, 275, and 268% respectively. Each of their standard deviations fell within each other's range.

The PVA cryogel poked with holes and the Velcro both show a decrease in yield elongation percentage from the plain 30% wt PVA cryogel. The poked holes samples have an average decrease of 32% to an elongation of 181% and the Velcro mold has a elongation value of 200% which is a 25% reduction. These values fall within each other's standard deviation ranges [162,200] and [160,240] respectively.

Gassed 20% wt PVA cryogel had a ride range of sampled elongation. Sample 5 had an elongation of 76% while Sample 3 was found to be 224%. The average was 154%, which is a 44% decrease from plain 20%.

10% salt had the highest average elongation percentage at 396% ±98. This is a 158% increase from plain 10% PVA cryogel. 20% PVA cryogel with salt had the second lowest at 163% ±92 which was a 41% decrease in average. The elongation percent was reduced 40% from 10% to 20% salt.

Most of the composite materials maintained similar elongation percentages to the nonporous PVA cryogels. With an elongation of 207%, 2% CS had a significant reduction of 22% from plain 30% wt PVA cryogel. However 4% CS, 5% CaPO4, and 10% CAPO4 all had elongation percentages that were not considered statistically significant from 30%.

In general, a trend can be seen that PVA cryogel with unfilled pores have a reduced elongation percentage than that of plain and composite PVA cryogel. PVA cryogel that was poked, molded with Velcro, gassed, and cast with 20% PVA cryogel all showed this. The only one that was different was that of 10% salt. Those that had particles embedded within it showed similar elongations except for 2% CS. 2% CS has four samples with a standard deviation 20% of the average's value. Sample 4 of 2% CS extended to 263% of its original length. This shows that it is possible for 2% CS to have a similar elongation the rest of the composite materials which can possibly be achieved with better manufacturing practices. In addition, those with unfilled pores also tended to have larger standard deviations percentages than the other types of PVA cryogel. This could be because of the variability in size and position of formed pores.

The threshold for yield elongation percentage was decided to be similar to that of cartilage: 30%. All tested materials easily achieved this benchmark. The lowest elongation found, gaseous 20% PVA cryogel at 154% elongation, is over 500% larger than the maximum cartilage strain.

Table 6: Calculated Tensile Strength, Elongation, and Young's Modulus

(Continued on the next 3 pages)

Type of PVA	Sample Number	Width (mm)	Thickness (mm)	Tensile Strength (Mpa)	Elongation (%)	Young's Modulus (MPa)
10% PVA	1	10.72	2.79	0.41	268	0.07
	2	10.78	2.93	0.34	251	0.06
	3	11.16	2.33	0.43	262	0.09
	4	12.18	2.65	0.39	252	0.08
	5	11.67	2.18	0.39	215	0.09
	6	11.3	2.77	0.25	177	0.11
	7	11.6	2.08	0.51	218	0.12
			Average	**0.39**	**250**	**0.08**
			Stdev	**0.03**	**20**	**0.01**

Type of PVA	Sample Number	Width (mm)	Thickness (mm)	Tensile Strength (Mpa)	Elongation (%)	Young's Modulus (MPa)
20% PVA	1	11.26	2.66	1.090	293	0.209
	2	11.43	2.54	1.181	279	0.252
	3	11.92	2.74	1.038	263	0.248
	4	11.24	2.85	1.245	277	0.266
			Average	**1.14**	**278**	**0.24**
			Stdev	**0.09**	**12**	**0.02**

Type of PVA	Sample Number	Width (mm)	Thickness (mm)	Tensile Strength (Mpa)	Elongation (%)	Young's Modulus (MPa)
30% PVA	1	12.50	4.17	2.554	291	1.248
	2	11.82	3.62	2.532	248	1.168
	3	11.90	3.55	2.500	280	1.171
	4	12.42	3.72	2.323	242	1.193
			Average	**2.48**	**265**	**1.20**
			Std. Dev.	**0.11**	**24**	**0.04**

Type of PVA	Sample Number	Width (mm)	Thickness (mm)	Tensile Strength (Mpa)	Elongation (%)	Young's Modulus (MPa)
Poked Holes 30% PVA	1	11.71	3.40	2.33	204	1.22
	2	11.77	4.23	1.82	159	1.24
	3	11.52	3.82	2.27	197	1.23
	4	11.02	3.15	2.17	181	1.09
	5	11.66	3.58	2.06	166	1.40
			Average	**2.13**	**181**	**1.24**
			Stdev	**0.20**	**19**	**0.11**

Type of PVA	Sample Number	Width (mm)	Thickness (mm)	Tensile Strength (Mpa)	Elongation (%)	Young's Modulus (MPa)
Velcro Mold 30% PVA	1	10.40	3.05	1.92	240	0.82
	2	9.49	2.75	1.34	153	1.02
	3	11.22	3.12	1.48	226	0.81
	4	10.40	3.15	1.28	183	0.87
			Average	**1.50**	**200**	**0.88**
			Stdev	**0.29**	**40**	**0.09**

Type of PVA	Sample Number	Width (mm)	Thickness (mm)	Tensile Strength (Mpa)	Elongation (%)	Young's Modulus (MPa)
Gas 20% PVA	1	12.00	2.78	0.06	114	0.04
	2	11.47	4.25	0.06	215	0.03
	3	10.90	2.66	0.11	224	0.04
	4	11.66	3.74	0.06	148	0.03
	5	11.81	3.50	0.04	76	0.04
	6	11.22	4.00	0.05	124	0.04
	7	11.60	3.60	0.07	177	0.03
			Average	**0.06**	**154**	**0.04**
			Stdev	**0.02**	**55**	**0.01**

Type of PVA	Sample Number	Width (mm)	Thickness (mm)	Tensile Strength (Mpa)	Elongation (%)	Young's Modulus (MPa)
Salt 10% PVA	1	10.50	5.16	0.31	380	0.06
	2	10.10	6.31	0.17	387	0.06
	3	11.09	5.80	0.18	590	0.06
	4	10.00	4.52	0.17	327	0.06
	5	10.90	4.71	0.20	335	0.05
	6	8.48	4.35	0.26	357	0.07
			Average	**0.21**	**396**	**0.06**
			Stdev	**0.06**	**98**	**0.01**

Type of PVA	Sample Number	Width (mm)	Thickness (mm)	Tensile Strength (Mpa)	Elongation (%)	Young's Modulus (MPa)
Salt 20% PVA	1	11.15	6.35	0.19	112	0.17
	2	11.37	6.06	0.21	122	0.17
	3	12.04	7.30	0.43	301	0.24
	4	11.66	6.79	0.15	117	0.15
			Average	**0.25**	**163**	**0.18**
			Stdev	**0.13**	**92**	**0.04**

Type of PVA	Sample Number	Width (mm)	Thickness (mm)	Tensile Strength (Mpa)	Elongation (%)	Young's Modulus (MPa)
2% CS 30% PVA	1	11.65	4.30	1.56	214	1.24
	2	11.43	4.01	1.24	178	1.03
	3	11.30	3.88	1.46	175	1.15
	4	11.57	4.30	1.87	263	1.37
			Average	**1.53**	**207**	**1.20**
			Stdev	**0.26**	**41**	**0.14**

Type of PVA	Sample Number	Width (mm)	Thickness (mm)	Tensile Strength (Mpa)	Elongation (%)	Young's Modulus (MPa)
4% CS 30% PVA	1	11.40	4.53	2.42	267	1.57
	2	11.51	4.30	2.83	280	1.68
	3	11.66	4.59	2.36	267	1.50
			Average	**2.54**	**271**	**1.58**
			Stdev	**0.25**	**7**	**0.09**

Type of PVA	Sample Number	Width (mm)	Thickness (mm)	Tensile Strength (Mpa)	Elongation (%)	Young's Modulus (MPa)
5% CaPO4 30% PVA	1	11.88	4.24	1.95	305	0.74
	2	12.20	3.38	2.40	286	0.77
	3	12.30	4.03	2.25	281	0.80
	4	12.35	4.12	1.85	279	0.84
			Average	**2.11**	**288**	**0.79**
			Stdev	**0.26**	**12**	**0.04**

Type of PVA	Sample Number	Width (mm)	Thickness (mm)	Tensile Strength (Mpa)	Elongation (%)	Young's Modulus (MPa)
10% CaPO4 30% PVA	1	11.86	3.30	2.77	305	1.04
	2	11.63	3.43	2.73	286	1.05
	3	11.30	3.45	2.46	281	1.13
	4	11.62	3.50	2.57	279	1.00
	5	11.40	3.49	2.77	267	1.07
	6	11.99	3.42	2.67	276	1.08
			Average	**2.66**	**282**	**1.06**
			Stdev	**0.12**	**13**	**0.04**

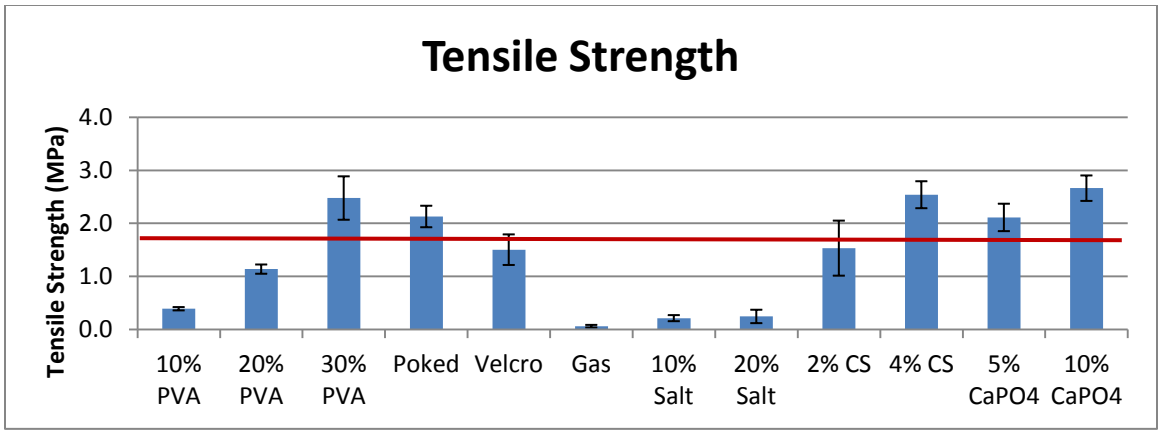

Figure 29: Comparison of Tensile Strengths for Porous PVA cryogel

Red line notes the acceptance criteria of 1.71MPa

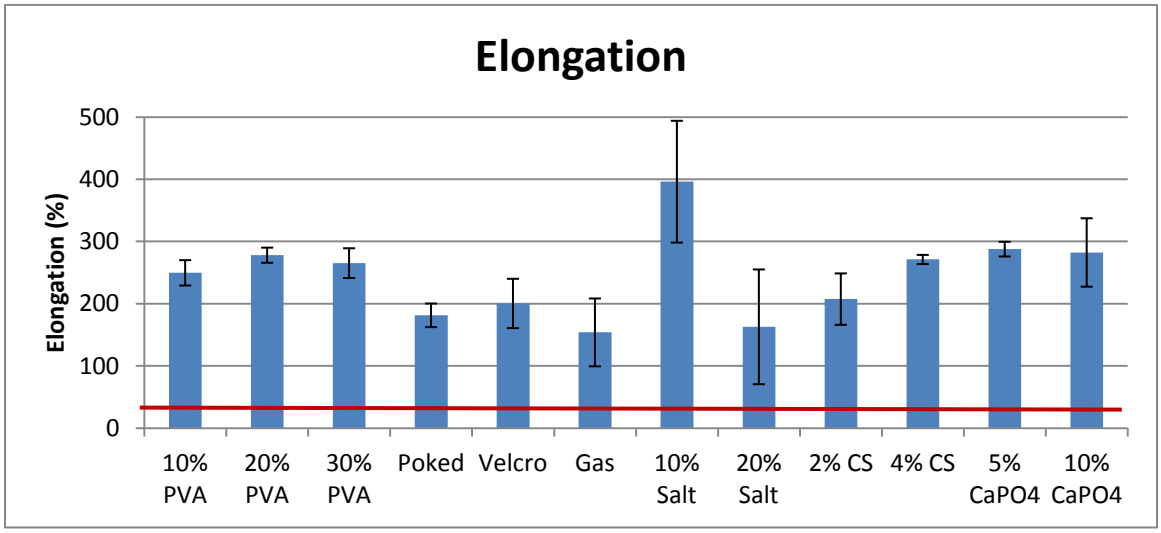

Figure 30: Comparison of Elongation Percentages for Porous PVA cryogel

Red line notes the acceptance criteria of 30%

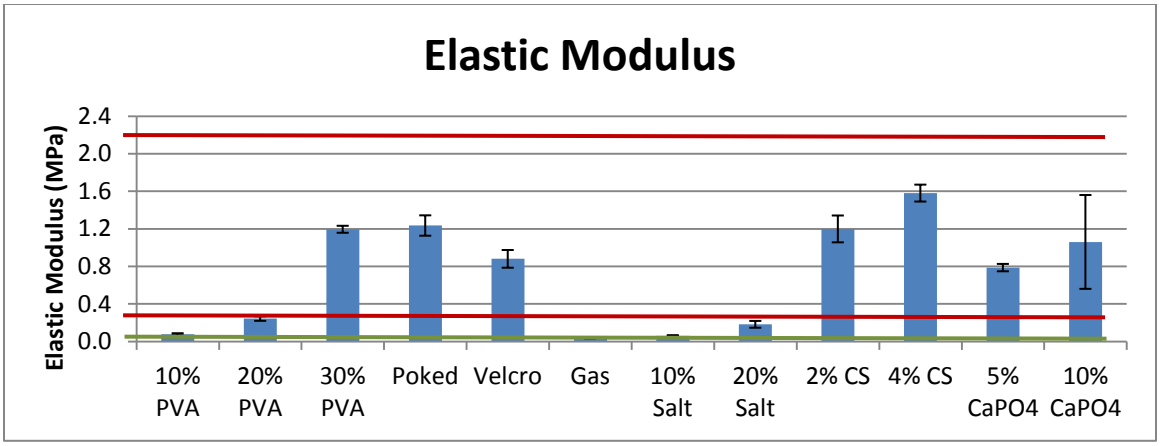

Figure 31: Comparison of Elastic Modulus for Porous PVA cryogel

Red line notes the acceptance criteria range for cartilage [0.3,2.3]MPa. Green line notes the acceptance criteria range for adipose tissue [0.005,0.05]MPa.

Table 7: Tensile Strength and Elastic Modulus Statistical Significance Comparison

P-value < .05 considered significant and is highlighted in blue

Type of PVA 1	Type of PVA 2	Tensile Strength P-value	Elongation P-value	Elastic Modulus P-value
10% PVA	20% PVA	0.000	0.007	0.000
20% PVA	30% PVA	0.000	0.195	0.000
30% PVA	Poked	0.015	0.001	0.238
30% PVA	Velcro	0.002	0.019	0.002
20% PVA	Gas	0.000	0.000	0.000
10% PVA	10% Salt	0.000	0.004	0.008
20% PVA	20% Salt	0.000	0.043	0.018
10% Salt	20% Salt	0.328	0.003	0.003
30% PVA	2% CS	0.001	0.031	0.481
30% PVA	4% CS	0.360	0.333	0.005
2% CS	4% CS	0.002	0.026	0.004
30% PVA	5% CaPO4	0.030	0.080	0.000
30% PVA	10% CaPO4	0.018	0.128	0.001
5% CaPO4	10% CaPO4	0.009	0.259	0.000

Tear Strength

Tear strength (T_s) is calculated in kiloNewtons per meter (kN/m) of thickness by the formula

$$T_s = \frac{F}{d}$$

Where F is the maximum force (in Newtons) obtained from the test and d is the median thickness of each piece in milimeters.

Samples were tested in tension using the 'zig-zag' shape shown in Figure 11 according to standard ASTM D624. The thickness of each sample was noted before every test and is listed along with the calculated tear strength in Table 8. A graphical representation is displayed in Figure 32 and statistical data to determine significant difference is shown in Table 9.

Tear strength for plain 10% wt PVA cryogel was found to be 1.345kN/m. It was found to have increased 40% to 2.26kN/m for 20% wt PVA cryogel and quadrupled to 9.11kN/m for 30% wt PVA cryogel.

An increase in the average value was seen in samples that were composed of plain PVA cryogel.

The 30% PVA cryogel that was poked with holes increased in tear strength by 30% to become 13.06kN/m. The one molded with Velcro showed a 20% increase from plain 30% wt PVA cryogel, however with a P-value of 0.079 it is not considered statistically significant. Reducing the standard deviation of 30% wt PVA cryogel through more samples could likely show that there is an increase.

Using the gas method on 20% wt PVA cryogel reduced the tear strength 74% to 0.585kN/m. This is the lowest tear strength found out of all the samples.

While there is an increase on the average value of the tear strength of the salt method, the change was not statistically significant in comparison to the plain counterparts. 10% salt had an average increase of 38% but the P-value was 0.071. 20% salt showed an average increase of 30% but had a P-value of 0.083. A 58% increase was seen between 10% salt and 20% salt.

While increasing chitosan increased tear strength, the opposite was true for CaPO4. 2% CS showed an average increase from plain 30% wt PVA cryogel of 25% to make the average 11.36kN/m, but a P-value of 0.094 makes the difference not significant. 4% CS had a value of 15.31kN/m and is a 35% increase from the 2% CS composite. The CaPO4 composites were both found to not be statistically significant from plain 30%. 5% CaPO4 showed a tear strength of 10.75kN/m and 10% CaPO4 was 16% lower at 9.00kN/m.

Table 8: Calculated Tear Strength

(Continued on the next 3 pages)

Type of PVA	Sample	Thickness (m)	Tear Strength (kN/m)
10% PVA	1	0.00254	1.042
	2	0.00212	2.124
	3	0.0023	1.027
	4	0.00215	1.165
	5	0.00228	1.420
	6	0.00244	1.880
	7	0.00215	0.758
		Average	1.345
		Std. Dev.	0.495

Type of PVA	Sample	Thickness (m)	Tear Strength (kN/m)
20% PVA	1	0.0031	2.693
	2	0.0033	2.382
	3	0.0030	1.872
	4	0.0040	2.182
	5	0.0034	2.168
		Average	2.259
		Std. Dev.	0.303

Type of PVA	Sample	Thickness (m)	Tear Strength (kN/m)
30% PVA	1	0.0032	6.41807
	2	0.0041	8.81335
	3	0.0036	8.48685
	4	0.0039	12.71997
		Average	9.110
		Std. Dev.	2.630

Type of PVA	Sample	Thickness (m)	Tear Strength (kN/m)
Poked Holes 30% PVA	1	0.0039	12.200
	2	0.0041	14.361
	3	0.0038	13.791
	4	0.0038	11.899
		Average	13.063
		Std. Dev.	1.199

Type of PVA	Sample	Thickness (m)	Tear Strength (kN/m)
Velcro Mold 30% PVA	1	0.0030	13.36
	2	0.0030	12.36
	3	0.0030	11.62
	4	0.0030	9.96
	5	0.0030	10.64
		Average	11.585
		Std. Dev.	1.347

Type of PVA	Sample	Thickness (m)	Tear Strength (kN/m)
Gas 20% PVA	1	0.0035	0.83599
	2	0.0035	0.28162
	3	0.0035	0.71547
	4	0.0035	0.50616
		Average	0.585
		Std. Dev.	0.244

Type of PVA	Sample	Thickness (m)	Tear Strength (kN/m)
Salt 10% PVA	1	0.0052	1.924
	2	0.0062	1.270
	3	0.0049	2.428
	4	0.0043	1.782
		Average	1.851
		Std. Dev.	0.476

Type of PVA	Sample	Thickness (m)	Tear Strength (kN/m)
Salt 20% PVA	1	0.0065	2.640
	2	0.0065	1.601
	3	0.0065	3.085
	4	0.0065	3.834
	5	0.0065	3.454
		Average	2.923
		Std. Dev.	0.861

Type of PVA	Sample	Thickness (m)	Tear Strength (kN/m)
2% CS 30% PVA	1	0.0043	13.162
	2	0.0042	11.476
	3	0.0042	9.802
	4	0.0040	11.473
	5	0.0043	10.903
		Average	11.363
		Std. Dev.	1.215

Type of PVA	Sample	Thickness (m)	Tear Strength (kN/m)
4% CS 30% PVA	1	0.0048	16.181
	2	0.0047	13.333
	3	0.0046	17.686
	4	0.0045	14.059
		Average	15.315
		Std. Dev.	1.990

Type of PVA	Sample	Thickness (m)	Tear Strength (kN/m)
5% CaPO4 30% PVA	1	0.0041	8.800
	2	0.0040	10.316
	3	0.0038	11.709
	4	0.0040	12.234
		Average	10.765
		Std. Dev.	1.540

Type of PVA	Sample	Thickness (m)	Tear Strength (kN/m)
10% CaPO4 30% PVA	1	0.0044	8.140
	2	0.0045	9.141
	3	0.0041	9.707
		Average	8.996
		Std. Dev.	0.793

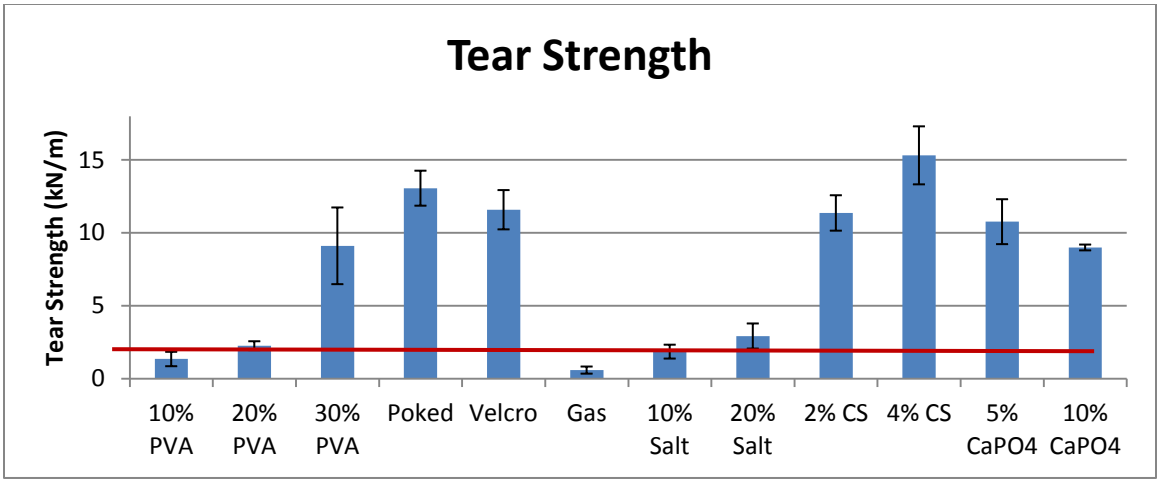

Figure 32: Comparison of Tear Strength for Porous PVA cryogel

Table 9: Tear Strength Statistical Significance Comparison

p-value < .05 considered significant and is highlighted in blue

Type of PVA 1	Type of PVA 2	Tensile Strength P-value
10% PVA	20% PVA	0.001
20% PVA	30% PVA	0.007
30% PVA	Poked	0.025
30% PVA	Velcro	0.079
20% PVA	Gas	0.000
10% PVA	10% Salt	0.071
20% PVA	20% Salt	0.083
10% Salt	20% Salt	0.027
30% PVA	2% CS	0.094
30% PVA	4% CS	0.005
2% CS	4% CS	0.010
30% PVA	5% CaPO4	0.164
30% PVA	10% CaPO4	0.470
5% CaPO4	10% CaPO4	0.055

Pore Size

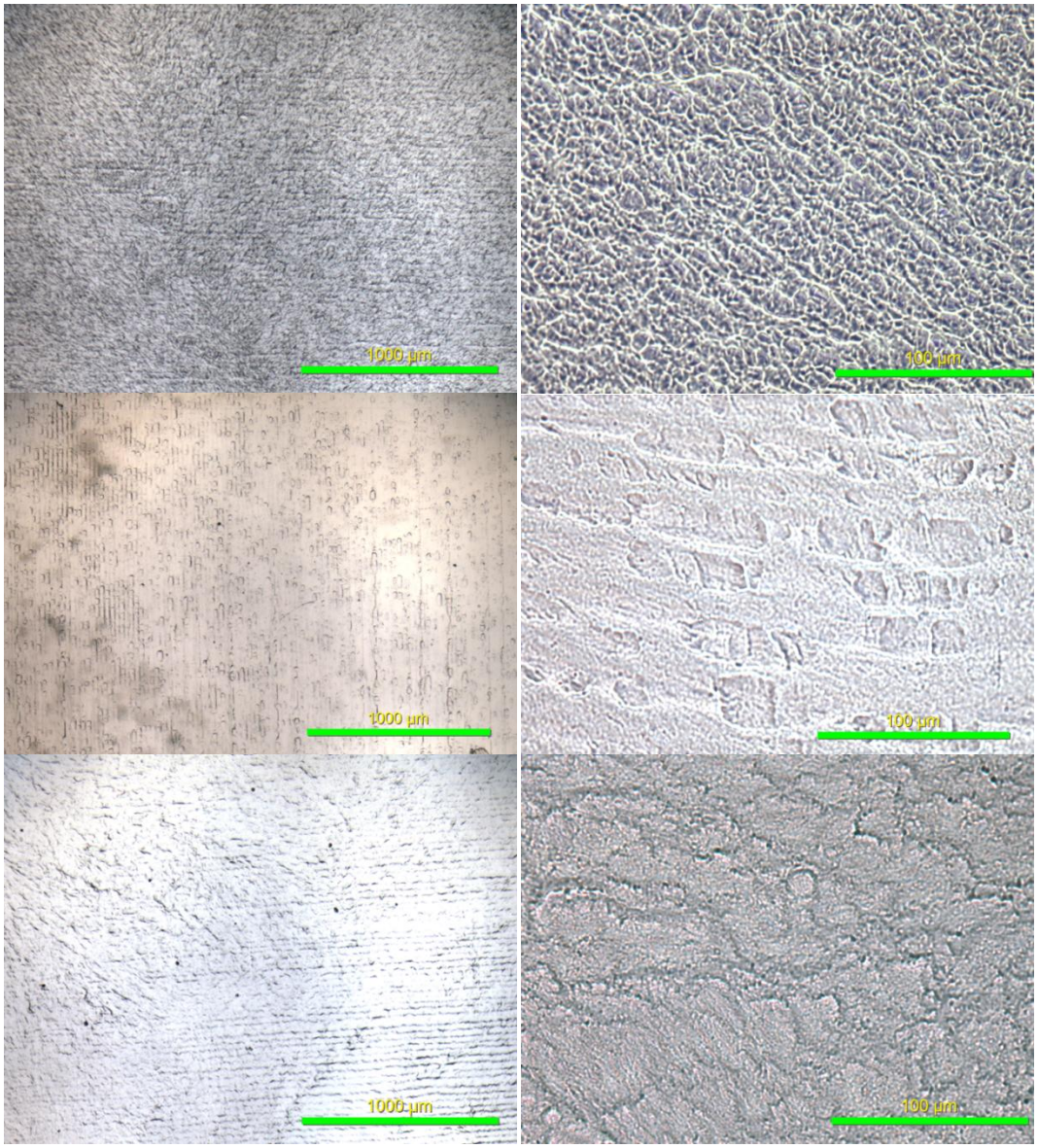

Figure 33: Images of Plain 10%, 20%, and 30% wt PVA cryogel

(A) 10% 2X Magnigication (B) 10% 2X Mag (C) 20% 2X Mag (D) 20% 2X Mag (E) 30% 2X Mag (F) 30% 2X Mag

Microscope images of the PVA cryogel samples are shown in Figure 33 through Figure 41. Table 10 is provided at the end of this section with a summary of the pore

sizes. The left side of Figure 33 displays images of the plain 10%, 20%, and 30% wt PVA cryogel at 2X magnification. The ridges seen are from the blade cutting the PVA cryogel. To show that PVA cryogel does not have any micropores, pictures of the samples were also taken at 20X magnification. From the images it can be seen that PVA cryogel is nonporous at 10%, 20%, and 30% wt.

Pressed Method

Figure 34 shows a section cut perpendicular to the direction that a 1mm diameter needle was pressed into 30% wt PVA cryogel. While the diameter of the needle used is larger than the desired pore size for cellular ingrowth, this method left smaller diameter pores. The range of pore diameters were between 60-170µm with an mean of 125µm. The pores created have on average a diameter 88% less than the needle used to create them. The smaller holes can be attributed to PVA cryogel's elastic nature.

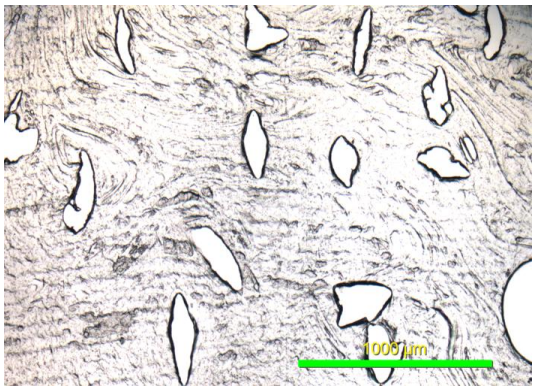

Figure 34: Sectioned Images of 30% wt PVA cryogel pressed with a 500µm needle

Molded Method

The images of Velcro are shown in Figure 35. Unlike the pores created by pressing in a needle through a solid block of PVA cryogel after it had undergone

freeze/thaw cycles, these were made by molding PVA cryogel over Velcro strips then running freeze/thaw cycles. This method involves molding the PVA cryogel around Velcro pillars instead of removing hydrogel material. Part A of Figure 35 was sectioned parallel to the Velcro pad that the PVA cryogel was molded over. The pattern of the Velcro is clearly visible. These holes were found to have a diameter of 250µm. The sample shown in Part B was sectioned perpendicular to the Velcro pad. This angle shows the depth the Velcro penetrated the PVA cryogel. The outline of the Velcro shape can been seen as a thin cylinder that ends at a larger sized diameter half spherical cap. The depth of the Velcro was measured to be about 1mm.

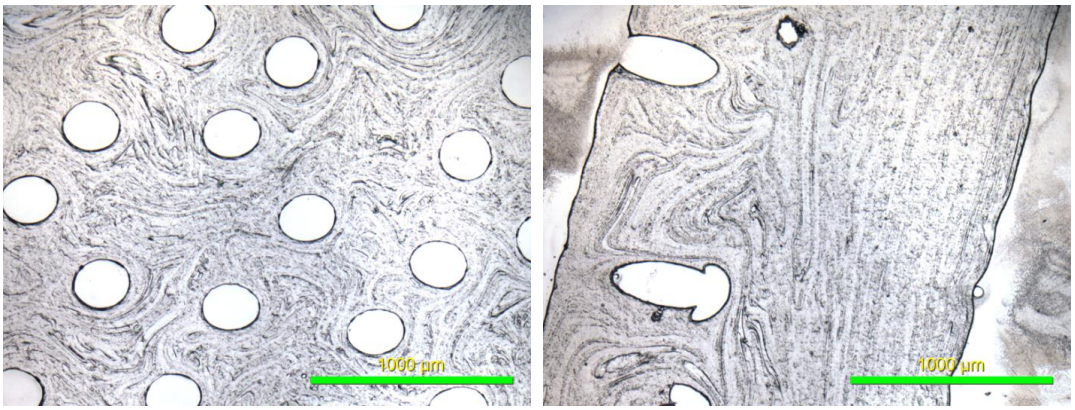

Figure 35: Sectioned Images of PVA cryogel Pressed with Velcro

(A) Sectioned parallel to the Velcro pad (B) Sectioned perpendicular to the Velcro pad

Casting/Particulate Leaching Method

Salt with diameters ranging from 150-600µm were used for the solvent casting/ particulate leaching method. Images of the formed pores are shown in Figure 36. Part A shows 10% wt PVA cryogel pressed into the salt. Most of the pores are shown to be open and connecting to multiple other porous spaces. The pore size ranged from 100-800µm with a mean size of 450µm. Part B shows the 20% wt PVA cryogel pressed into

salt. The pores are less interconnected and smaller than the 10% wt PVA cryogel cast over salt. The pore range was found to be 50-250µm with a mean of 150µm. The pores also have less of a defining shape to them while the pores from 10% wt PVA cryogel are mostly in the shape of squares with curved corners, i.e. the shape of the salt. In addition, the 10% wt PVA cryogel could be pressed up to 3cm in depth into the salt. The depth of the 20% wt PVA cryogel can be seen in Part C of Figure 36. It was found to be about 1mm.

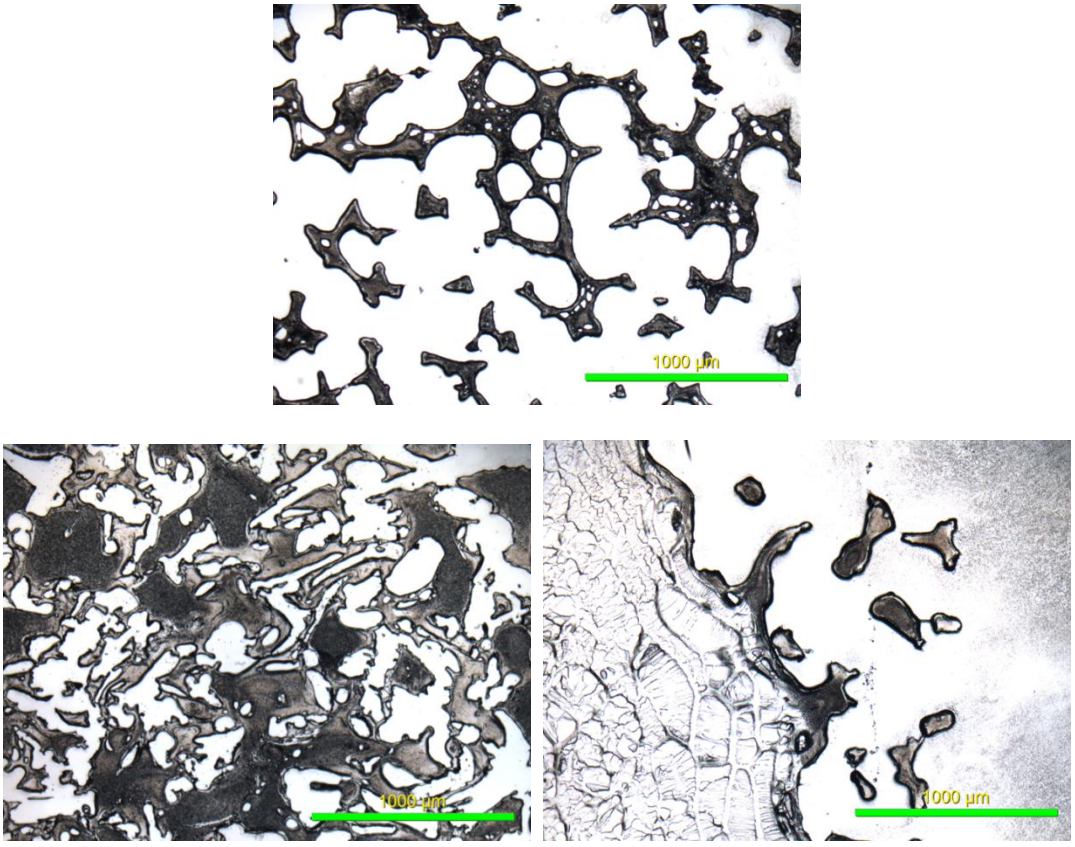

Figure 36: Sectioned Images of PVA cryogel pressed into salt crystals

(A) 10% wt PVA cryogel (B) 20% wt PVA cryogel parallel (C) 20% wt PVA cryogel perpendicular

Gas Method

Figure 37 is an image of porous PVA cryogel created through the gas method. These pores are more circular in shape and have defined boarders. This shows that the pores are less interconnectivity than that of salt. Pore sizes ranged from 20-600µm with a mean of 220µm and they proliferated throughout the PVA cryogel sample but not uniformly.

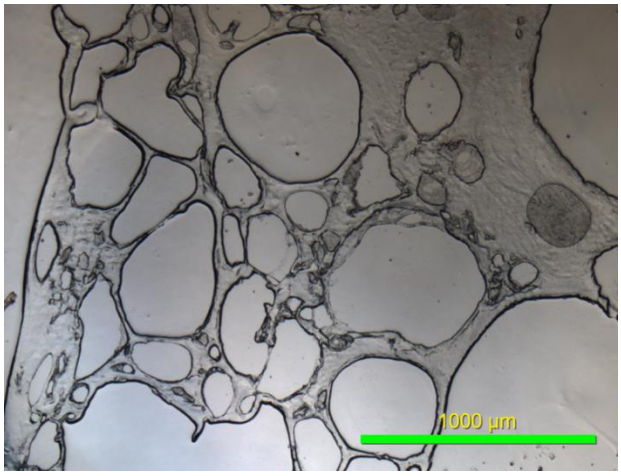

Figure 37: Sectioned Image of Porous PVA cryogel Created Through Gas Method

PVA cryogel/CS Composite Method

The flakes of chitosan were combined with the PVA cryogel in the autoclave to create the composite material were imaged with the microscope and are shown in Figure 38. The small flakes range in size from 5-15µm. There are also larger flakes present that have diameters as large as 200µm. Sections of the produced PVA cryogel/CS composite are shown in Figure 39. Part A displays 30% wt PVA cryogel mixed with 2% chitosan. The pore range is 20-300µm with a mean of 80µm. The larger pores are most likely from when some chitosan clumped together as well as from some of the larger CS flakes. Part B displays PVA cryogel mixed with 4% chitosan. The pores ranged from 20-500µm with

a mean of 100µm. The higher prevalence of larger sized pores can be attributed to the larger quantity of CS added to the mixture and which led to more clumping of the flakes.

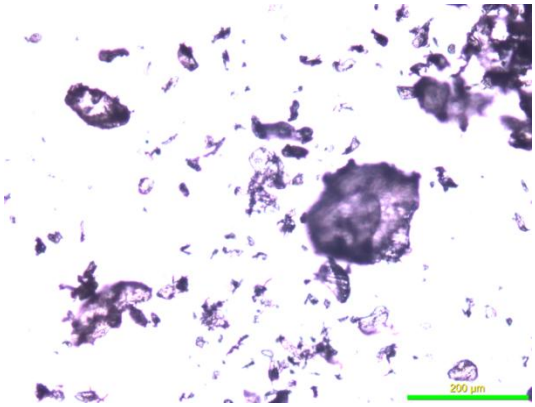

Figure 38: Image of Chitosan Flakes

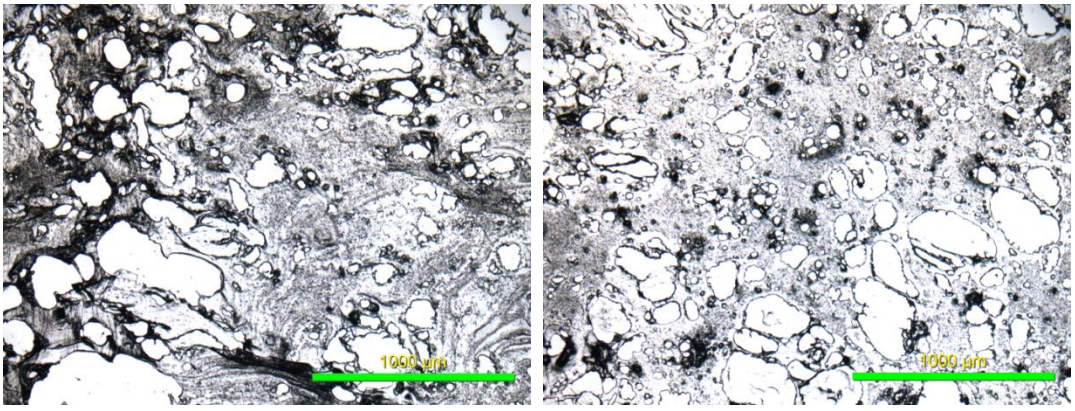

Figure 39: Sectioned Images of PVA cryogel mixed with Chitosan

(A) 2% CS (B) 4% CS

PVA cryogel/CaPO4 Composite Method

PVA cryogel was cooked with CaPO4 powder to create the final porous composites. Images of the CaPO4 powder are shown in Figure 40. The small dots pictured are between 3 and 5µm in size. The larger dots are from the CaPO4 clumping together and are both 50µm in diamteter. Finally, Figure 41 displays 30% wt PVA cryogel mixed with calcium phosphate. Part A shows the sample at 2X magnitude while

Part B is at 10X magnification. These small black dots are the CaPO4 embedded within the PVA cryogel. Pore sizes range from 5-15µm with a mean of 8µm. Part C is a section of PVA cryogel with 10% CaPO4 added and it is magnified in Part D. It can be observed that the 10% CaPO4 images are slightly darker than their 5% counterparts because a higher density of the embedded compound. The pore range for 10% CaPO4 is 5-20µm with a mean of 10µ.

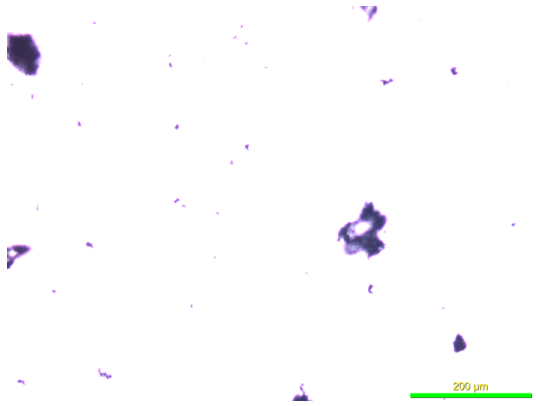

Figure 40: Images of CaPO4 Powder

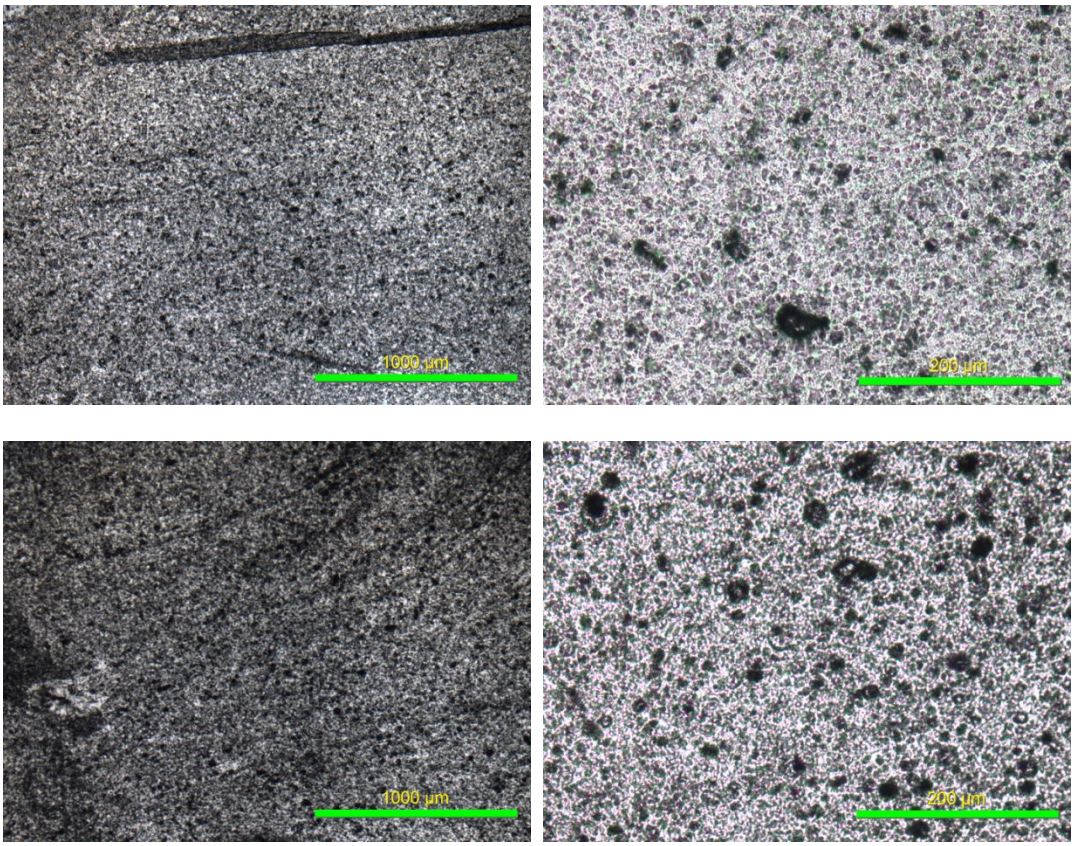

Figure 41: Sectioned Images of PVA cryogel mixed with $CaPO_4$

(A) 5% $CaPO_4$ (B) Close up of 5% $CaPO_4$ (C) 10% $CaPO_4$ (D) Close up of 10% $CaPO_4$

In Relation to Facial implant Criteria

The pore size range, mean pore size, interconnectivity of the pores, and the depth of the pores is summarized in Table 10. Fibrous ingrowth can be seen in pores with diameters between 5 and 15µm while bone regeneration typically requires pore diameters ranging from 100 to 400µm but can be as high as 700µm.

Table 10: Pore Size Range and Interconnectivity of Manufactured Porous PVA cryogel

Type	PVA %	Pore Size Range (µm)	Mean (µm)	Interconectivity	Depth (mm)
Poke	30	60-170	125	Unidirectional	Throughout
Velcro	30	250	250	Unidirectional	1
Salt	10	100-800	450	Yes	3
Salt	20	50-250	150	Yes	1-1.5
Gas	20	20-600	220	No	Throughout
2% CS	30	20-300	80	Partial	Throughout
4% CS	30	20-500	100	Partial	Throughout
5% CaPO4	30	5-15	8	No	Throughout
10% CaPO4	30	5-20	10	No	Throughout

The pores of the 30% PVA cryogel pressed with a needle had a diameter range of 60-170µm. The 1mm diameter needle used was thick enough to create some pores that will encourage bone growth. A larger mean pore size can be obtained by using a larger needle and a smaller one can lead the pores to be within the fibrous ingrowth range if desired. The consistent pore size of 250µm created by molding the PVA cryogel over Velcro shows that it can be used to encourage bone ingrowth. Again, changing the size of the extrusions can alter the pore size to be as large or as small as desired.

Implants that become interconnected to the neighboring bone will be then anchored to the bone and are less likely to migrate. Preventing the implant from creating dissymmetry or noticeable imperfections is critical when dealing with facial implants. Based on their pore size range, 10% salt, 20% salt, gaseous PVA cryogel, and both chitosan composites would all allow bone ingrowth. All their mean pore diameters were 100µm or above as well except for 2% CS with a measured mean diameter of 80µm. This means that over half of the pores were under 100µm and are not the size required for

bone ingrowth. Doubling the chitosan to 4% CS showed a 20µm increase in mean pore size to 100µm.

Both 5% and 10% CaPO4 had pore sizes that fell within the fibrous ingrowth range (5-15µm and 5-20µm respectively). While this does not give the strength that bone ingrowth would give, it does allow some stability. In addition, implants with fibrous ingrowth cause little tissue damage to its surrounding area when removed. PVA cryogel/CaPO4 composites could be used in the case of temporary implants where they help prevent implant slippage but give ease of removal.

Porosity Percentage

The ratio of porosity was determined through image analysis in Matlab. Figure 42 displays examples of the microscope images before and after they were analyzed. Part A shows an image of gaseous PVA cryogel then Part B displays it after it was transformed into a 2-tone black and white image. Part C and D show the same process for the CaPO4 images.

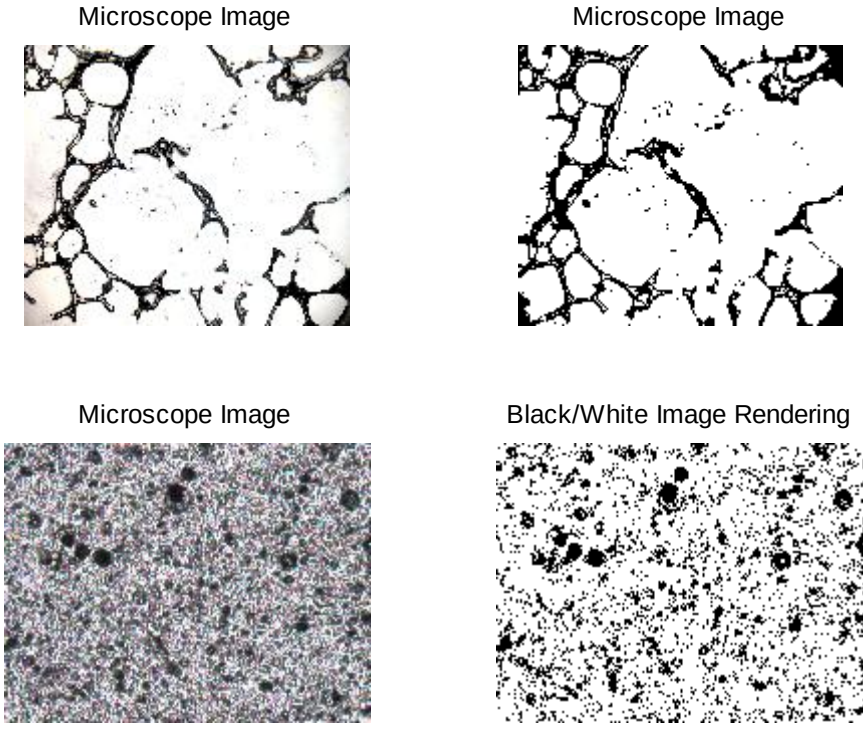

Figure 42: Before/After Images converted in Matlab to obtain porosity percentage (A) Image of porous PVA cryogel obtained through gas method (B) 2-Tone black/white image (C) Image of porous PVA cryogel/CaPO4 composite (D) 2-Tone black/white image

In Relation to Facial Implant Criteria

The average porosity ratios of the manufactured porous PVA cryogel are presented in Table 11. The porosities listed were found through the created Matlab

function. The images used to measure porosity were from multiple molded samples per batch of manufactured PVA cryogel and at least two separate batches were made at different times. The higher the porosity percentage of a material, the more structural linkage of the ingrowth material within the implant to ensure attachment and prevent slippage. An implant should strive to have a minimum porosity of 30% to help this bonding.[52] The samples that meet this minimum are gaseous PVA cryogel (74%) and those cast over salt (61% and 31%).

Table 11: Porosity Ratio of Manufactured Porous PVA cryogel

% wt PVA	30	30	20	10	20	30	30	30	30
Samples	Poked	Velcro	Gas	10% Salt	20% Salt	2% CS	4% CS	5% CaPO4	10% CaPO4
Porosities	0.05	0.09	0.80	0.73	0.35	0.13	0.20	0.16	0.23
	0.08	0.14	0.72	0.68	0.37	0.12	0.15	0.17	0.20
	0.03	0.09	0.69	0.71	0.30	0.10	0.17	0.18	0.24
	0.02	0.12	0.78	0.68	0.24	0.12	0.17	0.14	0.23
	0.03	0.18	0.67	0.72	0.27	0.09	0.21	0.17	0.23
	0.01	0.10	0.76	0.67	0.26	0.10	0.20		
	0.03	0.15		0.31	0.31	0.17	0.16		
	0.01	0.03		0.38	0.38				
		0.01							
Average	0.03	0.10	0.74	0.61	0.31	0.12	0.18	0.16	0.23
Stdev	0.02	0.05	0.05	0.17	0.05	0.03	0.02	0.02	0.01

Swelling

Only the plain PVA cryogel underwent tests to determine its increase in volume from a dehydrated to rehydrated state. Each sample was dried one week to remove all water then was placed in deionized water for two weeks. The results are listed in Table 12 and are compared in Figure 43.

Density of the samples was determined by weighing a large sample then measuring its volume in a graduated cylinder. With all water removed, the composition for each would only be made of PVA cryogel. This would lead one to expect the densities of the dried PVA cryogels would all have similar densities. The dried 10%, 20%, and 30% had densities 1.13, 1.12, and 1.14g/mL respectively. The values are within 1% of each other. After swelling, it can be seen that the densities increased with increasing weight percent. The densities of 10%, 20%, and 30% wt PVA cryogel became 1.03, 1.05, and 1.08g/mL respectively. Since 10% PVA cryogel has the highest water content per weight, it is expected that it would have the density closest to water (1.00g/mL).

The weight of five samples was measured for each weight percent then volume was calculated from this and the density. The change in the calculated volume from the dehydrated to hydrated state is the swelling ratio. 10% wt PVA cryogel showed an increase in volume of 250% from a dried sample. 20% wt PVA cryogel had an increase of 240% and 30% was 197%.

The swelling data collected show the beginning of a trend in which the swelling ratio decreases with the increase of PVA cryogel weight percent. 10% wt PVA cryogel

contains the highest percentage of water, so was expected to have a larger volume change from hydrated to dried and vise versa.

Table 12: Swelling Percents (Increase in Volume) of Plain PVA cryogel

		Dehydrated			Hydrated			
PVA	**Sample**	**Density (kg/m^3)**	**PVA wt (g)**	**PVA vol (mL)**	**Density (kg/m^3)**	**PVA wt (g)**	**PVA vol (mL)**	**Swelling (%)**
10%	1	1126	0.39	0.35	1026	1.29	1.26	262
	2		0.64	0.56		1.96	1.91	239
	3		0.37	0.33		1.21	1.18	261
	4		0.79	0.70		2.35	2.29	228
	5		0.43	0.38		1.40	1.36	260
							Average	**250**
							Stdev	**15**

		Dehydrated			Hydrated			
PVA	**Sample**	**Density (kg/m^3)**	**PVA wt (g)**	**PVA vol (mL)**	**Density (kg/m^3)**	**PVA wt (g)**	**PVA vol (mL)**	**Swelling (%)**
20%	1	1123	1.21	1.07	1047	3.853	3.68	243
	2		1.09	0.97		3.443	3.29	238
	3		0.89	0.79		2.833	2.71	242
	4		1.27	1.13		4.083	3.90	245
	5		1.16	1.03		3.592	3.43	232
							Average	**240**
							Stdev	**5**

		Dehydrated			Hydrated			
PVA	**Sample**	**Density (kg/m^3)**	**PVA wt (g)**	**PVA vol (mL)**	**Density (kg/m^3)**	**PVA wt (g)**	**PVA vol (mL)**	**Swelling (%)**
30%	1	1138	1.39	1.22	1080	4.02	3.72	205
	2		2.457	2.16		6.68	6.18	186
	3		2.23	1.96		6.11	5.66	189
	4		1.08	0.95		3.06	2.84	200
	5		1.73	1.52		4.97	4.60	203
							Average	**197**
							Stdev	**8**

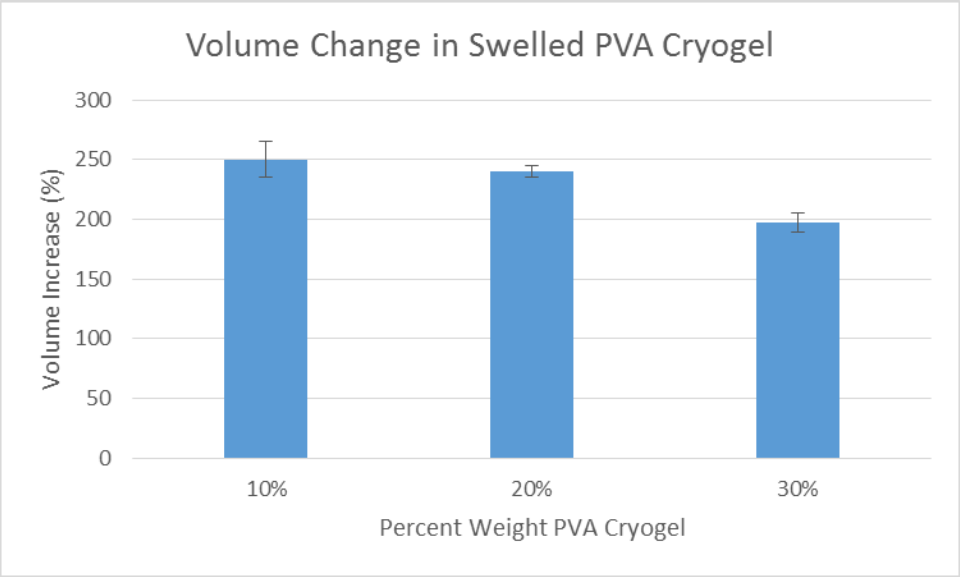

Figure 43: Comparison of Swelling Percent (Increase in Volume) from Dehydrated to Fully Hydrated for PVA Cryogel

Summary

A summary of all calculated values of mechanical and porous characteristics is displayed in Table 13.

Table 13: Summary of Properties of Tested PVA cryogel Materials

% wt PVA	Acceptance Criteria	10	20	30	30	30	20	10	20	30	30	30	30
Sample		10%	20%	30%	Poked	Velcro	Gas	10% Salt	20% Salt	2% CS	4% CS	5% CaPO4	10% CaPO4
Young's Modulus (MPa)	[0.005,0.05]	0.08	0.24	1.20	1.24	0.88	0.04	0.06	0.18	1.20	1.58	0.79	1.06
Tensile Strength (Mpa)	≥1.71	0.39	1.14	2.48	2.13	1.50	0.06	0.21	0.25	1.53	2.54	2.11	2.66
Elongation (%)	≥30	250	278	265	181	200	154	396	163	207	271	288	282
Tear Strength (kN/m)	≥2.0	1.34	2.26	9.11	13.06	11.59	0.58	1.85	2.92	11.36	15.31	10.76	9.00
Pore Size (μm)	[10,30] , [100,700]	-	-	-	60-170	250	100-800	50-250	20-600	20-300	20-500	5-15	5-20
Porosity (%)	[30,90]	-	-	-	3	10	74	61	31	12	18	16	23
Swelling Ratio	≥.5	2.5	2.4	1.97	-	-	-	-	-	-	-	-	-

CHAPTER 4

DISCUSSION

Many of the materials of the formulations tested would meet the goal of simultaneously achieving softness ([0.005,0.05]MPa for fat, [0.3,2.3]MPa for cartilage), surface porosity (≥0.3), and swelling ratio (≥0.5) for facial implants that are significantly better than the current devices. The selection of the best material for a particular implant would depend on the intended use. For instance, a nasolabial fold implant should have the softness of fat with light porosity, and more swelling. However, an ear implant should be stiffer like cartilage and have a small dimensional swelling.

Mechanical Properties

In respect to facial implants such as those for the nose and chin, the FDA recommends potential materials to undergo tests described in ASTM F881. These include tensile and tear tests to determine the material's tensile strength, yield elongation, modulus of elasticity, and tear strength. These mechanical properties of popular biomaterials on the market have been determined and are listed for reference in Table 14. The values for silicone are from the 510(k) summary for silicone facial implants by Hanson Medical while the values for Medpor and Gore-Tex were found in literature.

Table 14: Mechanical Properties of Popular Biomaterials

Property	Silicone	Medpor	Gore-Tex
Tensile Strength (MPa)	6.55	23	12
Elongation (%)	650	4	600
Young's Modulus (MPa)	2.07	227-307	6
Tear Strength (kN/m)	1.03	45	179
Reference	[89]	[21, 90-92]	[92-94]

Elasticity

In the literature, the rigidity of the implant was constantly mentioned as an issue with current facial implant materials. As seen in Table 14, the Young's modulus' for silicone, Medpor, and Gore-Tex are 2.07MPa, 227-307MPa, and 6MPa respectively. The elastic range of cartilage is [0.3,2.3]MPa. All the porous PVA cryogel samples made with 30% wt PVA cryogel fell within this range for cartilage. The same cannot be same for other biomaterials. Silicone with a modulus of 2.07MPa is the only one within the range of softness. Since the Young's modulus of cartilage increases as the depth of cartilage increases, 2.07MPa only falls within the range of the lowest depth (bottom 20%) of cartilage. Gore-Tex is much more ridged than cartilage with a modulus of 6MPa while Medpor is more similar to bone than cartilage. With a value that range from 227-307MPa, Medpor is the most rigid option used for facial implants and is two magnitudes greater than that of cartilage. One of the most common complaints for Medpor is that its stiffness makes it feel unnatural. With an elastic modulus that falls within the range of cartilage, porous PVA cryogel made with 30% wt PVA cryogel can offer a more natural feeling implant to the patient.

The modulus of elasticity of adipose tissue was found to range from 0.005-0.050MPa. 10% wt PVA cryogel cast over salt and gaseous 20% wt PVA cryogel met this criteria. These mechanical properties cannot be compared directly to those of popular dermal fillers due to their fluid nature. For general purposes, though, the elastic modulus of poly(methyl methacrylate) (PMMA) was found. This is the material of the only permanent dermal filler option and it is administered in the shape of microspheres. The Young's modulus of this material can range from 1800-3100MPa.[95] With the modulus of PMMA being five magnitudes greater than the surrounding tissue, the porous PVA cryogel samples would have a more natural feel underneath the skin.

Tensile Strength

The minimum tensile strength for a cartilage replacement was found to be 1.71MPa.[46] When looking at some of the most common biomaterials, it can been seen that they all have a tensile strength much higher than cartilage. Silicone is the closest and it is more than triple the minimum value. Gore-Tex has a tensile strength six times greater than cartilage, and Medpor is a whole factor greater at 23MPa. All tensile strengths determined from the created samples are closer in value to cartilage than those of current biomaterials, and all the porous PVA cryogel made with 30% wt PVA cryogel met this minimum standard.

Elongation

The standard recommendations by the FDA[42] states the elongation percentage of a cartilage replacing implant should be at least 200%. Since cartilage deformation begins after a 30% change in length, this value was chosen as the minimum elongation.

All porous PVA cryogel samples met this threshold. Silicone met the 200% elongation requirement of ASTM F881 with a value of 650% as did Gore-Tex with a value of 600%. Medpor, however, only has an elongation of 4% before it breaks. Having an implant that can stretch to at least the length of the surrounding tissue can help prevent an implant from having a unnatural feel, especially one in the face that is regularly under stress. In regards to elongation, all the porous PVA cryogel samples created would be more suited than Medpor for facial implants.

Tear Strength

The FDA does not have a recommended tear strength for facial implants, but cartilage was found to have a tear strength range of [2.0,2.4]kN/m.[48] An implant should have the same tear strength as cartilage if not higher to prevent it from becoming damaged. Both plain 20% and 30% wt PVA cryogel have a tensile strength of at least 2.0kN/m as well as almost all of their porous counterparts.

In comparison to other biomedical implants, silicone actually has tear strength beneath that of cartilage at 1.03kN/m.[96] This could lead it to tear internally while the surrounding cartilage stays intact, however none of the literature reviewed listed this occurrence. Only gaseous PVA cryogel presented a lower value, thus all but gaseous PVA cryogel would be an improved implant than silicone in regards to tear strength. Both Medpor and Gore-Tex have strengths magnitudes greater than cartilage at 45kN/m and 179kN/m respectively.

Summary of Mechanical Characteristics

While the elastic modulus of cartilage typically ranges from 0.3 to1.3MPa, it can be as high as 2.3MPa. 30% wt PVA cryogel and all its counterparts were found to have a Young's modulus within this range. Their values are more similar to that of cartilage than those materials on the market that can be as high as 23MPa. 30% wt PVA cryogel and all its porous counterparts either are the same tensile strength range as cartilage or are within the same magnitude while current biomaterials are many times greater. The elongation percentage of every sample was found to be greater than 30% (the maximum of cartilage). The required minimum tear strength to match cartilage was found in all samples except 10% wt and gaseous PVA cryogel. When comparing all mechanical properties, the values of the porous samples made with 30% wt PVA cryogel have equivalent values to cartilage unlike current biomaterials.

In regards to a filler for adipose tissue, the elasticity range is 0.005-0.05MPa. 10% wt PVA cryogel, its salt porous counterpart, and gaseous PVA cryogel all had similar elastic moduli. These were 0.08MPa, 0.21MPa, and 0.06MPa respectively. While elasticity cannot be compared directly to current dermal fillers, the material of the microspheres within the permanent filler (PMMA) has a modulus five magnitudes greater than fat. These porous PVA cryogels have a softness equivalent to that of adipose tissue unlike the current permanent option for patients in regards to dermal fillers.

Pore Structure Characteristics

Pore size and porosity percentages were determined by sectioning and imaging the implant. These values can be used to determine the likelihood of cellular ingrowth and eventual implant attachment after implantation. A wide range of pores and interconnectivity were observed with the created porous PVA cryogel samples. Information about these different pore structures show that some of the porous implants would have a greater chance of cellular ingrowth than others.

Pore Size

As stated earlier, fibrous ingrowth can be seen in pores with diameters between 5 and 15µm while bone regeneration typically requires pore diameters ranging from 100 to 400µm but can be as high as 700µm.[49-51] A chart comparing the porous PVA cryogel's pore range values to those of cellular ingrowth and current biomaterials is shown in Figure 44.

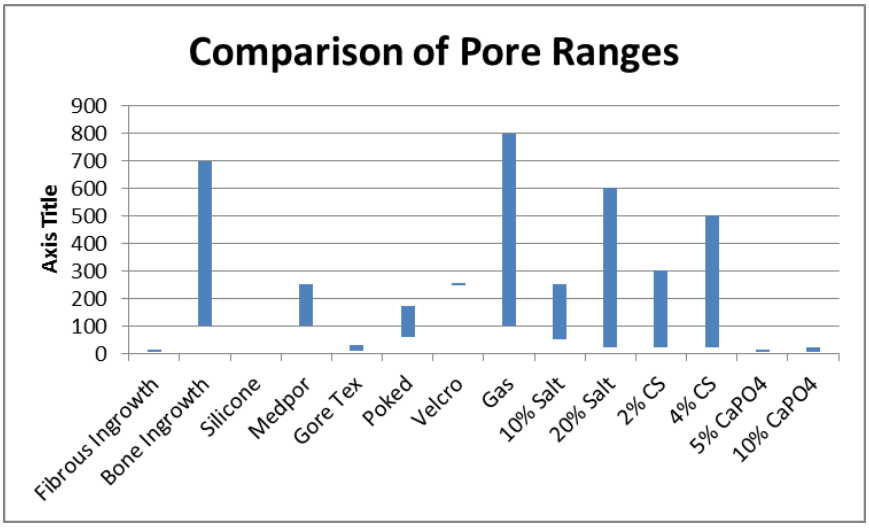

Figure 44: Comparison of Pore Ranges

Compares Cellular Ingrowth Ranges, PVA cryogel Samples, and Current Biomaterials

Having a porous implant, regardless of the pore diameter, allows for the body's surrounding environment to grow into it. All the porous samples manufactured are superior to nonporous silicone in this regard. Medpor has a pore diameter range of 100-250μm which is suitable for bone growth. Five of the porous PVA cryogel samples created also meet this standard. Gore-Tex is considered to be a microporous structure. Its pore range is 10-30μm which allows fibrous ingrowth.[97] The microporous calcium phosphate composites manufactured are then similar in utility.

Porosity

The higher the porosity percentage of a material, the more structural linkage of the ingrowth material within the implant to ensure attachment and prevent slippage. An implant should strive to have a minimum porosity of 30% to help this bonding.[52] The samples that meet this minimum are gaseous PVA cryogel (74%), those cast over salt (61% and 31%), and the CaPO4 composites (59% and 67%). A graph of the porosities of the samples is shown in Figure 45 with the red line marking the 30% minimum.

In relation the current biomaterials on the market, all the porous PVA cryogel samples created have an advantage over silicone in regards to porosity. One reason for silicone's decrease in popularity in America is due to its high likelihood of movement and rejection from the body. Having porous PVA cryogel allows the body to grow into the implant and prevent it from shifting. Both Medpor and Gore-Tex both have porosities above 30% (46% and 70% respectively). Bone ingrowth has been proven to occur within Medpor within two weeks of implementation.[90] Fibrous ingrowth has been seen within Gore-Tex in under a week.[8]

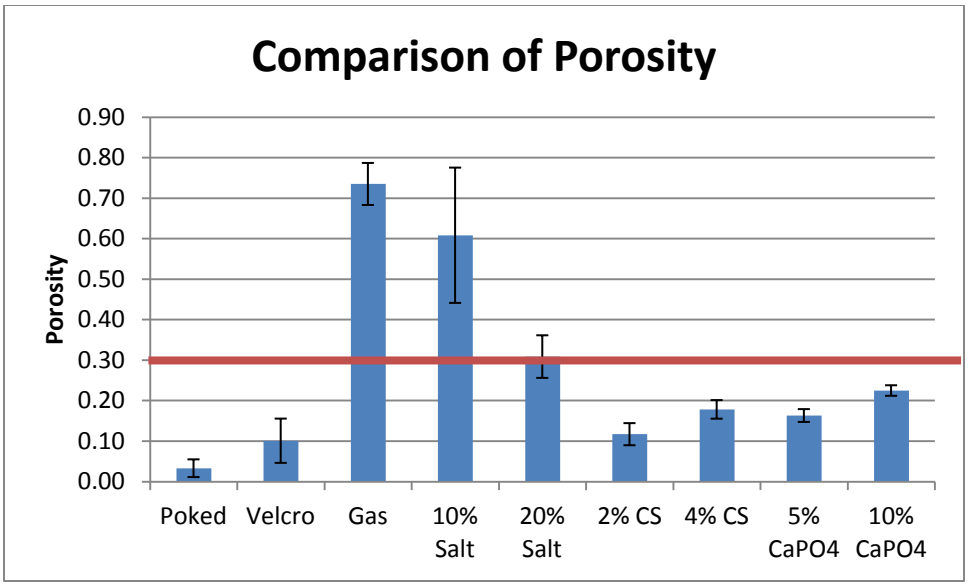

Figure 45: Comparison of Porosities

Red line marks minimum porosity needed for intercellular linkage during ingrowth

Surface Texture

In this research, porous PVA cryogel was created to allow cellular ingrowth into facial implants. This causes the implant to have a textured surface instead of a smooth one. While the merits of a smooth verses textured implant surface has not been researched for facial implants, they have been extensively studied with breast implants in relation to capsular contracture. This is the occurrence when the scar tissue that forms around the implant contracts and tightens. This can lead to an aesthetic change of the implant and discomfort for the patient. If the capsular contracture is severe enough, it must be corrected by surgery.[98]

There is overwhelming evidence that suggests that the type of textured breast implants have a lower capsular contracture rate than smooth ones. Barnsley et al. analyzed randomized controlled trials comparing implants with different surfaces to find

that smooth surfaced implants are five times more likely to have capsular contracture occur. Wong el al., in another review of previous studies, also found that textured implants experience capsular contracture less than smooth implants as well as it was independent of the pore size (30-70μm and 300-800μm) of the textured implant.[99] Collis et al. studied the long term affects of breast implants surfaces at ten years after implantation. He observed a capsular contracture rate of 65% for patients with smooth implants compared to 11% of textured.[100]

While there is not research that compares surface texture to the rate of capsular contracture in facial implants, studies show the benefit of textured breast implants over smooth implants. If this is the same for facial implants, then this suggests another benefit of the manufactured porous PVA cryogel implants in this study in comparison to current silicone facial implants as well as those made with plain PVA cryogel.

Summary of Porous Characteristics

Both the pore size and the porosity percentage are important for cellular ingrowth. The pore size determines ingrowth type while a high porosity allows the tissue to interconnect and create a strong hold between the implant and the surrounding area. In addition, the texturing of the implant can possibly prevent capsular contraction. The salt samples and gaseous PVA cryogel, and the chitosan composites all have pore sizes that will allow for bone ingrowth. The fine powder of the calcium phosphate created a microporous composite which is more suitable for fibrous ingrowth. In regards to a minimum porosity, the PVA cryogel cast over salt and gaseous PVA cryogel both presented a porosity high enough to allow tissue interconectivity. Thus, when

considering porous structure, the salt and gaseous PVA cryogel are suitable for bone ingrowth. Although the 30% PVA cryogel that was poked and molded do not meet these standards, if desired, this method can utilized for industry with different sized tools.

Comparing Porosity to Mechanical Properties

The porosity of the materials was compared to the mechanical characteristics to identify any trends. Scatter plots comparing these characteristics are displayed in Figure 46 and Figure 47. The most obvious trend can be seen with comparing porosity to tear strength (the red squares in the plot). An inverse relation is observed between them. Those with higher porosities were found to have lower tear strengths.

Trends are not as obvious with Young's modulus (green triangles) and tensile strength (blue diamonds). Below a level of 30% porosity, these two mechanical values are scattered without noticeable trends. Above a level of 30% porosity, there is a clear drop in the Young's modulus and tensile strength values as compared to the values below 30%. A value of approximately 30% porosity appears to be a threshold of some type.

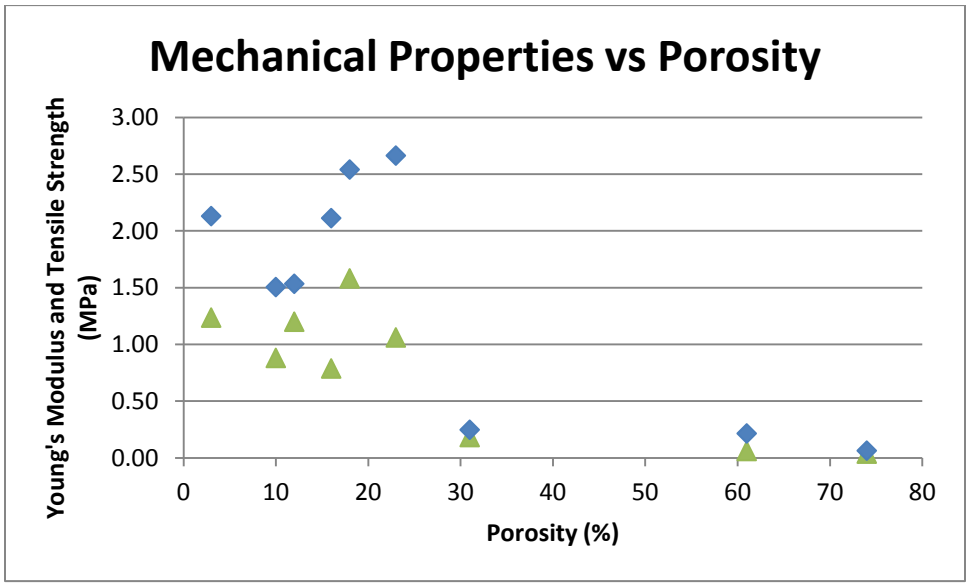

Figure 46: Comparing Mechanical Properties to Porosity

Green Triangles represent Young's modulus. Blue Diamonds represent tensile strength.

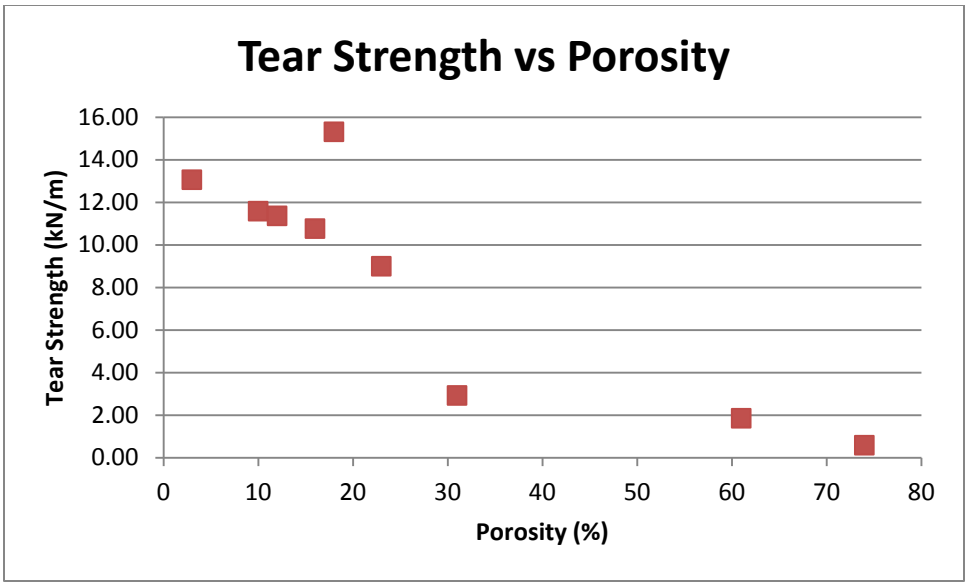

Figure 47: Comparing Tear Strength to Porosity

Rule of Mixtures

After the material mechanical characteristics were determined experimentally, they were compared to their theoretical values calculated using the rule of mixtures. The general rule of mixtures is used in material science as a means to predict the mechanical properties of composite materials, including the elastic modulus.[101] The rule of mixtures uses the elastic modulus of the matrix material (E_m) and of its reinforcement fiber material (E_f) to calculate the elastic modulus of the composite. The volume fraction of the reinforcement material is identified as v_f. These series of equations can calculate the elastic modulus when the reinforcement fibers are in three positions.[102, 103] When the fibers are parallel to the direction of the applied force, the longitudinal modulus (E_L) can be calculated using the following equation.

$$\boldsymbol{E_L = E_f v_f + E_m(1 - v_f)}$$

The transverse modulus (E_T) is the elastic modulus when the direction of the fibers in perpendicular to that of the applied force. This is shown in the equation below.

$$\boldsymbol{E_T = \frac{E_f E_m}{E_f(1 - v_f) + E_m v_f}}$$

Finally, the longitudinal and transverse modulus can be combined to find the random modulus (E_R) in which there is no order to the direction of the fibers. The equation is shown below.

$$E_R = \frac{3}{8}E_L + \frac{5}{8}E_T$$

E_m was obtained from the mechanical testing. The elastic moduli for 10, 20, and 30% wt PVA cryogels were found to be 0.08, 0.24, and 1.20MPa respectively. The

values for E_f were found in literature: 65MPa for chitosan [104] and 100MPa[105] for calcium phosphate. E_f for air is zero.

A table showing the calculations for E_L, E_T, and E_R are shown in Table 15. A graph comparing the theoretical longitudinal elastic moduli (E_L) to those found through mechanical testing is shown in Figure 48.

For the poked and Velcro PVA cryogels, the theoretical elastic moduli values were 1.16 and 1.08 MPa, which represent differences of 6 and 23% from their respective valves found through mechanical testing. The elastic modulus of porous PVA cryogel, which was created using the gas method, was found to be 0.06MPa, which is 50% greater than the 0.04 MPa found through experimental methods. When comparing the theoretical and experimental elastic results from the porous PVA created using salt, the theoretical values were 48% and 9% less than what was found experimentally for 10% and 20% respectively. The chitosan composite had theoretical elastic values about eight times greater than the experimental ones and the calcium phosphate theoretical values were twenty-two times greater.

All of the non-composite porous PVA cryogels created were found to have elastic moduli within the same order of magnitude that were found experimentally and within 50% of those value. The composites, however, had theoretical values that were much greater than the experimental values. The purpose of the rule of mixtures is to predict mechanical values of composite materials. The input values used to determine these theoretical values included some found experimentally (porosity of the composites and the elastic modulus of plain PVA cryogel) and in literature (elastic modulus' of chitosan

and calcium phosphate). Having incorrect values for any one of these inputs could have altered the theoretical output from the rule of mixtures and have caused this discrepancy.

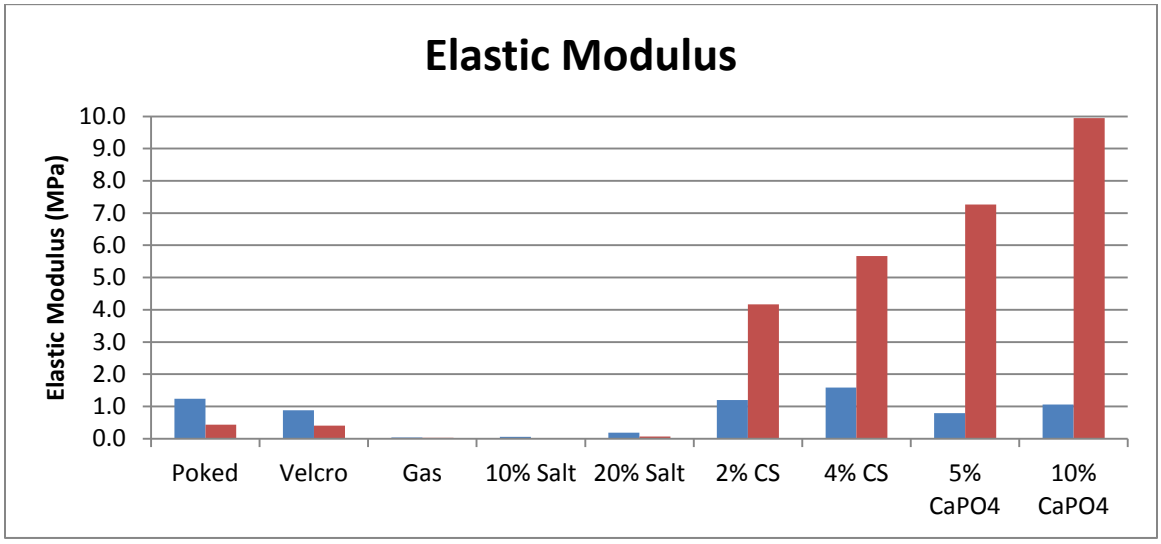

Figure 48: Comparing Longitudinal Modulus to Experimental Findings

Blue represents the elastic modulus' found through experimentation.

Red represents the theoretical longitudinal modulus calculated using the rule of mixtures.

Table 15: Theoretical Values Using Rule of Mixtures

Porous PVA	v_f	E_f	E_m	E_L	E_T	E_R
Poked	0.03	0	1.2	1.16	0.00	0.44
Velcro	0.1	0	1.2	1.08	0.00	0.41
Gas	0.74	0	0.24	0.06	0.00	0.02
10% salt	0.61	0	0.08	0.03	0.00	0.01
20% salt	0.31	0	0.24	0.17	0.00	0.06
2% CS	0.12	65	1.2	8.86	1.36	4.17
4% CS	0.18	65	1.2	12.68	1.46	5.67
5% CaPO4	0.16	100	1.2	17.01	1.43	7.27
10% CaPO4	0.23	100	1.2	23.92	1.55	9.94

Swelling

Increasing weight percent PVA cryogel showed a decrease in overall swelling percent. 10% wt PVA cryogel increased 250% in size while 30% wt PVA cryogel increased 197%. When injecting a dermal filler, a greater swelling rate would lead to a smaller sized needle when it is administered to the patient. Thus, a material such as 10% wt PVA cryogel would be more suitable than its larger weight counterparts for injection purposes.

Summary

Table 16 relates the parameters for facial implants given in Table 4 in the Introduction to the values found of all the PVA cryogel samples. A green check mark indicates that the value of the sample's characteristic is within the range and/or has a value closer than current materials on the market. A red 'X' shows that it did not meet this standard.

The swelling ratio is not shown in the table due to the fact that the test was not administered to the porous implants. Decreasing the weight percent of PVA within the hydrogel was shown to increase the swelling ratio. All weight percents increased in volume (250%, 240%, and 197% for 10%, 20%, and 30% wt PVA cryogel) much greater than the wanted 50%. It is a prediction that the porous PVA cryogel weight counterparts will have similar volume increases, however more tests will have to be performed to determine whether or not this is true.

Table 16: Visual Representation of Equivalence of Value to Required Characteristic

Basis	Characteristic	Acceptance Criteria	Poked (30% PVA)	Velcro (30% PVA)	Gas (20% PVA)	Salt (10% PVA)	Salt (20% PVA)	2% CS (30% PVA)	4% CS (30% PVA)	5% CaPO4 (30% PVA)	10% CaPO4 (30% PVA)
Adipose Tissue	Young's Modulus (MPa)	[0.005,0.05]	X	X	✔	✔	X	X	X	X	X
Cartilage	Young's Modulus (MPa)	[0.3,2.3]	✔	✔	X	X	X	✔	✔	✔	✔
	Tensile Strength (Mpa)	≥1.71	✔	✔	X	X	X	✔	✔	✔	✔
	Elongation (%)	≥30	✔	✔	✔	✔	✔	✔	✔	✔	✔
	Tear Strength (kN/m)	≥2.0	✔	✔	X	X	✔	✔	✔	✔	✔
Fibrous	Pore Size (μm)	[10,30]	X	X	X	X	X	X	X	✔	✔
Bone	Pore Size (μm)	[100,700]	✔	✔	✔	✔	✔	✔	✔	X	X
Callular Ingrowth	Porosity (%)	[30,90]	X	X	✔	✔	✔	X	X	X	X

Limitations

The pore characteristics were determined from images taken by a Nikon Eclipse E600 microscope from sections of the PVA cryogel samples. The sections were of different areas of the samples and images were taken of different areas within the image. While these images were taken at areas that had pores similar to the section as a whole, the nonumiform nature of the pores could mean the actual average pore size and porosity could be larger or smaller than calculated. In addition, this method was chosen because of ease of accessibility to the required machines. Other methods to determine these characteristics found in literature include porosimetry and SEM images. Porosimetry, however would require the extra material in the CS and CaPO4 composited to be dissolved out before the test and both machines were not available for use.

The samples underwent rather crude execution of the testing methods in regards to determining their mechanical properties. As stated above, ASTM standards D412 and D624 were followed. The testing machine utilized was chosen because it was the only one that was accessible and tall enough to pull the specimens to their complete length. It did not have auto tightening grips suggested by the standards. The specimens were tightened as much as possible prior to the beginning of the test, then again halfway though when the grip of the specimen became loose. The machine was located in an open room not in a temperature controlled air circulation chamber. The tests specified that the specimens should be maintained at 23°C±2 for three days prior. While they were stored at room temperature, no measures were taken to ensure the specified temperature during transport or testing nor the desired air flow rate. While the machine did measure

the change in length between the grips, it did not measure the beginning grip length. This was performed using calipers. The desired thickness for the samples was 3.0±0.3mm. As can be seen in Table 6 and Table 8, the thicknesses did not always meet this standard. Those that formed within the mold expanded and contracted through the freeze/thaw cycles to differing thicknesses. The salt samples were formed in tubes and after swelling in water to leach out the salt and were hand carved to try to give them a shape as similar as possible to the desired specifications. Within the tear test, the nick that had to be cut into every specimen was hand done with a scalpel. The nick depth is specified at 0.5±0.05mm, however is could have been slightly outside the range due to human error. Finally, the standards display their tested accuracy at the end of the documents. While most standard deviations of the characteristics are small, the percent elongation's standard deviation was tested to be as high as 50% of its average value. This shows that a large standard deviation for elongation is normal and expected when utilizing this standard.

The mechanical tests performed on the samples did not simulate the surrounding environment they would be in after implantation as well as did not predict long time wear. The ASTM standards require the tests specimens to be maintained at 23°C±2, however the average body temperature is about 37°C. This change in temperature could potentially alter the mechanical values determined. In addition, the CS and CaPO4 composite materials were not porous during testing. Porosity will develop in these samples after implantation over time as the body absorbs the CS and CaPO4. Becoming porous may change the mechanical properties of the materials as well. In addition, the implants should last indefinitely within the body. While PVA cryogel is

nonbiodegradable within the body, long term influence of the surround tissues and fluid was not assessed in these experiments.

Finally, ASTM F881 requires the hardness of the material be determined with a durometer based on ASTM D2240. This machine, or any compression tool, was unavailable for use. Testing the material's characteristics in compression is needed for when predicting the material's overall performance after implantation. Facial implants will experience compression forces during daily use, thus the compression characteristics of potential implant materials should be determined before they are released to the market.

Potential Future Work

Except for the salt samples, the tests performed were on samples that had been removed from the mold but were not placed in deionized water and swelled. Due to the chance that they may change, mechanical properties after swelling should be found to more accurately determine their values *in vivo*.

Another test is to determine cellular ingrowth. While under the preferred conditions such as pore size and the proper surrounding environment, cells should grow into the implant. Tests should be performed to determine the effectiveness of the pores on cellular ingrowth.

The samples were created out of desire to make facial implants, but their use could extend into other volume filling implants. Pores allow them to integrate with the body to reduce unwanted movement and prevent extrusion. Possible examples could include current PVA cryogel implants such as cartilage knee replacement to other areas such as bone void fillers or breast implants. Designers should consider porous PVA cryogel as another material choice for future implants.

Conclusions

Porous PVA cryogels were shown to be a suitable candidate for the application of facial implants.

Hydrogels manufactured with 30% wt PVA showed an elastic modulus equivalent to that of cartilage as well as with other mechanical characteristics. Pore sizes susceptible to the ingrowth of both bone and fibrous tissue were observed as well as porosities large enough to encourage attachment. When looking at all the characteristics of the samples as a whole, the PVA/chitosan composites as well as those with altered surface finish such as the molded PVA should be considered suitable as an alternative material for facial cartilage replacement. These would be used when there is a need for a strong attachment due to bone ingrowth. For the purpose of fibrous ingrowth, especially if there is a desire to later remove the implant, the PVA/CaPO4 composites would be suitable.

In regards to dermal fillers, porous PVA cryogels manufactured with lower PVA weights should be considered as alternatives to current injectable materials. This includes gaseous 20% wt PVA cryogel and 10% wt PVA cryogel cast over salt. Not only did these fall within the elastic range of adipose tissue, but samples manufactured with lower PVA weights showed higher volume increases when dried then saturated. The porous 10% wt PVA cryogel manufactured with the salt leaching method is recommended when a high amount of cellular ingrowth is desired. A 10% wt PVA cryogel combined with CaPO4 should be used for a lighter attachment.

REFERENCES

1. Baker, M.I., et al., *A review of polyvinyl alcohol and its uses in cartilage and orthopedic applications.* Journal of Biomedical Materials Research Part B: Applied Biomaterials, 2012. **100**(5): p. 1451-1457.
2. Williams, S., *Mechanical Testing of a New Biomaterial for Potential Use as a Vascular Graft and Articular Cartilage Substitute*, in *Mechanical Engineering*. 1998, Georgia Institute of Technology.
3. *List of Medical Devices, by Product Code, that FDA classifies as Implantable, Life-Saving, and Life-Sustaining Devices for purposes of Section 614 of FDASIA amending Section 519(f) of the FDC Act*, F.a.D. Administration, Editor. 2013.
4. Surgeons, A.S.o.P. *2013 Cosmetic Plastic Surgery Statistics*. 2014 [cited 2014; Available from: www.plasticsurgery.org.
5. *Saline, Silicone Gel, and Alternative Breast Implants* F.a.D. Administration, Editor. 2006.
6. *Product Classification*. 2014, U.S. Food and Drug Administration: U.S. Food and Drug Administration Website.
7. Adams, J.S., *Grafts and implants in nasal and chin augmentation. A rational approach to material selection.* Otolaryngologic clinics of North America, 1987. **20**(4): p. 913-930.
8. Lin, G. and W. Lawson, *Complications using grafts and implants in rhinoplasty.* Operative Techniques in Otolaryngology-Head and Neck Surgery, 2007. **18**(4): p. 315-323.
9. Conrad, K., C.S. Torgerson, and G.S. Gillman, *Applications of Gore-Tex implants in rhinoplasty reexamined after 17 years.* Archives of facial plastic surgery, 2008. **10**(4): p. 224-231.
10. Rah, D., *Art of Replacing Facial Bone Defects.* Yonsei Medical Journal, 2000. **41**(6).
11. Adams, J., *Graphs and implants in chin and nasal augumentation: A Rational Approach to Material Selection.* The Otolaryngologic Clinics of North America, 1987. **20**(4).
12. McCurdy, J.A., *Augmentation rhinoplasty with silicone prostheses.* Operative Techniques in Otolaryngology-Head and Neck Surgery, 2008. **19**(1): p. 72-78.
13. Dresner, H.S. and P.A. Hilger, *An overview of nasal dorsal augmentation.* Semin Plast Surg, 2008. **22**(2): p. 65-73.
14. Berghaus, A., *Alloplastic materials in rhinoplasty.* Current Opinion in Otolaryngology & Head and Neck Surgery, 2006. **14**(4).
15. Silver, W.E.D., Mathew J.; DeJoseph, Louis M. , *Implants and Fillers for Facial Plastic Surgery.*
16. Ersek, R., *Transplantation of Purified Autologous Fat: A 3-Year Follow-Up is Disappointing.* Plastic Reconstruction Surgery, 1991. **82**(2): p. 219-227.
17. Murakami, C.S., T.A. Cook, and R.A. Guida, *Nasal reconstruction with articulated irradiated rib cartilage.* Archives of Otolaryngology–Head & Neck Surgery, 1991. **117**(3): p. 327-330.

18. Ham, K., S. Chung, and S. Lee, *Complications of oriental augmentation rhinoplasty.* Annals of the Academy of Medicine, Singapore, 1983. **12**(2 Suppl): p. 460-462.
19. Wellisz, T., *Clinical experience with the Medpor porous polyethylene implant.* Aesthetic plastic surgery, 1993. **17**(4): p. 339-344.
20. *<Alloplastic materials in rhinoplasty (review).pdf>*.
21. Park, H., et al, *Biomechanical properties of high-density polyethylene for pterional prosthesis.* Neurological research, 2002. **24**(7): p. 671-676.
22. Romo III, T., A.P. Sclafani, and P. Sabini, *Use of porous high-density polyethylene in revision rhinoplasty and in the platyrrhine nose.* Aesthetic plastic surgery, 1998. **22**(3): p. 211-221.
23. Godin, M.S., S.R. Waldman, and C.M. Johnson, *Nasal augmentation using Gore-Tex: a 10-year experience.* Archives of facial plastic surgery, 1999. **1**(2): p. 118-121.
24. Jin, H.-R., et al., *A multicenter evaluation of the safety of Gore-Tex as an implant in Asian rhinoplasty.* American journal of rhinology, 2006. **20**(6): p. 615-619.
25. Conrad, K.T., Cory; Gillman, Grant, *Applications of GORE-TEX Implants in Rhinoplasty Reexamined After 17 Years.* ARCH FACIAL PLAST SURG, 2008. **10**(4).
26. Gross, E.J., et al., *Mersilene mesh chin augmentation: a 14-year experience.* Archives of facial plastic surgery, 1999. **1**(3): p. 183-189.
27. Gross, E., et al, *Mersilene Mesh Chin Augmentation A 14-Year Experience.* Archives of Facial Plastic Surgery, 1999. **1**(3): p. 183-189.
28. *Serious Problems With Proplast-Coated TMJ Implant*, F.a.D. Administration, Editor. 1990.
29. *Dermal Filler Devices*, F.a.D. Administration, Editor. 2008.
30. Housman, T.S., et al., *What specialties perform the most common outpatient cosmetic procedures in the United States?* Dermatologic Surgery, 2008. **34**(1): p. 1-8.
31. Lemperle, G., et al., *ArteFill® permanent injectable for soft tissue augmentation: II. Indications and applications.* Aesthetic plastic surgery, 2010. **34**(3): p. 273-286.
32. *Wrinkle Fillers Approved by the Center for Devices and Radiological Health*, U.S.F.a.D. Administration, Editor. 2013.
33. Jacovella, P.F., *Use of calcium hydroxylapatite (Radiesse®) for facial augmentation.* Clinical interventions in aging, 2008. **3**(1): p. 161.
34. Gold, M., *The science and art of hyaluronic acid dermal filler use in esthetic applications.* Journal of cosmetic dermatology, 2009. **8**(4): p. 301-307.
35. Kablik, J., et al., *Comparative physical properties of hyaluronic acid dermal fillers.* Dermatologic Surgery, 2009. **35**(s1): p. 302-312.
36. Lowe, N.J., et al., *Hyaluronic acid skin fillers: adverse reactions and skin testing.* Journal of the American Academy of Dermatology, 2001. **45**(6): p. 930-933.
37. Narins, R.S., et al., *Twelve-Month Persistency of a Novel Ribose–Cross-linked Collagen Dermal Filler.* Dermatologic surgery, 2008. **34**(s1): p. S31-S39.

38. Silvers, S.L., et al., *Prospective, open-label, 18-month trial of calcium hydroxylapatite (Radiesse) for facial soft-tissue augmentation in patients with human immunodeficiency virus-associated lipoatrophy: one-year durability.* Plastic and reconstructive surgery, 2006. **118**(3S): p. 34S-45S.
39. Bass, L.S., et al., *Calcium Hydroxylapatite (Radiesse) for Treatment of Nasolabial Folds Long-Term Safety and Efficacy Results.* Aesthetic Surgery Journal, 2010. **30**(2): p. 235-238.
40. Jansen, D.A. and M.H. Graivier, *Evaluation of a calcium hydroxylapatite-based implant (Radiesse) for facial soft-tissue augmentation.* Plastic and reconstructive surgery, 2006. **118**(3S): p. 22S-30S.
41. Park, T.H., et al., *Clinical experience with polymethylmethacrylate microsphere filler complications.* Aesthetic plastic surgery, 2012. **36**(2): p. 421-426.
42. ASTM, *Standard Specification for Silicone Elastomer Facial Implants*. 2006.
43. Laasanen, M., et al., *Biomechanical properties of knee articular cartilage.* Biorheology, 2003. **40**(1): p. 133-140.
44. Krouskop, T.A., et al., *Elastic moduli of breast and prostate tissues under compression.* Ultrasonic imaging, 1998. **20**(4): p. 260-274.
45. Sarvazyan, A., et al., *Biophysical bases of elasticity imaging*, in *Acoustical imaging*. 1995, Springer. p. 223-240.
46. Richmon, J.D., et al., *Tensile biomechanical properties of human nasal septal cartilage.* American journal of rhinology, 2005. **19**(6): p. 617-622.
47. Akizuki, S., et al., *Tensile properties of human knee joint cartilage: I. Influence of ionic conditions, weight bearing, and fibrillation on the tensile modulus.* Journal of Orthopaedic Research, 1986. **4**(4): p. 379-392.
48. Kempson, G., *Mechanical Properties of articular cartilage*. 2nd ed. Freeman MAR (ed.): Adult Articular Cartilage. 1979, Tunbridge Wells, England: Pitman Medical.
49. Annabi, N., et al., *Controlling the porosity and microarchitecture of hydrogels for tissue engineering.* Tissue Engineering Part B: Reviews, 2010. **16**(4): p. 371-383.
50. Burg, K.J., S. Porter, and J.F. Kellam, *Biomaterial developments for bone tissue engineering.* Biomaterials, 2000. **21**(23): p. 2347-2359.
51. Mullen, L., et al., *Selective Laser Melting: A regular unit cell approach for the manufacture of porous, titanium, bone in-growth constructs, suitable for orthopedic applications.* Journal of Biomedical Materials Research Part B: Applied Biomaterials, 2009. **89**(2): p. 325-334.
52. Bruchman, W.C., C.W. Bolton, and J.R. Bain, *Prosthesis for tensile load-carrying tissue and method of manufacture*. 1993, Google Patents.
53. Gill, H.S. and M.R. Prausnitz, *Does needle size matter?* Journal of diabetes science and technology, 2007. **1**(5): p. 725-729.
54. Stammen, J.A., et al., *Mechanical properties of a novel PVA hydrogel in shear and unconfined compression.* Biomaterials, 2001. **22**(8): p. 799-806.
55. Corkhill, P., A. Trevett, and B. Tighe, *The potential of hydrogels as synthetic articular cartilage.* Proceedings of the Institution of Mechanical Engineers, Part H: Journal of Engineering in Medicine, 1990. **204**(3): p. 147-155.

56. Hoffman, A.S., *Hydrogels for biomedical applications.* Annals of the New York Academy of Sciences, 2001. **944**(1): p. 62-73.
57. Holloway, J.L., A.M. Lowman, and G.R. Palmese, *Mechanical evaluation of poly (vinyl alcohol)-based fibrous composites as biomaterials for meniscal tissue replacement.* Acta biomaterialia, 2010. **6**(12): p. 4716-4724.
58. Hutmacher, D.W., *Scaffolds in tissue engineering bone and cartilage.* Biomaterials, 2000. **21**(24): p. 2529-2543.
59. Mikos, A.G. and J.S. Temenoff, *Formation of highly porous biodegradable scaffolds for tissue engineering.* Electronic Journal of Biotechnology, 2000. **3**(2): p. 23-24.
60. Zorlutuna, P., et al., *Microfabricated biomaterials for engineering 3D tissues.* Advanced Materials, 2012. **24**(14): p. 1782-1804.
61. Murphy, W.L., et al., *Salt fusion: an approach to improve pore interconnectivity within tissue engineering scaffolds.* Tissue engineering, 2002. **8**(1): p. 43-52.
62. Ma, P.X. and J.-W. Choi, *Biodegradable polymer scaffolds with well-defined interconnected spherical pore network.* Tissue engineering, 2001. **7**(1): p. 23-33.
63. Draghi, L., et al., *Microspheres leaching for scaffold porosity control.* Journal of materials science: materials in medicine, 2005. **16**(12): p. 1093-1097.
64. Park, J.S., et al., *< i> In vitro</i> and< i> in vivo</i> test of PEG/PCL-based hydrogel scaffold for cell delivery application.* Journal of Controlled Release, 2007. **124**(1): p. 51-59.
65. Freed, L.E., et al., *Neocartilage formation in vitro and in vivo using cells cultured on synthetic biodegradable polymers.* Journal of biomedical materials research, 1993. **27**(1): p. 11-23.
66. Goldstein, A.S., et al., *Effect of osteoblastic culture conditions on the structure of poly (DL-lactic-co-glycolic acid) foam scaffolds.* Tissue engineering, 1999. **5**(5): p. 421-433.
67. Rezwan, K., et al., *Biodegradable and bioactive porous polymer/inorganic composite scaffolds for bone tissue engineering.* Biomaterials, 2006. **27**(18): p. 3413-3431.
68. Kabiri, K., H. Omidian, and M. Zohuriaan-Mehr, *Novel approach to highly porous superabsorbent hydrogels: synergistic effect of porogens on porosity and swelling rate.* Polymer International, 2003. **52**(7): p. 1158-1164.
69. Keskar, V., et al., *In vitro evaluation of macroporous hydrogels to facilitate stem cell infiltration, growth, and mineralization.* Tissue engineering Part A, 2009. **15**(7): p. 1695-1707.
70. Zheng, Y., et al., *Performance of novel bioactive hybrid hydrogels in vitro and in vivo used for artificial cartilage.* Biomedical Materials, 2009. **4**(1): p. 015015.
71. Lee, J.-Y., B. Tan, and A.I. Cooper, *CO2-in-water emulsion-templated poly (vinyl alcohol) hydrogels using poly (vinyl acetate)-based surfactants.* Macromolecules, 2007. **40**(6): p. 1955-1961.
72. Cooper, A.I., *Polymer synthesis and processing using supercritical carbon dioxide.* Journal of Materials Chemistry, 2000. **10**(2): p. 207-234.

73. Butler, R., I. Hopkinson, and A. Cooper, *Synthesis of porous emulsion-templated polymers using high internal phase CO2-in-water emulsions.* Journal of the American Chemical Society, 2003. **125**(47): p. 14473-14481.
74. Palocci, C., et al., *Porous biomaterials obtained using supercritical CO2-water emulsions.* Langmuir, 2007. **23**(15): p. 8243-8251.
75. Ushio, K., et al., *Attachment of artificial cartilage to underlying bone.* Journal of Biomedical Materials Research Part B: Applied Biomaterials, 2004. **68**(1): p. 59-68.
76. Maher, S., et al., *Nondegradable hydrogels for the treatment of focal cartilage defects.* Journal of biomedical materials research Part A, 2007. **83**(1): p. 145-155.
77. Zheng, Y., et al., *Preparation and characterization of poly (vinyl alcohol)/hydroxylapatite hybrid hydrogels.* Journal of composite materials, 2007. **41**(17): p. 2071-2082.
78. Tang, Y., et al., *A thermosensitive chitosan/poly (vinyl alcohol) hydrogel containing hydroxyapatite for protein delivery.* Journal of Biomedical Materials Research Part A, 2009. **91**(4): p. 953-963.
79. Yan, L.P., et al., *Genipin-cross-linked collagen/chitosan biomimetic scaffolds for articular cartilage tissue engineering applications.* Journal of Biomedical Materials Research Part A, 2010. **95**(2): p. 465-475.
80. Qi, B., et al., *The preparation and cytocompatibility of injectable thermosensitive chitosan/poly (vinyl alcohol) hydrogel.* Journal of Huazhong University of Science and Technology [Medical Sciences], 2010. **30**: p. 89-93.
81. Wu, G., et al., *< i> In vitro</i> behaviors of hydroxyapatite reinforced polyvinyl alcohol hydrogel composite.* Materials Chemistry and Physics, 2008. **107**(2): p. 364-369.
82. de Souza Costa-Júnior, E., M.M. Pereira, and H.S. Mansur, *Properties and biocompatibility of chitosan films modified by blending with PVA and chemically crosslinked.* Journal of Materials Science: Materials in Medicine, 2009. **20**(2): p. 553-561.
83. ASTM, *Standard Test Methods for Vulcanized Rubber and Thermoplastic Elastomers—Tension*. 2008.
84. ASTM, *Standard Test Method for Tear Strength of Conventional Vulcanized Rubber and Thermoplastic Elastomers*. 2012.
85. *Silicone Implants*. Available from: http://qliniqmedical.nl/qliniq_bv_gezicht_implantaten_neus_kin.htm.
86. Barry, J.J., et al., *Supercritical carbon dioxide: putting the fizz into biomaterials.* Philosophical Transactions of the Royal Society A: Mathematical, Physical and Engineering Sciences, 2006. **364**(1838): p. 249-261.
87. Qi, B.-w., et al., *Chitosan/poly (vinyl alcohol) hydrogel combined with Ad-hTGF-β1 transfected mesenchymal stem cells to repair rabbit articular cartilage defects.* Experimental Biology and Medicine, 2013. **238**(1): p. 23-30.
88. Qi, H., K. Joyce, and M. Boyce, *Durometer hardness and the stress-strain behavior of elastomeric materials.* Rubber chemistry and technology, 2003. **76**(2): p. 419-435.

89. Qi, B.W., et al., *Chitosan/poly(vinyl alcohol) hydrogel combined with Ad-hTGF-beta1 transfected mesenchymal stem cells to repair rabbit articular cartilage defects.* Exp Biol Med (Maywood), 2013. **238**(1): p. 23-30.
90. Spector, M., et al., *Bone growth into porous high-density polyethylene.* Journal of biomedical materials research, 1976. **10**(4): p. 595-603.
91. Nayyer, L., et al., *Design and development of nanocomposite scaffolds for auricular reconstruction.* Nanomedicine: Nanotechnology, Biology and Medicine, 2014. **10**(1): p. 235-246.
92. Bang, B.W., et al., *The biodurability of covering materials for metallic stents in a bile flow phantom.* Digestive diseases and sciences, 2012. **57**(4): p. 1056-1063.
93. Bäckdahl, H., et al., *Mechanical properties of bacterial cellulose and interactions with smooth muscle cells.* Biomaterials, 2006. **27**(9): p. 2141-2149.
94. Giesen, E., et al., *Mechanical properties of cancellous bone in the human mandibular condyle are anisotropic.* Journal of biomechanics, 2001. **34**(6): p. 799-803.
95. *PMMA*, in *Material Property Database*. 2004, MIT.
96. Medical, H., *Duralistic Chin Implants*, F.a.D. Administration, Editor. 1997.
97. Foundation, C.H. *Robert W. Gore*. Available from: http://www.chemheritage.org/discover/online-resources/chemistry-in-history/themes/petrochemistry-and-synthetic-polymers/synthetic-polymers/gore.aspx.
98. Barnsley, G.P., L.J. Sigurdson, and S.E. Barnsley, *Textured surface breast implants in the prevention of capsular contracture among breast augmentation patients: A meta-analysis of randomized controlled trials.* Plastic and reconstructive surgery, 2006. **117**(7): p. 2182-2190.
99. Wong, C.-H., et al., *Capsular contracture in subglandular breast augmentation with textured versus smooth breast implants: a systematic review.* Plastic and reconstructive surgery, 2006. **118**(5): p. 1224-1236.
100. Collis, N., et al., *Ten-year review of a prospective randomized controlled trial of textured versus smooth subglandular silicone gel breast implants.* Plastic and reconstructive surgery, 2000. **106**(4): p. 786-791.
101. Alger, M.S.M., *Polymer Science Dictionary*. 2nd ed. 1997: Springer Publishing.
102. Mallick, P.K., *Fiber Reinforced Composites: Materials, Manufacturing and Design*. 2nd ed. 1993, New York: Marcel Decker, Inc.
103. Roylance, D., *Introduction to composite materials.* Department of Materials Science & Engineering, Massachusetts Institute of Technology, Camridge, 2000.
104. Nishino, T., R. Matsui, and K. Nakamae, *Elastic modulus of the crystalline regions of chitin and chitosan.* Journal of Polymer Science Part B: Polymer Physics, 1999. **37**(11): p. 1191-1196.
105. Al-Sanabani, J.S., A.A. Madfa, and F.A. Al-Sanabani, *Application of calcium phosphate materials in dentistry.* International journal of biomaterials, 2013. **2013**.